

**DEVELOPMENT OF A COMPUTERIZED  
THERMAL CONDUCTIVITY MEASUREMENT SYSTEM  
UTILIZING THE TRANSIENT NEEDLE PROBE TECHNIQUE:  
AN APPLICATION TO HYDRATES IN POROUS MEDIA**

**GREGORY B. ASHER**

ProQuest Number: 10796307

All rights reserved

INFORMATION TO ALL USERS

The quality of this reproduction is dependent upon the quality of the copy submitted.

In the unlikely event that the author did not send a complete manuscript and there are missing pages, these will be noted. Also, if material had to be removed, a note will indicate the deletion.



ProQuest 10796307

Published by ProQuest LLC (2019). Copyright of the Dissertation is held by the Author.

All rights reserved.

This work is protected against unauthorized copying under Title 17, United States Code  
Microform Edition © ProQuest LLC.

ProQuest LLC.  
789 East Eisenhower Parkway  
P.O. Box 1346  
Ann Arbor, MI 48106 – 1346

---

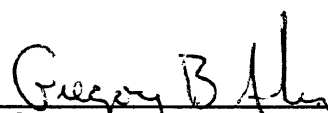
## SUBMITTAL


---

A thesis submitted to the Faculty and Board of Trustees of the Colorado School of Mines in partial fulfillment of the requirements of Doctor of Philosophy in Chemical Engineering and Petroleum Refining.

Golden, Colorado

Date May 12, 1987

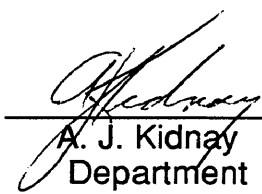
Signed   
Gregory B. Asher

Approved   
E. Dendy Sloan  
Co-Thesis Advisor

Approved   
Michael S. Graboski  
Co-Thesis Advisor

Golden, Colorado

Date 5/12/87

  
A. J. Kidnay  
Department Head  
Chemical Engineering  
and Petroleum Refining

---

## ABSTRACT

---

A computerized thermal conductivity measurement system utilizing the transient needle probe technique was developed for solids and viscous liquids. The thermal conductivity is determined by nonlinear regression of the experimental data for the needle probe, and the estimate of the conductivity is a maximum likelihood estimator. A mathematical heat transfer model is employed that accounts for the probe thermal conductivity and volumetric heat capacity. This model permits measurements at shorter experimental times compared to models that do not account for the probe properties.

Thermal conductivities of solids and liquids with waterlike viscosities are determined with an accuracy of 4%. The solids tested and their conductivities are: 1) ice,  $2.29 \text{ W}\cdot\text{m}^{-1}\cdot\text{K}^{-1}$  at 269 K, 2) tetrahydrofuran hydrate,  $0.486 \text{ W}\cdot\text{m}^{-1}\cdot\text{K}^{-1}$  at 273 K, and 3) tertiary butyl alcohol,  $0.122 \text{ W}\cdot\text{m}^{-1}\cdot\text{K}^{-1}$  at 293 K. The liquids tested and their conductivities at 298 K are: 1) water,  $0.623 \text{ W}\cdot\text{m}^{-1}\cdot\text{K}^{-1}$ , 2) glycerin,  $0.292 \text{ W}\cdot\text{m}^{-1}\cdot\text{K}^{-1}$ , 3) 1-methylnaphthalene,  $0.135 \text{ W}\cdot\text{m}^{-1}\cdot\text{K}^{-1}$ , and 4) tertiary butyl alcohol,  $0.110 \text{ W}\cdot\text{m}^{-1}\cdot\text{K}^{-1}$ . The water measurements demonstrate that this system is also capable of measuring the conductivity of electrolytes.

In an application of this system the thermal conductivity of methane hydrate, Structure I, in Ottawa Sands was determined to be  $2.75 \text{ W}\cdot\text{m}^{-1}\cdot\text{K}^{-1}$  at 275 K. This study showed that the thermal conductivity of the hydrate reservoir does not depend on the structure, Structure I or Structure II, of the in situ hydrates.

T-3335

*In Memory of My Father*

***RICHARD ALFRED ASHER***

***1937-1985***

---

## TABLE OF CONTENTS

ITEM	PAGE
ABSTRACT.....	iii
DEDICATION.....	iv
TABLE OF CONTENTS.....	v
LIST OF FIGURES.....	ix
LIST OF TABLES.....	xi
NOMENCLATURE.....	xii
ACKNOWLEDGEMENTS.....	xv

---

### CHAPTER 1 INTRODUCTION

---

1.0 INTRODUCTION.....	2
1.1 LITERATURE REVIEW.....	7
1.1.1 THERMAL CONDUCTIVITY NEEDLE PROBE REVIEW.....	7
1.1.2 HYDRATES AND THERMAL CONDUCTIVITY REVIEW.....	11

---

### CHAPTER 2 MATHEMATICAL MODELS FOR THE NEEDLE PROBE

---

2.0 INTRODUCTION.....	15
2.1 PROBE FACTORS AND EFFECTS.....	18
2.1.1 PROBE FINITE HEAT CAPACITY.....	20
2.1.2 PROBE FINITE THERMAL CONDUCTIVITY.....	25
2.1.3 PROBE FINITE LENGTH.....	32
2.2 SAMPLE FACTORS AND EFFECTS.....	36
2.2.1 SAMPLE FINITE SIZE.....	36
2.2.2 SAMPLE TEMPERATURE DEPENDENCY.....	39
2.2.3 INDUCED CONVECTION IN LIQUIDS.....	39
2.2.4 THERMAL CONTACT.....	40
2.4 CONCLUSION.....	43

---

---

 CHAPTER 3

**ALGORITHMS FOR DATA ACQUISITION AND ANALYSIS**


---

3.0 INTRODUCTION.....	45
3.1 DATA ACQUISITION ALGORITHM.....	48
3.2 DATA ANALYSIS ALGORITHM BASIS.....	51
3.2.1 OPTIMUM SOLUTION REGION.....	53
3.2.2 REGRESSION AND LAGRANGE MULTIPLIERS.....	57
3.3 ALGORITHMS FOR UNKNOWN SAMPLE PROPERTIES.....	60
3.3.1 LONG TIME SOLUTION FOR SAMPLE.....	60
3.3.2 SHORT TIME SOLUTION FOR SAMPLE.....	63
3.4 ALGORITHM FOR UNKNOWN PROBE PROPERTIES.....	66
3.5 CONCLUSION.....	69

---



---

 CHAPTER 4

**THERMAL CONDUCTIVITY MEASUREMENT SYSTEM**


---

4.0 INTRODUCTION.....	71
4.1 SYSTEM HARDWARE SPECIFICATIONS.....	72
4.1.1 THERMAL CONDUCTIVITY NEEDLE PROBE.....	72
4.1.2 PERSONAL COMPUTER AND INTERFACING.....	76
4.2 SYSTEM HARDWARE INSTALLATION.....	79
4.3 SYSTEM SOFTWARE.....	82
4.4 CONCLUSION.....	86

---



---

 CHAPTER 5

**SYSTEM VERIFICATION ON SOLIDS AND LIQUIDS**


---

5.0 INTRODUCTION.....	88
5.1 THERMAL CONDUCTIVITY SYSTEM CALIBRATION.....	90
5.1.1 COMPUTER AND INTERFACING CALIBRATION.....	90
5.1.2 PROBE THERMISTOR CALIBRATION.....	91
5.2 INITIAL MEASUREMENTS ON SOLIDS.....	94
5.2.1 SOLID TERTIARY BUTYL ALCOHOL.....	94
5.2.2 TETRAHYDROFURAN HYDRATE.....	98
5.2.3 WATER ICE.....	98

5.3 INITIAL MEASUREMENTS ON LIQUIDS.....	101
5.3.1 LIQUID TERTIARY BUTYL ALCOHOL.....	101
5.3.2 LIQUID 1 - METHYLNAPHTHALENE.....	106
5.3.3 LIQUID GLYCERIN.....	106
5.4 MEASUREMENT OF PROBE PROPERTIES.....	108
5.5 MEASUREMENTS WITH SOLUTION ANALYSIS.....	111
5.5.1 LIQUID WATER.....	114
5.5.2 LIQUID TOLUENE.....	114
5.6 SELECTION OF THE LONG OR SHORT TIME SOLUTION.....	119
5.7 CONCLUSION.....	122

---

---

**CHAPTER 6**  
**AN APPLICATION TO HYDRATES IN POROUS MEDIA**

---

6.0 INTRODUCTION.....	125
6.1 EFFECTIVE THERMAL CONDUCTIVITY.....	126
6.1.1 THE CONTINUOUS PHASE.....	127
6.1.2 THE DISCONTINUOUS PHASE.....	128
6.2 HYDRATE FORMATION AROUND PROBE.....	129
6.3 MEASUREMENTS ON HYDRATES IN SEDIMENTS.....	132
6.4 CONCLUSION.....	139

---

---

**CHAPTER 7**  
**CONCLUSIONS AND RECOMMENDATIONS**

---

7.0 CONCLUSIONS.....	141
7.1 RECOMMENDATIONS.....	143

---

---

<b>REFERENCES.....</b>	<b>144</b>
------------------------	------------

---



---

APPENDIX A  
**MATHEMATICAL MODELING ADDENDUM**

---

A.1 FINITE CONDUCTOR MODEL EXPANSION.....	149
A.2 TERMS FOR SHORT TIME DATA ANALYSIS.....	153
A.2.1 TERMS FOR UNKNOWN SAMPLE.....	153
A.2.2 TERMS FOR UNKNOWN PROBE.....	156

---

---

APPENDIX B  
**THERMAL CONDUCTIVITY SYSTEM SOFTWARE MANUAL**

---

B.0 INTRODUCTION.....	155
B.1 LOG IN AND OPERATING PROCEDURES.....	156
B.2 PROGRAM CODE.....	175

---

---

## LIST OF FIGURES

TITLE	PAGE
1.1 Application of the Thermal Conductivity Needle Probe.....	4
1.2 Structures of Hydrates (Clathrate Inclusion Compounds).....	12
2.1 Needle Probe: Radial Heat Conduction Between Concentric Cylinders..	16
2.2 Probe Finite Heat Capacity Variation of Temperature with Time.....	23
2.3 Probe Finite Heat Capacity Effect on Long Time Solution.....	24
2.4 Inner Probe Temperature Profiles.....	28
2.5 Probe Centerline Temperature Dependence on $\beta$ and $\omega$ .....	30
2.6 Probe Finite Thermal Conductivity Effect on Long Time Solution.....	31
2.7 Theoretical Probe Response versus Time for Tetrahydrofuran Hydrate...	35
2.8 Thermal Wave Penetration into the Surrounding Medium.....	38
2.9 Thermal Contact Resistance Effect on Long Time Solution.....	42
3.1 Typical Experimental Responses for the Needle Probe.....	46
3.2 Comparison of Curve Fitting for Various Degrees of Accuracy.....	50
3.3 Acquisition and Analysis on 1-Methylnaphthalene.....	56
4.1 Thermal Conductivity System Hardware.....	72
4.2 Schematic for Precision D.C. Power Amplifier.....	78
4.3 Switcher Installation Diagram.....	81
4.4 Thermal Conductivity System Software Installation Requirements.....	84
4.5 Thermal Conductivity System Program Flow Diagram.....	85
5.1 Thermistor Resistance and Residuals for the Needle Probe TCP111.....	93
5.2 Experimental Response Behavior of Various Solids.....	96
5.3 Acquisition and Analysis on Solid Tertiary Butyl Alcohol.....	97
5.4 Acquisition and Analysis on Tetrahydrofuran Hydrate.....	99
5.5 Acquisition and Analysis on Water Ice.....	100
5.6 Experimental Response Behavior of Various Liquids.....	103
5.7 Acquisition and Analysis on Liquid Tertiary Butyl Alcohol.....	104
5.8 Acquisition and Analysis on Liquid Glycerin.....	107
6.1 Schematic of the Hydrate Formation Cell.....	130
6.2 Thermal Conductivities of Water, Ice, Methane Gas, and Methane Hydrate in Ottawa Sand .....	133
6.3 Summary of Hydrate Measurements in Sediments .....	137

B.1	Menu Bar, Menu List, and System Control Guidelines.....	161
B.2	Dialog Box Guidelines.....	162
B.3	Data Editor Guidelines.....	163
B.4	Graph Editor Guidelines.....	164
B.5	Thermal Conductivity System Log In Procedure.....	165
B.6	Operating Procedure 1.....	166
B.7	Operating Procedure 2.....	167
B.8	Operating Procedure 3.....	168
B.9	Operating Procedure 4.....	169
B.10	Operating Procedure 5.....	170
B.11	Operating Procedure 6.....	171
B.12	Operating Procedure 7.....	172
B.13	Operating Procedure 8.....	173
B.14	Operating Procedure 9.....	174
B.15	Operating Procedure 10.....	175
B.16	Operating Procedure 11.....	176
B.17	Operating Procedure 12.....	177

---

---

## LIST OF TABLES

TITLE	PAGE
2.1 Needle Probe Experimental Factors and Effects.....	16
3.1 Method of Data Analysis Reported in Literature and This Work.....	47
3.2 Transient Needle Probe Model Equation.....	52
4.1 Developmental and Required Thermal Conductivity System Hardware..	74
5.1 Measured Thermal Conductivities of Various Solids.....	95
5.2 Measured Thermal Conductivities of Various Liquids.....	102
5.3 Thermal Conductivity Measurements on 1-Methylnaphthalene.....	112
5.4 Solution Analysis for Measurements on Liquid 1-Methylnaphthalene...	113
5.5 Thermal Conductivity Measurements on Liquid Water.....	115
5.6 Solution Analysis for Measurements on Liquid Water.....	116
5.7 Thermal Conductivity Measurements on Liquid Toluene.....	117
5.8 Solution Analysis for Measurements on Liquid Toluene.....	118
5.9 Summary of Thermal Conductivity Measurements.....	123
B.1 Summary of the Operating Procedures.....	165

---

---

## NOMENCLATURE

---



---

### ENGLISH DESCRIPTION

---

a	Radius of the probe.
$b_i$	Estimates of the equation parameters $\beta_i$ .
c	Radial thickness of the contact resistance layer.
C	$\exp(\gamma) = 1.7811\dots$ , the exponential of Euler's constant.
F	Function to minimize in linear regression.
g	Acceleration of gravity.
$g_i, G_i$	Constraining equations.
H	Thermal contact resistance coefficient.
$J_0(\cdot)$	Bessel function of the first kind, zero order.
$J_1(\cdot)$	Bessel function of the first kind, first order.
k	Thermal conductivity of the sample.
$k_1$	Thermal conductivity of the probe.
$k_c$	Thermal conductivity of the contact resistance layer.
L	Probe length.
$L^*$	$L / a$ , ratio of probe length to probe radius.
m	Total number of experiments performed.
M	Number of multiple experiment thermal conductivities used in determining an average thermal conductivity.
n	Number of data points for linear regression, a subset of N.
N	Total number of time increments in an experiment.
Q	Step power supplied per unit probe length.
r	Radial distance.
$R_{p,i}$	$p = 1, 2, \dots$ , time dependent error term for $i^{\text{th}}$ experimental point.
s	Arithmetic average of all sample standard deviations.
$s_i$	Sample standard deviation for the $i^{\text{th}}$ time increment.

$s_k$	Standard deviation for an set of apparent thermal conductivities.
$s^2(b_i)$	Estimate of the variance of the parameter $\beta_i$ .
$t$	Time elapsed since Q began and time for onset of convection.
$t_i$	Time at $i^{\text{th}}$ time increment in an experiment.
$T$	Temperature rise at the probe and medium interface.
$T_1$	Temperature rise of the probe at a given position.
$T_{j,i}$	Temperature rise for the $j^{\text{th}}$ experiment, $i^{\text{th}}$ time increment.
$\bar{T}_i$	Average temperature rise for $j$ experiments, $i^{\text{th}}$ time increment.
$u_{p,i}$	$p = 1, 2, \dots$ , error term for linear regression for $i^{\text{th}}$ experimental point.
$Y_0(\cdot)$	Bessel function of the second kind, zero order.
$Y_1(\cdot)$	Bessel function of the second kind, first order.
$z$	Confidence interval multiplier.

---

## GROUPED DESCRIPTION

---

$\Delta k$	Confidence in the apparent thermal conductivity measurement.
$\Delta t$	Constant time interval for temperature measurement.
$N\Delta t$	Time length of the experiment.
$(\rho C_p)$	Volumetric heat capacity of the sample.
$(\rho C_p)_1$	Volumetric heat capacity of the probe.

---

---

**GREEK      DESCRIPTION**


---

$\alpha$	Thermal diffusivity of the medium.
$\beta$	$k / k_1$ , the ratio of the sample to probe thermal conductivity.
$\beta_c$	$k / k_c$ , the ratio of the sample to contact resistance layer thermal conductivity.
$\beta^*$	Volume expansivity of the liquid.
$\beta_i$	$i = 1, 2, 3, 4, 5, 6, \dots$ , equation parameters.
$\gamma$	0.5772..., Euler's constant.
$\epsilon_i$	Random measurement error for the $i^{\text{th}}$ experimental point.
$\lambda$	Lagrangian multipliers.
$\mu$	Viscosity of the liquid.
$\mu_i$	Actual temperature for the $i^{\text{th}}$ time increment.
$\pi$	3.14159265...
$\sigma$	Population standard deviation of the temperature measurement (assumed independent of the time increment).
$\Phi_k$	Set of equations that minimize F.
$\chi$	$(\alpha_1 / \alpha)^{-1/2}$ .
$\omega$	$2 (\rho C_p) / (\rho C_p)_1$ , twice the ratio of the sample to probe volumetric heat capacity.

---

---

## ACKNOWLEDGEMENTS

---

The author is grateful for the financial support of this work from the following sources: 1) Standard Oil of Ohio, Warrensville, Ohio, 2) Mining and Mineral Institute Fellowship, and 3) Department of Energy, Morgantown, Contract DE-FG21-86MC23063.

The author thanks Professor and co-advisor E. Dendy Sloan for his efforts in the initial development of the project and for acquiring the financial support, and thanks former Professor and co-advisor Michael Graboski for his insight in times of difficulty. Also, the committee members for their time and effort in assuring the quality of this work: Professors Bill Astle, Paul Bryan, Greg Holden, and Sami Selim.

The author also wishes to thank those who recommended ways to make this work's equipment better. Bruce Weiler, contact at Standard of Ohio and former Mines student, duplicated the equipment and was the first to use and test the equipment after primary development. Hamid Ouar formed all methane hydrates tested in this work and provided objective, constructive criticism for the use of the apparatus in hydrate measurements. The late Mark Bourrie provided valuable comments during the developmental stages of the software. Mark was a special friend and is sincerely missed.

Last, but not least, a special thanks for the spiritual support of: mother and step-father, Ruth Ann and Gordon Smith; sister and niece, Tami and Tania Vendetti.



CHAPTER 1

**INTRODUCTION**

---

## 1.0 INTRODUCTION

---

Thermal conductivity is an industrially important physical property. Data on the conductivities of many substances are scarce. Few means exist to readily determine this physical property. An instrument capable of automatically measuring unknown thermal conductivities would have widespread appeal.

Experimental determination of thermal conductivities was conducted and is documented herein. The study is composed of three phases. These are:

- 1) Development of a computerized thermal conductivity measurement system utilizing the transient needle probe technique,
- 2) Verification of the operation of the thermal conductivity system by testing various solids and liquids, and
- 3) Measurement of the unknown thermal conductivities of methane hydrates in porous media.

The first phase is a study of the mathematical models for the needle probe, the development of an algorithm for data acquisition and analysis, and the design of the thermal conductivity measurement system (details presented sequentially in Chapters 2, 3, and 4). Materials selected for the study in the second phase are those with well known conductivities, while the third phase consists of measuring materials of undocumented thermal conductivities (details for both phases are presented in Chapter 5).

The basic needle probe consists of a wire loop for heating and a thermistor for temperature measurement, both of which are mounted inside a small hypodermic needle (Figure 1.1). The basic concept of the needle probe operation is as follows:

- 1) The probe is initially inserted into the sample.
- 2) Thermal equilibrium is obtained between the probe and sample.
- 3) At time zero a step power input is supplied to the probe.
- 4) The temperature rise of the probe is monitored with respect to time.

Time requirements for the measurement of solids or liquids are generally on the order of minutes or seconds, respectively.

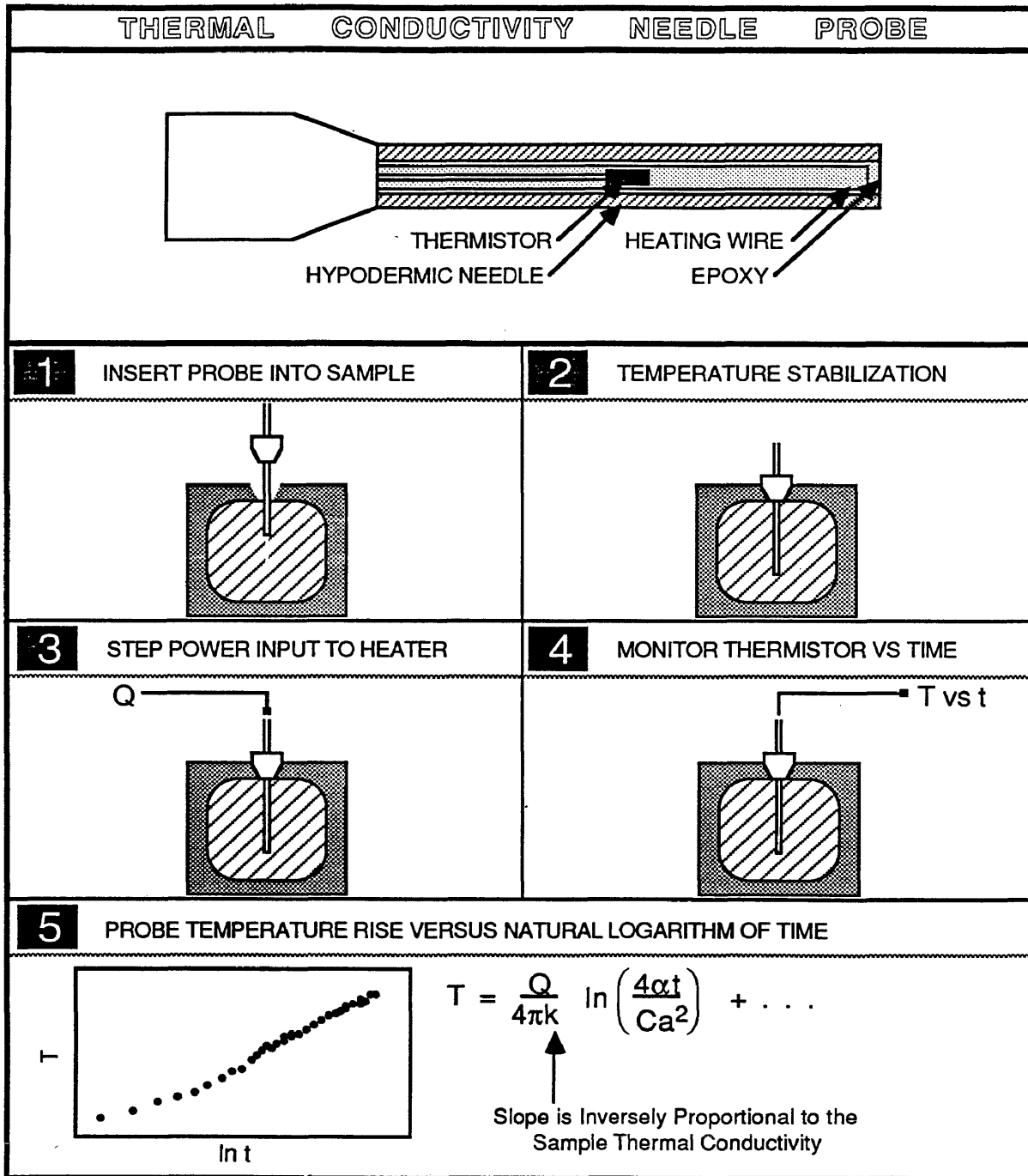
- 5) A linear plot of probe temperature rise versus the natural logarithm of time, yields a slope which is inversely proportional to the sample thermal conductivity.

Figure 1.1 demonstrates the application of the thermal conductivity needle probe.  $T$ , in this figure, refers to the probe temperature minus the initial temperature of the probe. In any needle probe experiment only three operating parameters are necessary. These parameters are:

- $Q$ , Time zero step power input supplied to the probe heater wire,
- $\Delta t$ , Constant time interval for temperature measurement, and
- $N\Delta t$ , Time length of the experiment.

Figure 1.1

Application of the Thermal Conductivity Needle Probe



The work presented herein advances the state of the art in needle probe experimentation in several ways. These are:

- 1) Experimental data analysis is done in a mathematical model which employs the probe thermal conductivity and volumetric heat capacity.
- 2) The needle probe can determine thermal conductivities for liquids, including electrolytes, with waterlike viscosities.
- 3) A system has been generated which automatically measures absolute thermal conductivities. Detailed knowledge of the transport phenomena involved is not required. Successful conductivity measurements require only knowledge of the system software. All aspects of the experimental procedure are computerized.

Estimates of natural gas existing in situ hydrated form, range between 5 and 12,000 percent of the proven United States gas reserves (Zielinski and McIver, 1982). Selim and Sloan (1985) are investigating the feasibility of utilizing these reserves as a natural gas resource. The application to hydrates presented herein is valuable for several reasons. Two of these are:

- 1) Predictive studies of the production rates from these reservoirs require hydrate thermal conductivities. This work contributes to the thermal conductivity data base of methane hydrates, which contains no published measurements.
- 2) The work proves the versatility and usefulness of the thermal conductivity measurement system.

Several goals were selected for this work so the system would have industrial appeal. First, all components have off-the-shelf availability and are relatively inexpensive. Second, the resulting apparatus has an operating system that requires minimal skill to operate. Last, the accuracy of this system is desired to be better than five percent for the measured thermal conductivity.

The material in this text is presented in the following order:

- 1) Literature Review
- 2) Mathematical Models for the Needle Probe
- 3) Algorithm for Data Acquisition and Analysis
- 4) Thermal Conductivity Measurement System
- 5) System Verification on Solids and Liquids
- 6) Application to Hydrates in Porous Media
- 7) Conclusions and Recommendations

Each of these subjects is a chapter in itself and builds upon the material presented in the previous chapters.

---

## 1.1 LITERATURE REVIEW

---

First a literature review is presented on the needle probe, and then a review is presented on hydrates and thermal conductivity. The current research helps to extend the knowledge base on thermal conductivity probes.

### 1.1.1 THERMAL CONDUCTIVITY NEEDLE PROBE REVIEW

Since its primary introduction by Von Herzen and Maxwell (1959) the thermal conductivity needle probe has been widely used for solids and saturated sediments. Most experimental applications employed either of two methods of data acquisition: the output of data to a strip-chart recorder, or to a digital voltmeter interfaced to a cassette recorder. Bloomer and Ward (1979) put their probe under microprocessor control, but their application was limited to sedimentary rock.

Analyzing the experimental data for thermal conductivity predictions is a cumbersome task. The methods of data analysis reported in the literature predicted the conductivity providing that the probe was calibrated on a known material of similar properties to the test material. Basic data analysis used for determining thermal conductivity for the needle probes is presented in Carslaw and Jaeger (1959). The equation used is:

$$T = (Q/4\pi k) \ln(4\alpha t/Ca^2) \quad (1.1)$$

Where the variables are defined as follows:

a = radius of the probe,

$C = \exp(\gamma) = 1.7811\dots$ , the exponential of Euler's constant,

$k$  = thermal conductivity of the medium,

$Q$  = step power supplied per unit probe length,

$t$  = time elapsed since  $Q$  began,

$T$  = temperature rise at the probe and medium interface,

$\alpha$  = thermal diffusivity of the medium, and

$\pi = 3.14159265\dots$

Past investigators (listed in the next paragraph) determined deviations from this model by: 1) conducting a calibration experiment on a material of known properties,  $(Q/4\pi k)$ , 2) obtaining the slope of the semilogarithmic plot of temperature rise versus time for this experiment,  $(Q/4\pi k)^*$ , 3) conducting an experiment on an unknown and determining the slope,  $(Q/4\pi k)_U$ , 4) adjusting the slope of the unknown by the correction factor of the from the calibration experiment,  $(Q/4\pi k)_U^* = (Q/4\pi k)_U * (Q/4\pi k)^* / (Q/4\pi k)$ , and then 5) determining the best estimate of the conductivity from  $(Q/4\pi k)_U^*$ .

Perhaps the most oft cited probe is that of Von Herzen and Maxwell (1959). Their probe used the basic needle probe design mentioned above. Von Herzen and Maxwell's probe has a diameter of 0.086 centimeters (0.034 inches) and a length to diameter ratio of 74.4. Length to diameter ratios ranging from 20 to 100 are common for the needle probe. Other authors have used needle probes of a slightly modified configuration or exactly the same configuration as that of Von Herzen and Maxwell (1959). These authors are Woodside and Messmer (1961), Gerard, Langseth, and Ewing (1962), Von Herzen and Uyeda (1963), Nason and Lee (1964), Langseth, Grim, and Ewing



(1965), Lachenbruch and Marshall (1966), Corry, Dubois, and Vacquier (1968), Mitchell, ASCE, and Kao (1978), Bloomer and Ward (1979), and Stoll and Bryan (1979).

Several factors are important in probe construction. These are:

- Probe thermistor placement,
- Placement and control of the heating element, and
- Probe length to diameter ratio.

The probe thermistor placement is such that it maximizes the fit to the simplified model, Equation 1.1. To properly fit this heat transfer model the probe should be isothermal and infinite in extent, but in reality this is never the case. According to the model derivation by Carslaw and Jaeger (1959), the temperature should be measured at the probe and medium interface. Due to the mechanical design of the needle probe, the temperature is measured at the centerline of the probe, which is not at the same temperature as the interface. Since the probe is finite in length the thermistor is typically located at probe midlength. This minimizes the axial end effects, which is necessary because these effects are not included in the model.

Heater placement and control are also such that the fit to the simplified model is maximized. The model assumes that the heat generation is uniform within the probe. For the small scale of the needle probe, uniform heat generation is accomplished by running the heater wire axially along the probe. Not only is the placement of the heating element important, but the stability of the power supplied to the probe heater is important. Mitchell, ASCE, and Kao

(1978) found that a one percent variation in the heater current can lead to a twenty percent variation in the measured thermal conductivity.

The length to diameter of the probe is another important factor. The probe temperature versus time response can vary strongly with the length to diameter of the probe. If the probe is too short axial effects will become significant, and the simplified model given above can no longer be used for data analysis. Blackwell (1956) developed a criterion that the probe length to diameter ratio must be greater than 20 to 30. The probes presented in the papers by the authors mentioned previously all satisfied this criteria.

Experiments are conducted after the probe has been built to maximize the fit of the simplified model. Unless the sample to be tested is formed around the probe a contact thermal resistance layer will exist. In the early portions of the experiment, contact resistance will cause severe nonlinearities in the semilogarithmic plot of temperature rise versus time (Morrow, 1979). To minimize the effect of this resistance layer several factors should be considered. These factors are: 1) the thickness of the layer should be as small as possible, 2) the mass of the layer should be small relative to that of the probe, and 3) the thermal conductivity of the layer should be large relative to that of the probe. A contact material of high conductivity can reduce the error caused by this resistance to less than one percent of the measured thermal conductivity. A low conductivity material, such as air, will add appreciable error to the measured thermal conductivity (Beck, 1965).

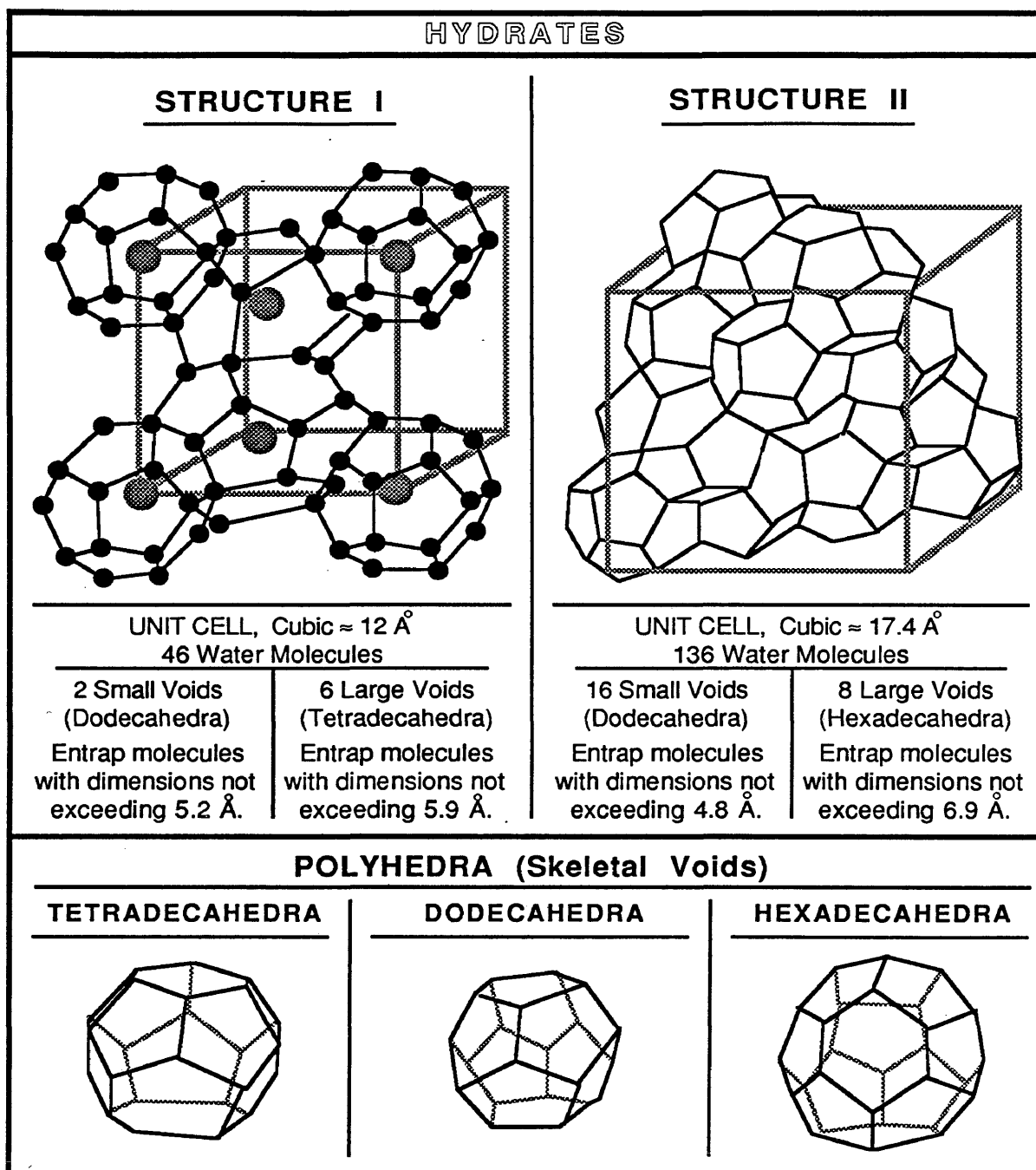
### 1.1.2 HYDRATE AND THERMAL CONDUCTIVITY REVIEW

Gas hydrates are clathrate inclusion compounds. Gas molecules are trapped as the *guest*, inside a cage of water molecules which is the *host*. Two different crystalline structures can occur, named Structure I and Structure II. Structure I or II hydrates form depending upon the composition of the gas. Propane forms Structure II hydrates while methane forms Structure I hydrates. Mixtures of methane and propane will form Structure I or Structure II hydrates depending upon the amount of propane present in the gas. The structures are diagrammed in Figure 1.2.

Tremendous quantities of natural gas exist in hydrated form. These hydrates represent a substantial natural gas resource, and currently there are researchers who are concerned with evaluating the feasibility of producing these reservoirs (Selim and Sloan, 1985). The locations of hydrate reservoirs and reservoir production modeling schemes are presented in: Katz (1971), Hitchon (1974), Makogen (1981), Goodman and Giussani (1982), Halleck (1982), Holder, Angert, John, and Yen (1982), Judge (1982), Macleod (1982), McGuire (1982), Weaver and Stewart (1982), Yamano, Uyeda, Aoki, and Shipley (1982), Holder (1983), and Pearson, Halleck, McGuire, Hermes, and Matthews (1983).

Production rates can be estimated by mathematically modeling the recovery of natural gas from a hydrate reservoir. Physical properties of hydrates are necessary for modeling hydrate dissociation, three of which are: 1) the heat capacity, 2) the heat of dissociation, and 3) the thermal conductivity.

Figure 1.2  
Structures of Hydrates (Clathrate Inclusion Compounds)



Many hydrate properties appear similar to those of water ice, while hydrate thermal conductivity is singularly different. Stoll and Bryan (1979) first determined that the thermal conductivity of propane hydrate is one-fourth to one-fifth that of ice. Recent work has verified this hydrate phenomena on ethylene oxide and tetrahydrofuran hydrates (Ross and Andersson, 1982) and Ross, Andersson, and Backstrom, 1981).

The thermal conductivity data base for hydrates is insufficient. Stoll and Bryan (1979) reported conductivity results on propane hydrates with and without sediments. Their results are questionable because they could not discern the composition of their hydrates and also because their hydrates appeared to be metastable, when considered in light of sound velocity measurements. Ross and Andersson (1982) reported work on hydrates which are not found in a naturally occurring hydrate reservoir.

In situ hydrates recovered from the Glomar Challenger leg in the Blake Bahama Ridge contain large amounts of sediment. Mid-America trench hydrates had a few percent sediment (Sloan, 1985). Proposed hydrates located in the permafrost region exist mainly in consolidated and unconsolidated sediments. The data base for hydrate thermal conductivity should contain values for methane hydrates with and without sediments; to date these data are not available.

# CHAPTER 2

## **MATHEMATICAL MODELS FOR THE NEEDLE PROBE**

---

## 2.0 INTRODUCTION

---

The intent of this chapter is to define the heat transfer models appropriate in predicting the experimental behavior of the transient needle probe. From this information, the experimental data acquisition and analysis is developed, a transient needle probe system is built, and the system operation is verified.

The goal of this heat transfer modeling is to determine the sample thermal conductivity via the transient needle probe technique. Figure 2.1 diagrams the physics of the technique. The complete model assumptions for the needle probe are given in Table 2.1. A mathematical model derived from all of these considerations is quite difficult to employ.

Instead of solving the model with the assumptions and effects presented in Table 2.1, this work employs a model with several simplifying assumptions:

- The probe has uniform physical properties.
- The probe has a finite thermal conductivity.
- The probe is infinitely long.
- The sample extends from the probe surface to infinity.
- Energy is transferred by radial conduction only.

The heat transfer model used with these constraints at long times is:

$$T = (Q/4\pi k) \ln(4\alpha t/Ca^2) + (Q/4\pi k_1) \quad (2.1)$$

Figure 2.1

## Needle Probe: Radial Heat Conduction Between Concentric Cylinders

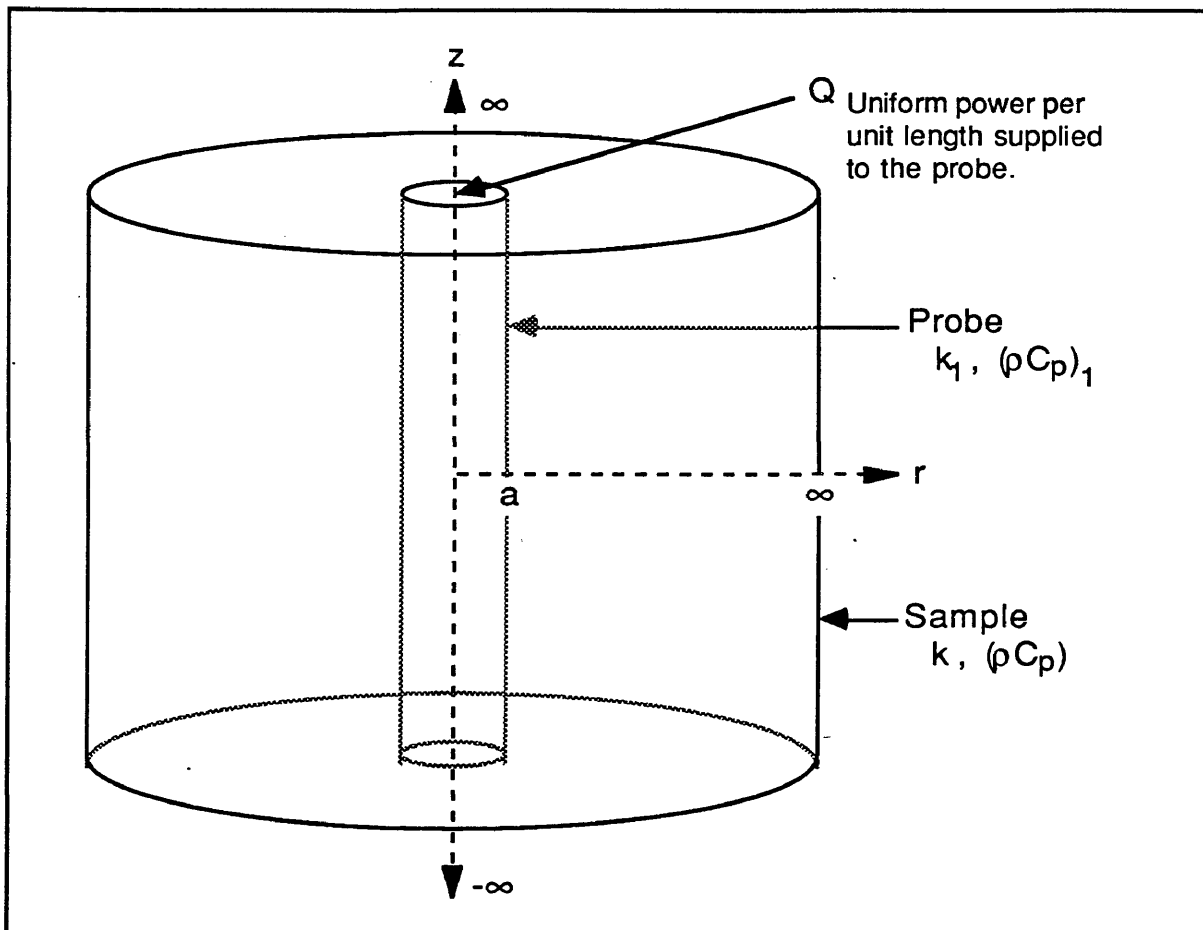




Table 2.1  
Needle Probe Experimental Factors and Effects

	FACTOR	EFFECT
PROBE	The probe has a finite heat capacity.	Heat supplied to the medium is time dependent.
	The probe has a finite thermal conductivity.	The temperature within the probe varies radially.
	The probe has a finite length and a finite diameter.	Radial and axial heat transfer coexist.
SAMPLE	The sample has a finite size.	The thermal wave emitted by the probe may penetrate through the sample.
	The sample has temperature dependent properties.	Temperature rise during experimentation is minimized.
	Convection may be induced in liquid samples.	Convective and conductive heat flow coexist.
	A probe to medium thermal contact resistance may exist.	The sample conductivity cannot be determined.

Where the variables are defined as follows:

$a$  = radius of the probe.

$C = \exp(\gamma) = 1.7811\dots$ , the exponential of Euler's constant.

$k$  = thermal conductivity of the medium.

$k_1$  = thermal conductivity of the probe.

$Q$  = step power supplied per unit probe length.

$t$  = time elapsed since  $Q$  began.

$T$  = temperature rise at the probe and medium interface.

$\alpha$  = thermal diffusivity of the medium.

$\pi = 3.14159265\dots$

A linear solution of probe temperature rise versus the natural logarithm of time, yields a slope inversely proportional to the medium thermal conductivity. The difference between this long time solution and the solution presented in Chapter 1 is imbedded in the intercept term. The major difference between this new model and the literature model is evident when long times cannot be reached.

The effects of the model assumptions compared to the factors and effects given in Table 2.1 are discussed in the remainder of this chapter. Chapter 3 presents how to use this information in designing an algorithm for data acquisition and analysis.

---

## 2.1 PROBE FACTORS AND EFFECTS

---

Several factors affect the response of the needle probe. The variables that characterize the effects are the following:

- Probe finite heat capacity; characterized by  $\omega = 2 (\rho C_p) / (\rho C_p)_1$ , twice the ratio of the sample to probe volumetric heat capacity.
- Probe finite thermal conductivity; characterized by  $\beta = k / k_1$ , the ratio of the sample to probe thermal conductivity.
- Probe finite length; characterized by  $L^* = L / a$ , the ratio of the probe length to the radius.

Due to the relationships between these three variables, it is not always possible to discuss one without the other. In the discussion of the probe heat capacity the probe is assumed infinitely conductive and infinitely long. In the discussion of the probe thermal conductivity the probe is assumed to have a finite heat capacity and infinite length. In the discussion on probe length the probe is assumed to have a finite heat capacity and thermal conductivity.

The model used for the heat capacity discussion assumes that the temperature is measured at the probe surface. If the probe is a perfect conductor, then the temperature is identical at all points within the probe. If the probe has a finite conductance, then a temperature profile will exist within the probe. Depending on the conductance of the probe, the centerline temperature may be significantly higher than the surface temperature. It is important to consider the temperature profiles within the probe.

### **2.1.1 PROBE FINITE HEAT CAPACITY**

The probe finite volumetric heat capacity will cause the power supplied to the medium to vary with time, depending on the magnitude of the ratio of the medium volumetric heat capacity to the probe volumetric heat capacity. Only the power supplied to the heater wire remains constant with time.

A model is necessary that accounts for the time variation of the power supplied to the sample, namely the model used by researchers in the past. The assumptions of this model are:

- The probe has uniform physical properties.
- The probe is infinitely long.
- The probe is infinitely conductive.
- The sample is infinite in extent.
- Energy is transferred only by radial conduction.

This model is referred to as the perfect conductor model in the text.

Laplace's equation and the appropriate boundary conditions for this model are:

$$\frac{\partial T}{\partial t} = \frac{\alpha}{r} \frac{\partial}{\partial r} \left( r \frac{\partial T}{\partial r} \right) \quad ; \quad t \geq 0, \quad a \leq r < \infty \quad (2.2)$$

Initial Condition,  
 $T = 0$

@  $t = 0, \quad 0 < r < \infty$

Boundary Conditions,

$$Q = \pi a^2 (\rho C_p)_1 \frac{\partial T}{\partial t} - (2\pi a) k \frac{\partial T}{\partial r}$$

@  $t > 0, \quad r = a$

$$T = 0$$

@  $t > 0, \quad r \rightarrow \infty$

The complete solution for the temperature at the probe and medium interface is (Carslaw and Jaeger, 1959):

$$T = \frac{2Q}{k\pi^3} \int_0^{\infty} \frac{(1 - e^{-\alpha t u^2/a^2})}{u^3 \{ \phi^2(u) + \psi^2(u) \}} du \quad (2.3)$$

Where,

$$\phi(u) = \frac{u}{\omega} J_0(u) - J_1(u)$$

$$\psi(u) = \frac{u}{\omega} Y_0(u) - Y_1(u)$$

$J_0(u)$  and  $J_1(u)$  are Bessel functions of the first kind, and

$Y_0(u)$  and  $Y_1(u)$  are Bessel functions of the second kind.

A solution at short times for this equation is (Carslaw and Jaeger, 1959):

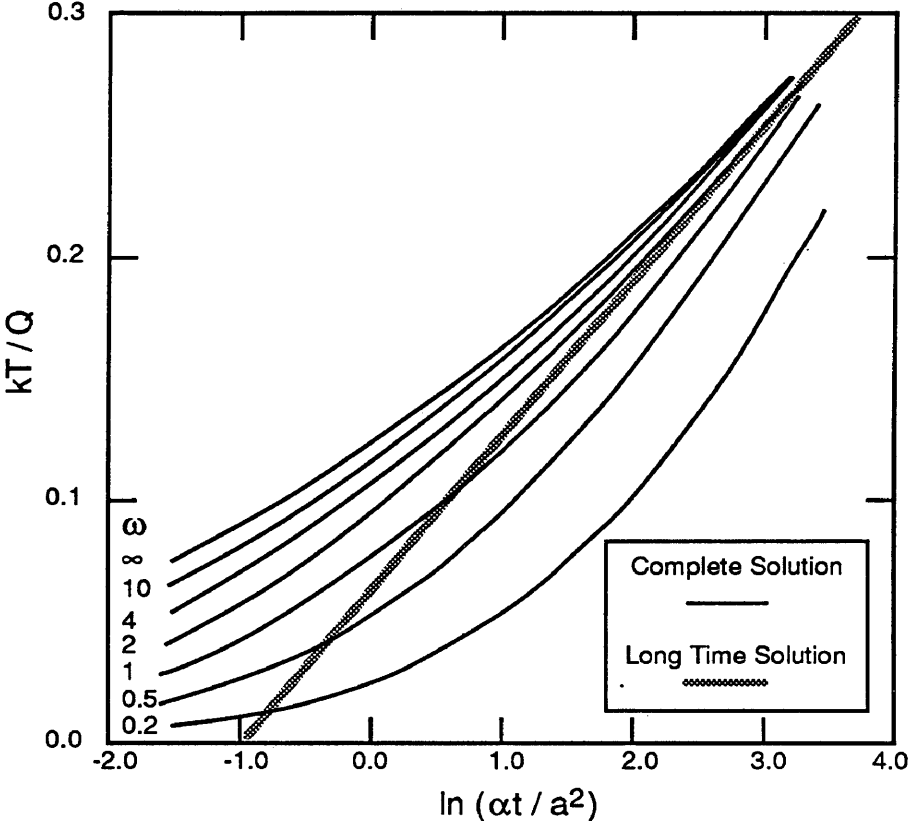
$$T = \frac{Q}{4\pi k} \left[ \ln \left( \frac{4\alpha t}{Ca^2} \right) + \left\{ 1 + \frac{\omega - 2}{\omega} \ln \left( \frac{4\alpha t}{Ca^2} \right) \right\} \frac{a^2}{2\alpha t} \right] \quad (2.4)$$

The ratio of the medium to probe volumetric heat capacities,  $\omega$ , controls the time required to reach the long time solution. Depending upon  $\omega$ , various degrees of curvature are exhibited in the early time portion of the semilogarithmic plot of temperature rise versus time. This effect is shown in Figure 2.2 (based on Jaeger,1958). In this figure,  $\omega = \infty$  corresponds to zero probe heat capacity, and as  $\omega$  decreases either the medium heat capacity decreases or the probe heat capacity increases.

As will be shown in the probe finite length discussion, the long time solution will not necessarily be valid. For these times the probe heat capacity must be known to determine the best estimate of the medium thermal conductivity. Figure 2.3 demonstrates how the measured thermal conductivity can vary when the heat capacity effect is not taken into account. The vertical axis of this graph is the ratio of the measured thermal conductivity using the long time solution (Equation 2.1 with  $k_1 = \infty$ ) to the measured thermal conductivity using the short time solution (Equation 2.4). In the experiments performed in this project,  $\omega$  is greater than 0.5 and less than 4.0. For this range of heat capacity ratios, this figure shows that the corrections to the measured thermal conductivity are less than  $\pm 10\%$  at  $\ln(\alpha t / a^2) > 4$ .

Figure 2.2

Probe Finite Heat Capacity Variation of Temperature with Time







## 2.1.2 PROBE FINITE THERMAL CONDUCTIVITY

The probe finite thermal conductivity will cause the temperature to vary radially within the probe depending on the magnitude of the ratio of the medium thermal conductivity to the probe thermal conductivity. During experimentation the temperature rise of the probe is measured at midlength of the centerline of the probe.

A model is necessary that accounts for the radial variation of the probe temperature. The model used for this discussion is the model presented by researchers in the past and employed in this work. To reiterate, the assumptions of this model are:

- The probe has uniform physical properties,
- The probe is infinitely long,
- The probe has a finite conductivity,
- The sample is infinite in extent, and
- Energy is transferred only by radial conduction.

This model, termed the finite conductor model, should reduce to the perfect conductor model as the conductivity ratio tends to zero.

Laplace's equation and the appropriate boundary conditions for this model are:

$$\frac{\partial T}{\partial t} = \frac{\alpha}{r} \frac{\partial}{\partial r} \left( r \frac{\partial T}{\partial r} \right) \quad ; \quad t \geq 0, \quad a \leq r < \infty \quad (2.5)$$

$$\frac{\partial T_1}{\partial t} = \frac{\alpha_1}{r} \frac{\partial}{\partial r} \left( r \frac{\partial T_1}{\partial r} \right) + \frac{Q}{(\rho C_p)_1 \pi a^2} \quad ; \quad t \geq 0, \quad 0 \leq r \leq a$$

Initial Condition,

$$T = 0$$

$$@ \quad t = 0, \quad 0 < r < \infty$$

Boundary Conditions,

$$T_1 \text{ is finite}$$

$$@ \quad t > 0, \quad r = 0$$

$$T = T_1$$

$$@ \quad t > 0, \quad r = a$$

$$-k \frac{\partial T}{\partial r} = -k_1 \frac{\partial T_1}{\partial r}$$

$$@ \quad t > 0, \quad r = a$$

$$T = 0$$

$$@ \quad t > 0, \quad r \rightarrow \infty$$

The complete solution for the temperature within the probe is (Carslaw and Jaeger, 1959):

$$T_1 = \frac{4Q}{k\pi^3} \int_0^{\infty} \frac{(1 - e^{-\chi^2 \alpha t u^2 / a^2})}{u^4 \{ \phi^2(u) + \psi^2(u) \}} f(u) du \quad (2.6)$$

Where:

$$\phi(u) = \frac{1}{\beta} J_1(u) J_0(\chi u) - \chi J_0(u) J_1(\chi u)$$

$$\psi(u) = \frac{1}{\beta} J_1(u) Y_0(\chi u) - \chi J_0(u) Y_1(\chi u)$$

$$f(u) = J_0(ru/a) J_1(u)$$

$$\chi = \sqrt{\alpha_1 / \alpha} = \sqrt{\omega / 2\beta}$$

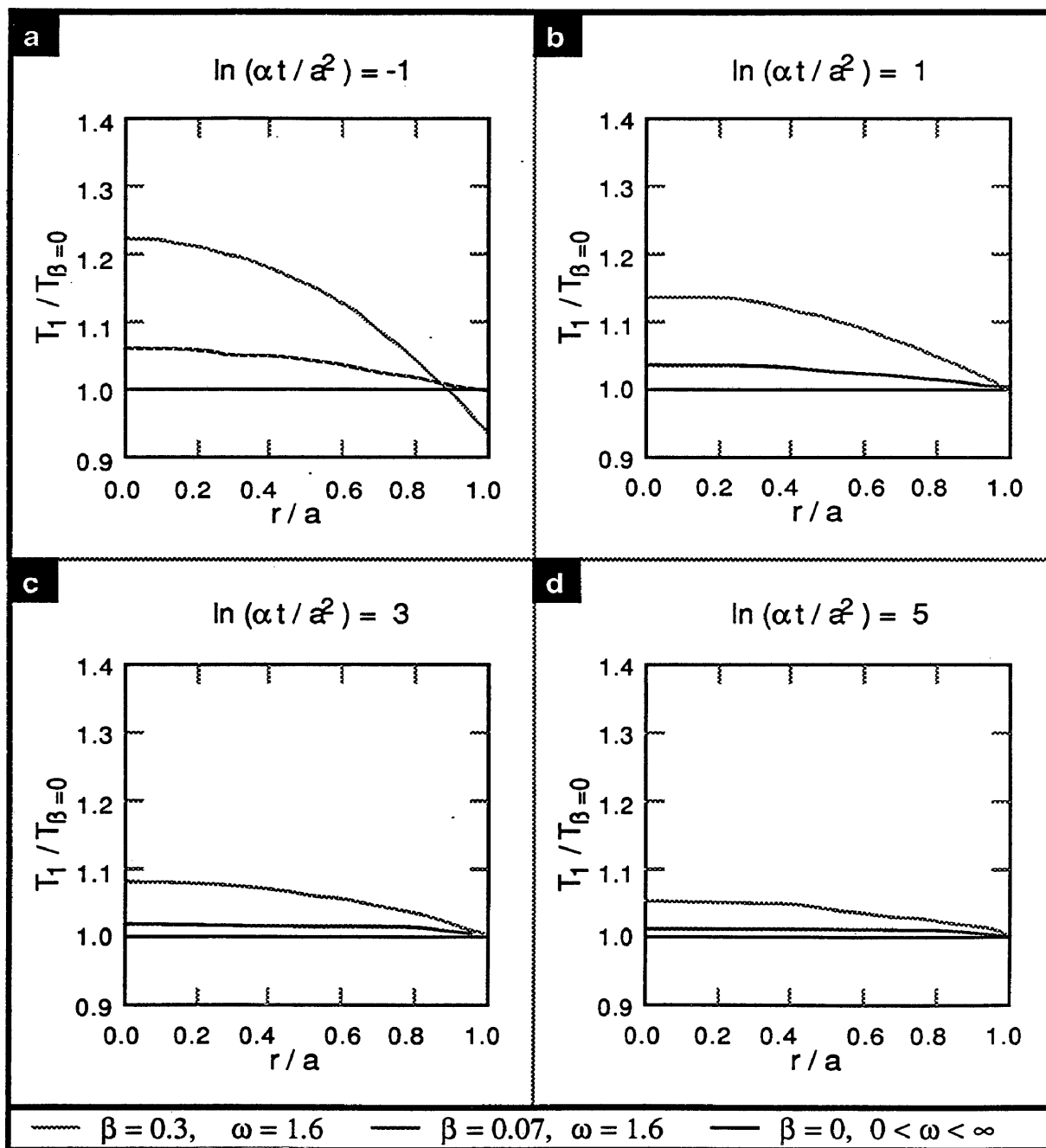
The solution for suitably short times has been solved by the author (derivation given in Appendix A) as:

$$\begin{aligned}
 T_1 = & \frac{Q}{4\pi k} \left[ \ln \left( \frac{4\alpha t}{Ca^2} \right) + \left\{ 1 + \frac{\omega - 2}{\omega} \ln \left( \frac{4\alpha t}{Ca^2} \right) \right\} \frac{a^2}{2\alpha t} \right. \\
 & + \left\{ \left( \frac{3}{8} - \frac{2}{\omega} + \frac{\pi^2}{8} \left( \frac{\omega - 2}{\omega} \right)^2 \right) + \left( \frac{-7}{4} + \frac{4}{\omega} + \frac{3}{2} \left( \frac{\omega - 2}{\omega} \right)^2 \right) \ln \left( \frac{4\alpha t}{Ca^2} \right) \right. \\
 & \left. \left. - \frac{3}{4} \left( \frac{\omega - 2}{\omega} \right)^2 \ln^2 \left( \frac{4\alpha t}{Ca^2} \right) \right\} \left( \frac{a^2}{2\alpha t} \right)^2 \right] \\
 & + \frac{Q}{4\pi k_1} \left[ (1 - (r/a)^2) - \left( \frac{1}{2} + (1 - (r/a)^2) \right) \frac{1}{\omega} \frac{a^2}{2\alpha t} \right. \\
 & + \left\{ 2 + 2(1 - (r/a)^2) + \beta \left( \frac{1}{3} - \frac{3}{2}(1 - (r/a)^2) + \frac{1}{4}(1 - (r/a)^4) \right) \right. \\
 & \left. \left. + \left( 2 - \frac{\omega}{2} - (\omega - 2)(1 - (r/a)^2) \right) \ln \left( \frac{4\alpha t}{Ca^2} \right) \right\} \left( \frac{1}{\omega} \frac{a^2}{2\alpha t} \right)^2 \right]
 \end{aligned} \tag{2.7}$$

At long times at the probe center this equation reduces to Equation 2.1.

It is important to model the temperature profiles within the probe, since the thermistor measures the temperature within the probe. Temperature profiles for various experimental approximations of the thermal conductivity ratio,  $\beta$ , and heat capacity ratio are presented in Figure 2.4. In this figure,  $T_1$  is the temperature within the probe (Equation 2.6), and  $T_{\beta=0}$  is the temperature of a perfect conductor probe (Equation 2.3). Plots are given at various levels of dimensionless time corresponding to actual times experimentally encountered.

Figure 2.4  
Inner Probe Temperature Profiles



From Figure 2.4 it is apparent that gross errors can occur when using the perfect conductor model to represent the centerline temperature of a probe of finite conductance. The temperature profiles are relatively flat near the probe centerline, and insignificant error is introduced by assuming that the thermistor measures the temperature at probe centerline.

A more extensive representation of the effect of varying  $\beta$  and  $\omega$  is presented in Figure 2.5. In this figure,  $T_{1,r=0}$  is the temperature at the centerline of a finite conductor probe (Equation 2.6), and  $T_{\beta=0}$  is the temperature of a perfect conductor probe (Equation 2.3). Plots are given at various levels of dimensionless time corresponding to actual times experimentally encountered. From the plots given in Figure 2.5, it is apparent that the error in assuming the probe is a perfect conductor can become quite large.

The temperature at the probe centerline can be significantly higher than the perfect conductor temperature, but the error in using the perfect conductor model to measure the thermal conductivity of the medium will not be as significant. The thermal conductivity is determined from the slope of temperature rise versus the natural logarithm of time, and these plots show the error in the slope will not be as great as the difference in the temperatures. Errors attributed to the assumption of a perfect conductance are shown in Figure 2.6 (this figure is determined from the derivative of temperature, given in Equation 2.6, with respect to the natural logarithm of time).

Figure 2.5

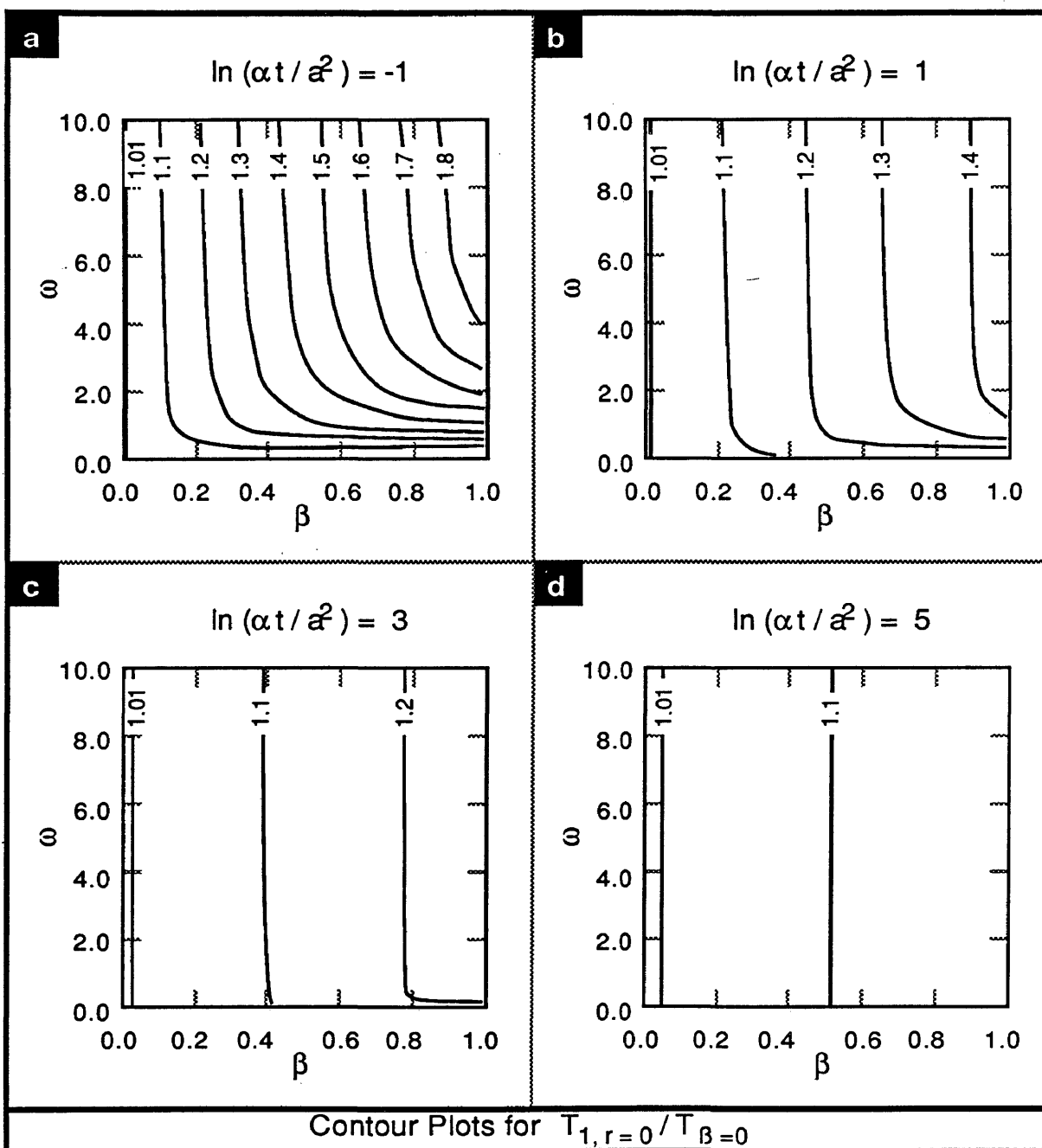
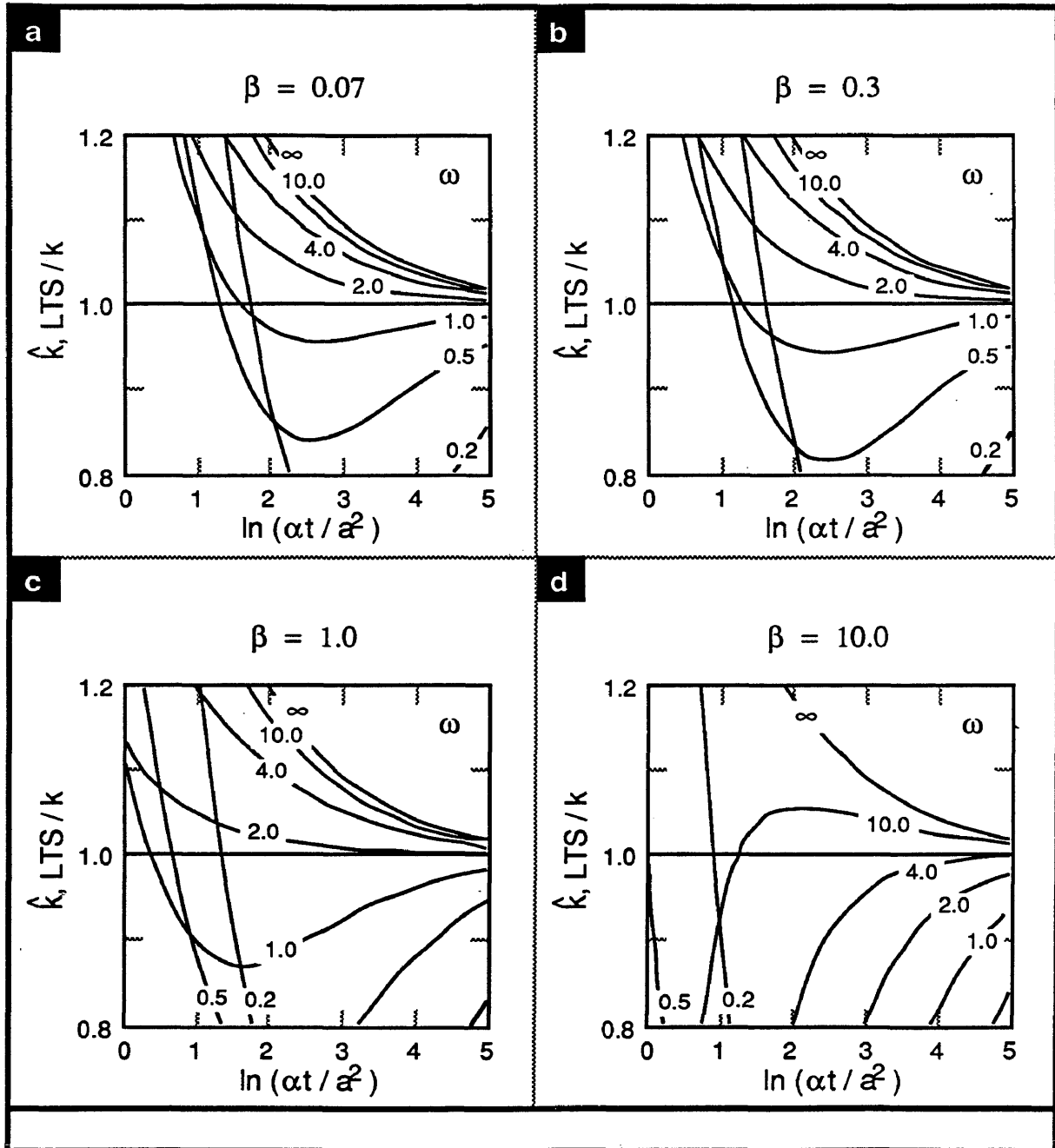
Probe Centerline Temperature Dependence on  $\beta$  and  $\omega$ 

Figure 2.6

Probe Finite Thermal Conductivity Effect on Long Time Solution



### 2.1.3 PROBE FINITE LENGTH

The probe finite length will cause axial heat flow to coexist with radial heat flow. Axial effects complicate the mathematics of probe response versus time, and if the effects are significant the infinitely long probe model is no longer valid.

A model is necessary that accounts for the effect of finite probe length. By making the probe sufficiently long and measuring the temperature at probe midlength, the error caused by assuming only radial flow can be made negligible within the experimental accuracy. Blackwell (1956) proposed a minimum length to diameter ratio of 20 to 30, and the studies here suggest that a length to diameter ratio greater than 30 is required.

The model used in this discussion is one presented in Kierkus, Mani, and Venart (1973). The assumptions of their model are:

- The probe has uniform physical properties,
- The probe has a finite length,
- The probe has a finite conductivity,
- The sample is infinite in extent radially and its height is equal to that of the probe, and
- Energy is transferred only by radial and axial conduction.

Throughout the text this model is referred to as the Kierkus, Mani, and Venart (1973) model.



Laplace's equation and the appropriate boundary conditions for this model are:

$$\frac{\partial T}{\partial t} = \frac{\alpha}{r} \frac{\partial}{\partial r} \left( r \frac{\partial T}{\partial r} \right) + \alpha \frac{\partial^2 T}{\partial z^2} \quad ; t \geq 0, a \leq r < \infty, 0 \leq z \leq L \quad (2.8)$$

Initial Condition,

$$T = 0$$

$$@ t = 0, 0 < r < \infty, 0 \leq z \leq L$$

Boundary Conditions,

$$T = 0$$

$$\begin{cases} @ t > 0, r \rightarrow \infty, 0 \leq z \leq L \\ @ t > 0, 0 < r < \infty, z = 0 \text{ \& } L \end{cases}$$

$$Q = \pi a^2 (\rho C_p)_1 \frac{\partial T}{\partial t} - (2\pi a) k \frac{\partial T}{\partial r} - \frac{2\pi a}{(L/a)} k_1 \frac{\partial T}{\partial z}$$

$$@ t > 0, r = a, 0 < z < L$$

The complete solution for the for the temperature at the surface of the probe at probe midlength is (Kierkus, Mani, and Venart,1973):

$$T = \frac{2Q}{k\pi^3} \sum_{i=0}^{\infty} \frac{(-1)^i}{(2i+1)} \int_0^{\infty} \frac{1 - \exp \left[ - \left\{ \left( \frac{(2i+1)\pi}{L/a} \right)^2 + u^2 \right\} \frac{\alpha t}{a^2} \right]}{\left[ \left( \frac{(2i+1)\pi}{L/a} \right)^2 + u^2 \right] \{ \phi^2(u) + \psi^2(u) \}} f(u) du \quad (2.9)$$

Where:

$$\phi(u) = \frac{1}{u} \left[ \left( \frac{1}{\omega} - \frac{1}{\beta} \right) \left( \frac{(2i+1)\pi}{L/a} \right)^2 + \frac{u^2}{\omega} \right] J_0(u) - J_1(u)$$

$$\psi(u) = \frac{1}{u} \left[ \left( \frac{1}{\omega} - \frac{1}{\beta} \right) \left( \frac{(2i+1)\pi}{L/a} \right)^2 + \frac{u^2}{\omega} \right] Y_0(u) - Y_1(u)$$

$$f(u) = J_0(u)\psi(u) - Y_0(u)\phi(u)$$

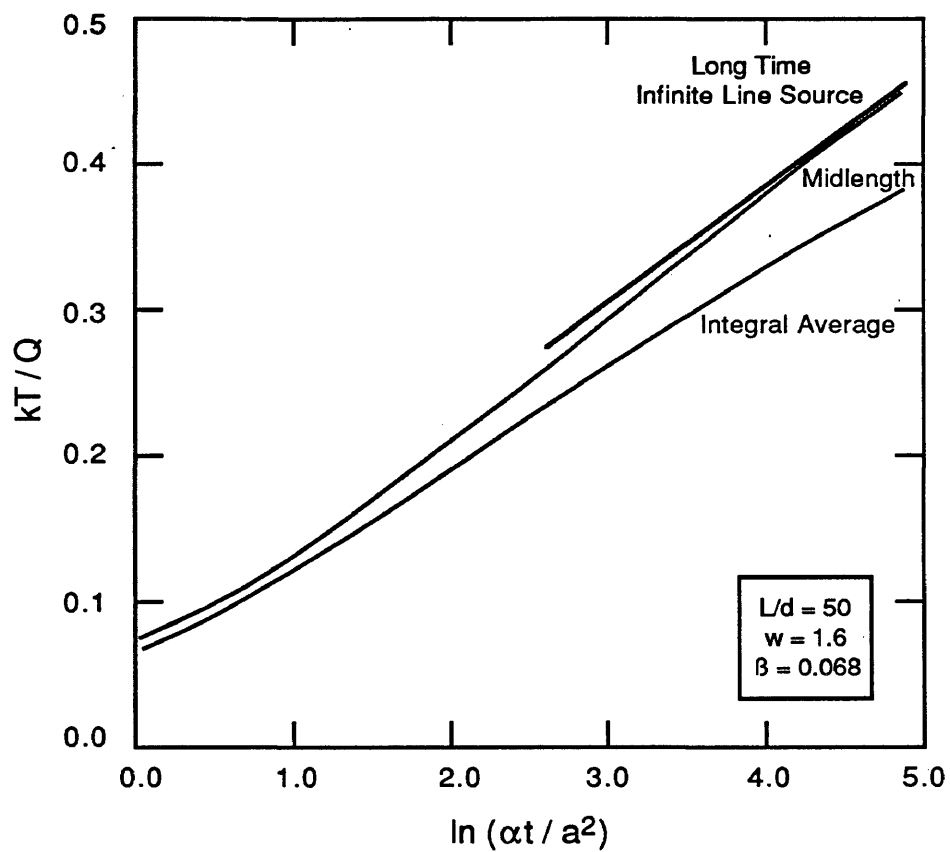
The following discussion is based on the probe testing tetrahydrofuran (THF) hydrate at 1 atm and 273 K;  $\rho = 0.89 \text{ gm.cm}^{-3}$ ,  $C_p = 2.22 \text{ J.gm}^{-1}.\text{K}^{-1}$ , and  $k = 5 \text{ mW.cm}^{-1}.\text{K}^{-1}$ . Assuming that the probe of this work is similar to the probe of Von Herzen and Maxwell (1959);  $\omega = 1.6$ ,  $\beta = 0.068$ , and  $L^* = 38.33$ .

A typical response for the probe was obtained through this finite line source solution for the given values of  $\omega$ ,  $\beta$ , and  $L^*$ . A graph of dimensionless temperature rise versus the natural logarithm of time is given in Figure 2.6. The curve labeled *Infinite Line Source* is from Equation 2.1 with  $k_1 = \infty$ , the curve labeled *Midlength* is from Equation 2.12, and the curve labeled *Integral Average* is the curve had the temperature been measured over the entire probe length. The computer program used in solving the solution of Kierkus, Mani, and Venart (1973) was a modified program of Perkins (1983). The modification entailed the calculation of the temperature at probe midlength rather than an integral average over the entire length of the probe.

Several conclusions are possible for general experimentation. First, measuring the temperature at probe midlength is a good method of minimizing axial end effects and approximating the long time infinite line source solution. Second, though the long time solution may never be reached, the error in assuming the probe is infinitely long is within the experimental accuracy. Using Equation 2.1 on the results from the Kierkus, Mani, Venart (1973) solution given in Figure 2.7, a thermal conductivity is obtained which is only 1.6 % different from the true conductivity. Finally, there is a time period in which axial effects are not significant. By analyzing experimental data within this time period, axial effects can be ignored without inducing significant error.

Figure 2.7

Theoretical Probe Response versus Time for Tetrahydrofuran Hydrate



---

## **2.2 SAMPLE FACTORS AND EFFECTS**

---

After the needle probe has been designed the experimental response depends upon the medium being tested. Several factors due to the sample which affect the response of the needle probe are:

- Sample finite size,
- Sample temperature dependency,
- Induced convection in liquids, and
- Thermal contact.

Each of these factors are discussed in this section.

### **2.2.1 SAMPLE FINITE SIZE**

As power is supplied to the probe a thermal wave moves out through the sample. If that sample is not large enough, then the thermal wave will reach the edge of the sample. After this occurrence the thermal conductivity cannot be determined from the models presented earlier.

A model is necessary that accounts for the penetration of a thermal wave into the medium. From this model, a sample size is selected such that the thermal wave never encounters the sample boundary. The model used for this discussion is the same as that presented in the probe finite heat capacity discussion, except instead of using the solution only at the probe sample interface the solution is extended out into the sample.

The complete solution for the temperature profile extending into the sample is (Carslaw and Jaeger, 1959).

$$T = \frac{Q}{k\pi^2} \int_0^{\infty} \frac{(1 - e^{-\alpha t u^2/a^2})}{u^2 \{ \phi^2(u) + \psi^2(u) \}} f(u) du \quad (2.10)$$

Where:

$$\phi(u) = \frac{u}{\omega} J_0(u) - J_1(u)$$

$$\psi(u) = \frac{u}{\omega} Y_0(u) - Y_1(u)$$

$$f(u) = J_0(ur/a)\psi(u) - Y_0(ur/a)\phi(u)$$

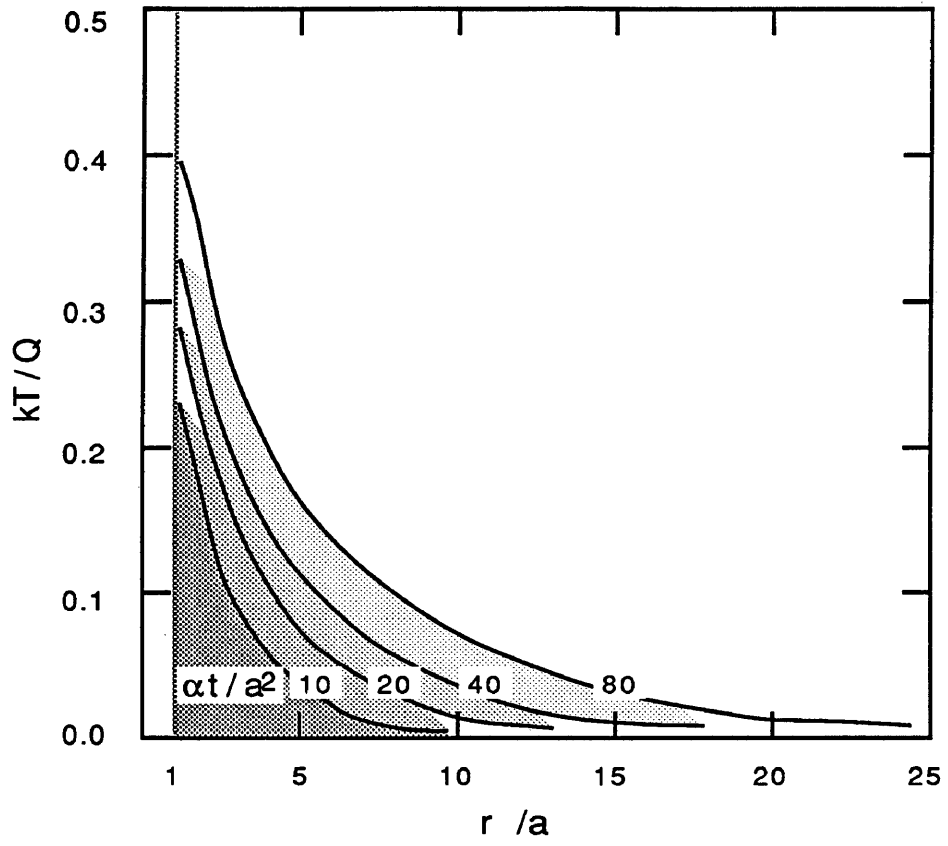
Values of the heat capacity ratio encountered in this work were modeled. It was found that the dimensionless thermal wave penetration ( $kT/Q$ ) was fairly insensitive to  $\omega$  with respect to dimensionless time ( $\alpha t/a^2$ ). The results for  $\omega = 2$  for the thermal wave penetration into the sample are shown in Figure 2.8. Assuming that the thermal wave ends when the temperature of the wave is less than one percent of the probe surface temperature, an equation predicting the thermal wave size is:

$$(r/a) = 3 (\alpha t/a^2)^{1/2} \quad (2.11)$$

The sample is sized such that the thermal wave never reaches the sample boundary. For the needle probe and samples used in this work, a sample radius to probe radius of greater than thirty is required.

Figure 2.8

Thermal Wave Penetration into the Surrounding Medium



### 2.2.2 SAMPLE TEMPERATURE DEPENDENCY

As the temperature increases during an experiment the physical properties of the medium change. For the compounds tested in this work this change in properties is not significant. To minimize this effect, the power supplied to the probe is minimized to minimize the temperature increase. The thermal conductivity is reported at one half of the experimental temperature increase. The error induced is not significant compared to the overall experimental inaccuracy.

### 2.2.3 INDUCED CONVECTION IN LIQUIDS

The power supplied to the probe will eventually cause convection in the liquid phase, and this induced convection will transport heat away from the probe at a faster rate than by conduction alone. Thereby nullifying the implementation of the models presented earlier.

Typically there is an induction time until heat transfer due to convection is significant to that by conduction. At the end of this, time a "rollover" will occur in the temperature profile. By analyzing the data before this time, the models presented earlier are still valid. A correlation for the onset of convection is (Pantaloni, Guyon, Velarde, Bailleux, and Finiels (1977):

$$\begin{aligned} \left(\frac{\alpha t}{a^2}\right)^{3/2} \ln\left(\frac{4\alpha t}{Ca^2}\right) &= 380 \left(\frac{a^3 \rho^2 g \beta^* (Q/k)}{\mu^2}\right)^{-1} \left(\frac{C_p \mu}{k}\right)^{-1} \\ &= 380 \cdot Gr^{-1} \cdot Pr^{-1} \end{aligned} \quad (2.12)$$

Where the variables are defined as previously, with new variables:

$g$  = acceleration of gravity,

$t$  = time for convection to become significant,

$\beta^*$  = volume expansivity of the liquid, and

$\mu$  = viscosity of the liquid.

If the viscosity of the liquid is large, then viscosity controls the onset of convection. Only viscosity is studied in the verification of the thermal conductivity system operation, because of doubt in the claim (Stoll and Bryan, 1979) that only liquids as viscous as glycerine can be measured by the needle probe.

## 2.2.4 THERMAL CONTACT

A thermal contact resistance layer may exist between the probe and the medium, therefore a temperature discontinuity will exist between the outer surface of the probe and the inner surface of the medium. This discontinuity is not accounted for in the probe mathematical models presented earlier.

The effect at short times for the thermal contact resistance layer on the solution for the perfect probe model is (Carslaw and Jaeger, 1959):

$$T = \frac{Q}{4\pi k} \left[ \ln \left( \frac{4\alpha t}{Ca^2} \right) + \left\{ 1 + \frac{\omega - 2}{\omega} \ln \left( \frac{4\alpha t}{Ca^2} \right) \right\} \frac{a^2}{2\alpha t} + \left( \frac{2k}{aH} \right) \left\{ 1 + \frac{a^2}{\alpha t} \right\} \right] \quad (2.13)$$

Where the variables are defined as previously, with the new variable:

$H$  = the thermal contact resistance coefficient.

If long times can be reached during experimentation, then the thermal conductivity can be determined regardless of the contact resistance. At long times the contact resistance affects only the intercept and not the slope of the

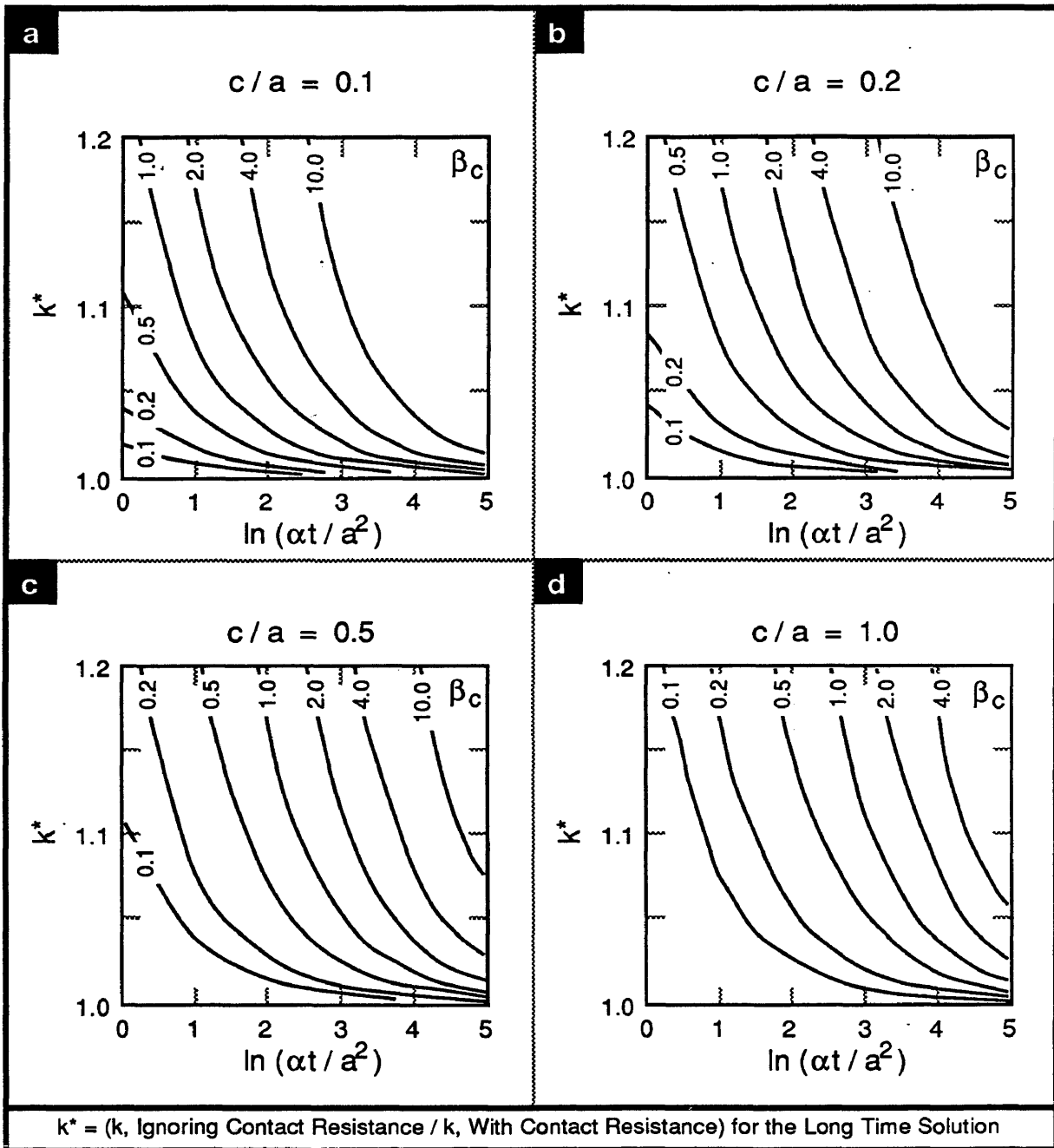


semilogarithmic plot of temperature rise versus time. Since the extent of the contact layer and the properties of the contact layer vary from experiment to experiment, there is no sufficient method for determining a best estimate of the thermal resistance and medium thermal conductivity.

The errors associated with assuming no contact resistance when there is contact resistance are shown in Figure 2.9. This figure is based on Equation 2.13. In this figure,  $c$  is the radial thickness of the contact resistance layer and  $\beta_c$  is the ratio of the sample thermal conductivity to the contact resistance layer thermal conductivity. As expected, the errors are minimized when the contact resistance layer is thin and its thermal conductivity large.

Figure 2.9

Thermal Contact Resistance Effect on Long Time Solution



---

## 2.3 CONCLUSION

---

The intent of this chapter was to define the heat transfer models appropriate in predicting the behavior of the transient needle probe during experimentation. From this information, the basis for experimental data acquisition and analysis is developed, and a transient needle probe system is built and its proper operation verified.

By considering many factors of the needle probe experimentation a model was selected for data analysis. The model chosen was the finite conductor model. To reiterate, the assumptions of this model are:

- The probe has uniform physical properties,
- The probe is infinitely long,
- The probe has a finite heat capacity,
- The probe has a finite conductivity,
- The sample is infinite in extent, and
- Energy is transferred only by radial conduction.

If long times can be reached, then thermal conductivities can be measured without knowing the probe properties. Estimation of the probe properties is required when it becomes necessary to analyze experimental data when short or long time solutions are valid. This estimation requires a solution which solves for the probe properties given an experiment on a medium of known properties.

# CHAPTER 3

## **ALGORITHM FOR DATA ACQUISITION AND ANALYSIS**

---

### 3.0 INTRODUCTION

---

In this chapter an algorithm for data acquisition and analysis is presented. The algorithm is based upon the mathematical modeling for the transient needle probe presented in Chapter 2.

The experimentation process (refer to Figure 1.1) controls the data acquisition and analysis. Typical experimental results are presented in Figure 3.1 for three compounds: a) 1-methylnaphthalene, b) water, and c) water ice. In this figure, the optimum solution region is the closet approach of the data to the long time infinite line source solution. Before this time, heat capacity or thermal conductivity effects are excessive, and after this time convective or axial effects are excessive.

An analysis of the data from the optimum solution region yields the best estimate of the sample thermal conductivity. Table 3.1 details the differences between the solution method presented in the literature (refer to Chapter 1) and the solution method presented in this work.

The presentation of the acquisition and analysis algorithm is in four parts:

- Data acquisition algorithm,
- Data analysis algorithm basis,
- Algorithms for unknown media properties, and
- Algorithm for unknown probe properties.

Figure 3.1

Typical Experimental Responses for the Needle Probe

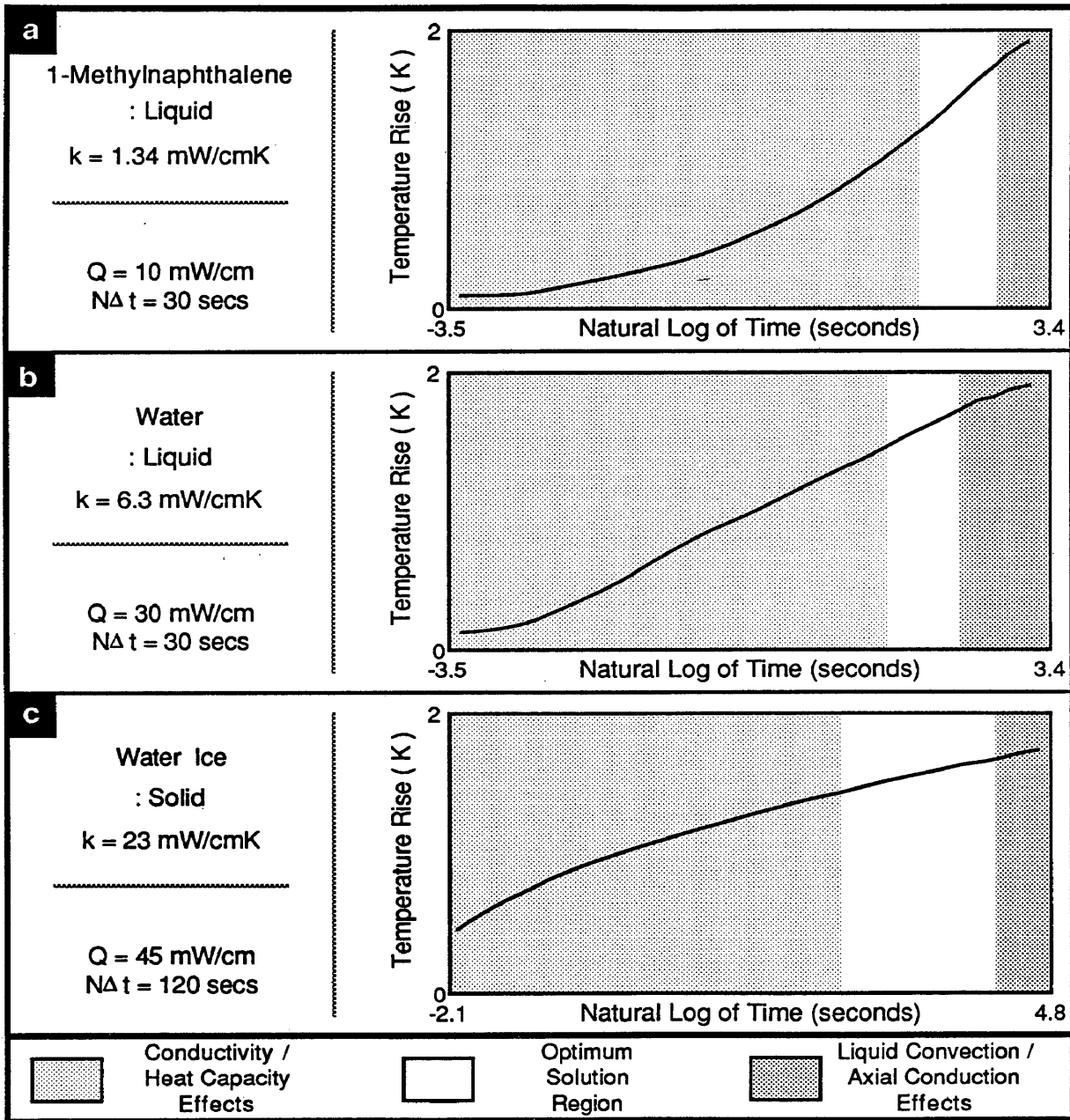


Table 3.1

Method of Data Analysis: Reported in Literature and This Work

<b>METHOD OF DATA ANALYSIS: REPORTED IN LITERATURE</b>	
$T = \frac{Q}{4\pi k} \ln \left( \frac{4\alpha t}{Ca^2} \right)$	
<b>CALIBRATION</b>	<b>EXPERIMENTATION</b>
<ol style="list-style-type: none"> <li>1. EXPERIMENT ON A MATERIAL OF KNOWN PROPERTIES, <math>(Q/4\pi k)</math>.</li> <li>2. DETERMINE THE SLOPE OF THE T vs ln t PLOT, <math>(Q/4\pi k)^*</math>.</li> </ol>	<ol style="list-style-type: none"> <li>1. EXPERIMENT ON AN UNKNOWN.</li> <li>2. DETERMINE THE SLOPE OF THE T vs ln t PLOT, <math>(Q/4\pi k)_u</math></li> <li>3. ADJUST THE SLOPE OF THE UNKNOWN BY THE KNOWN, <math>(Q/4\pi k)_u^* = (Q/4\pi k)_u \times (Q/4\pi k)^*/(Q/4\pi k)</math>.</li> </ol>

<b>METHOD OF DATA ANALYSIS: THIS WORK</b>	
$T = \frac{Q}{4\pi k} \left[ \ln \left( \frac{4\alpha t}{Ca^2} \right) + \left\{ 1 + \frac{\omega - 2}{\omega} \ln \left( \frac{4\alpha t}{Ca^2} \right) \right\} \frac{a^2}{2\alpha t} \right] + \frac{Q}{4\pi k_1} \left[ 1 - \frac{3}{2\omega} \frac{a^2}{2\alpha t} \right]$	
<b>CALIBRATION</b>	<b>EXPERIMENTATION</b>
<ol style="list-style-type: none"> <li>1. EXPERIMENT ON A MATERIAL OF KNOWN PROPERTIES, <math>k, (\rho C_p)</math>.</li> <li>2. ESTIMATE THE PROPERTIES OF THE PROBE, <math>k_1^*, (\rho C_p)_1^*</math>.</li> </ol>	<ol style="list-style-type: none"> <li>1. EXPERIMENT ON AN UNKNOWN.</li> <li>2. LOCATE THE OPTIMUM SOLUTION REGION OF THE T vs ln t PLOT.</li> <li>3. ESTIMATE THE UNKNOWN THERMAL CONDUCTIVITY FROM THE LONG OR SHORT TIME SOLUTION, <math>k_u^*</math></li> </ol>

---

### 3.1 DATA ACQUISITION ALGORITHM

---

Typically, for past work presented in the literature, a single experiment is conducted and the thermal conductivity is determined from that experiment. In this work multiple experiments are performed under identical conditions, and the temperature measurements at identical times are averaged. This procedure allows for a more detailed data analysis.

At any given time a range can be predicted within which the experimental temperatures will occur. This range is given as:

$$\bar{T}_i = \mu_i \pm \sqrt{\frac{z\sigma}{m}} \quad (3.1)$$

$$\bar{T}_i = \frac{1}{m} \sum_{j=1}^m T_{j,i} \quad (3.2)$$

Where:

$m$  = Total number of experiments performed.

$z$  = Depends upon the probability distribution function for the temperature measurements and the degree of confidence for the data.

$T_{j,i}$  = Measured temperature rise for the  $j^{\text{th}}$  experiment,  $i^{\text{th}}$  time increment.

$\mu_i$  = Actual temperature rise for the  $i^{\text{th}}$  time increment.

$\sigma$  = Population standard deviation (assumed independent of  $i$ ).

For a given measurement error the confidence that the measured temperature is the actual temperature increases as the number of experiments increase. The average temperature is a sufficient statistic, therefore no statistical information is lost with this parameter.



The population standard deviation,  $\sigma$ , is a measure of the accuracy in determining the actual temperature rise. It is determined by: 1) the inherent characteristics of the thermistor, 2) the methodology of measuring the resistance of the thermistor, and 3) the accuracy of the calibration process for the resistance versus temperature characteristics of the thermistor.

The temperature standard deviation is unknown, and it is estimated by the sample standard deviation, which is a sufficient statistic. The sample standard deviation,  $s$ , is:

$$s^2 = \frac{1}{N} \sum_{i=1}^N s_i^2 \quad (3.3)$$

$$s_i^2 = \frac{1}{(m-1)} \sum_{j=1}^m (T_{j,i} - \bar{T}_i)^2 \quad (3.4)$$

Where:

$N$  = Total number of time increments in an experiment.

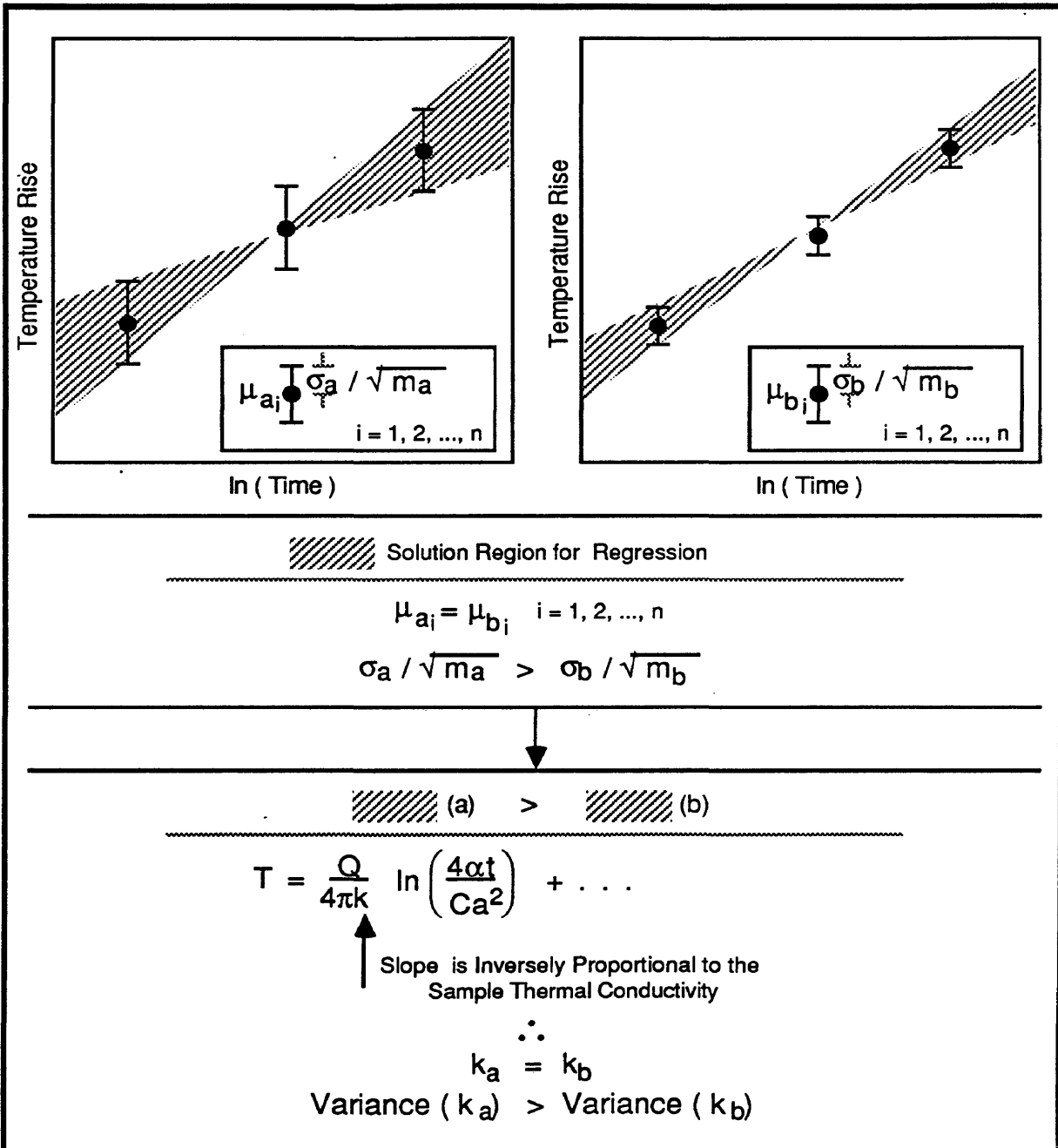
$s_i$  = Sample standard deviation for the  $i$ th time increment.

$s$  = Arithmetic average of all sample standard deviations.

A minimal variance in the temperature measurement maximizes the accuracy in the measured thermal conductivity. This is detailed in Figure 3.2, where a smaller variance in the temperature measurement gives a smaller variance in the measured thermal conductivity. If the variance in the temperature measurement is excessive, then a solution for the thermal conductivity may not be possible.

Figure 3.2

Comparison of Curve Fitting for Various Degrees of Accuracy



---

## 3.2 DATA ANALYSIS ALGORITHM BASIS

---

After the data from a transient needle probe experiment is acquired, then a data analysis procedure is used to determine the sample thermal conductivity. From Chapter 2, the equation for modeling the probe as a finite conductor is:

$$T = \beta_0 + \beta_1 \ln t + (\beta_2 + \beta_3 \ln t) t^{-1} + (\beta_4 + \beta_5 \ln t + \beta_6 \ln^2 t) t^{-2} \quad (3.5)$$

The equation parameters  $\beta_k$  are defined in Table 3.2. The temperature is at the probe centerline. Solutions for this model at long and short times are presented in this text, these are:

- Long Time Solution,

$$T = \beta_0 + \beta_1 \ln t \quad (3.6a)$$

- Short Time Solution,

$$T = \beta_0 + \beta_1 \ln t + (\beta_2 + \beta_3 \ln t) t^{-1} \quad (3.6b)$$

The basis for the data analysis algorithm is presented in two steps:

- 1) Filtering of the complete experimental temperature rise versus time data set to determine the data set for the optimum solution region.
- 2) Application of least squares regression on the complete model equation, and introduction of Lagrange multipliers into the least squares regression.

Table 3.2

## Transient Needle Probe Model Equation

$$T = \beta_0 + \beta_1 \ln t + (\beta_2 + \beta_3 \ln t) t^{-1} + (\beta_4 + \beta_5 \ln t + \beta_6 \ln^2 t) t^{-2}$$

$$\beta_0 = \frac{Q}{4\pi k} \ln \left( \frac{4\alpha}{Ca^2} \right) + \frac{Q}{4\pi k_1}$$

$$\beta_1 = \frac{Q}{4\pi k}$$

$$\beta_2 = \left[ \frac{Q}{4\pi k} \left\{ 1 + \frac{\omega-2}{\omega} \ln \left( \frac{4\alpha}{Ca^2} \right) \right\} - \frac{Q}{4\pi k_1} \frac{3}{2\omega} \right] \frac{a^2}{2\alpha}$$

$$\beta_3 = \frac{Q}{4\pi k} \left( \frac{\omega-2}{\omega} \right) \frac{a^2}{2\alpha}$$

$$\beta_4 = \left[ \frac{Q}{4\pi k} \left\{ \left( \frac{3}{8} - \frac{2}{\omega} + \frac{\pi^2}{8} \left( \frac{\omega-2}{\omega} \right)^2 \right) + \left( -\frac{7}{4} + \frac{4}{\omega} + \frac{3}{2} \left( \frac{\omega-2}{\omega} \right)^2 \right) \ln \left( \frac{4\alpha}{Ca^2} \right) - \frac{3}{4} \left( \frac{\omega-2}{\omega} \right)^2 \ln^2 \left( \frac{4\alpha}{Ca^2} \right) \right\} \right.$$

$$\left. + \frac{Q}{4\pi k_1} \left\{ \left( 4 - \frac{11k}{12k_1} \right) + \left( 4 - \frac{3\omega}{2} \right) \ln \left( \frac{4\alpha}{Ca^2} \right) \right\} \frac{1}{\omega^2} \right] \left( \frac{a^2}{2\alpha} \right)^2$$

$$\beta_5 = \left[ \frac{Q}{4\pi k} \left\{ \left( -\frac{7}{4} + \frac{4}{\omega} + \frac{3}{2} \left( \frac{\omega-2}{\omega} \right)^2 \right) - \frac{6}{4} \left( \frac{\omega-2}{\omega} \right)^2 \ln \left( \frac{4\alpha}{Ca^2} \right) \right\} \right.$$

$$\left. + \frac{Q}{4\pi k_1} \left( 4 - \frac{3\omega}{2} \right) \frac{1}{\omega^2} \right] \left( \frac{a^2}{2\alpha} \right)^2$$

$$\beta_6 = -\frac{Q}{4\pi k} \frac{3}{4} \left( \frac{\omega-2}{\omega} \right)^2 \left( \frac{a^2}{2\alpha} \right)^2$$

### 3.2.1 OPTIMUM SOLUTION REGION

From the optimum solution region for an experimental data set, as shown in Figure 3.1, the best estimate of the sample thermal conductivity is determined. At times other than in this region, there are several factors that adversely affect conductivity determinations:

- The shorter the time the more terms which must be included in the model. If the time is too short, then the short time solution will have insufficient terms to model the heat transfer. The short time solution may not be able to converge, and if it does the confidence in the answer is small.
- At short times the accuracy in the temperature measurement is comparable to experimental temperature increase. The short time solution may not be able to converge, and if it does the variance in the measured thermal conductivity is excessive.
- At times longer than the optimum solution region the heat transfer model in Table 3.2 is no longer applicable. Axial and convective effects are too dominant.

The problem is in determining the solution region for an experiment.

Three operating parameters,  $Q$ ,  $\Delta t$ , and  $N\Delta t$ , control the position of the solution region. Guidelines for selecting these parameters are:

- $Q$ , the power supplied per unit probe length controls the extent of the temperature increase. It must be large enough so that the experimental temperature increase is significant, typically 1 to 2 Kelvin. Also, it must be small enough such that the onset of convection (in liquids) occurs at the largest time possible.

- $\Delta t$ , the time step is selected such that there are greater than 600 data points per experiment. Fewer data points contribute to a larger variance in each apparent conductivity.
- $N\Delta t$ , the time length of the experiment must be large enough to ensure the onset of convection or axial heat flow effects. The onset of these effects causes the apparent thermal conductivity to increase. To avoid the taking of excessive data this onset time should be as close to the end of the experiment as possible.

The method to determine the optimum solution region for an experiment is:

- 1) The apparent thermal conductivities are calculated at several points along the experimental response curve, by employing the long time solution. The conductivities are termed apparent because it is assumed that the long time solution is valid. If the conductivity ratio,  $\beta$ , is large, then the beginning of the experiment is ignored. At short times a large conductivity ratio will cause severe nonlinearities in the experimental temperature response.
- 2) From this set of apparent conductivities, the minimum apparent conductivity and the corresponding time are determined. Not ignoring the early time portion for high conductivity ratios adversely affects finding the minimum apparent conductivity.

Figure 3.3 gives an example of an actual experiment on 1-methylnaphthalene. The temperature rise and apparent thermal conductivity versus natural log of

time are shown in Figure 3.3 a and b, respectively. Further details are presented in the discussion of measurements on solids and liquids.

Point estimates of the apparent thermal conductivity were calculated from the experimental data. Each point estimate is actually an estimate for a segment of the data whose average is the point. For a given point  $i$  ( $i = 1, 2, \dots, N$ ), the lower bound point  $j$  and the upper bound point  $k$  for the segment are:

$$j \approx i \cdot \exp(1 - f \ln f / (f-1)) \quad (3.7a)$$

$$k \approx j \cdot f \quad (3.7b)$$

$$f = N^\delta$$

Where  $\delta$  is the length of the segment in natural log of time divided by the natural log of the experimental time length. The minimum value,  $i_{\min}$ , and maximum value,  $i_{\max}$ , which  $i$  can take on are:

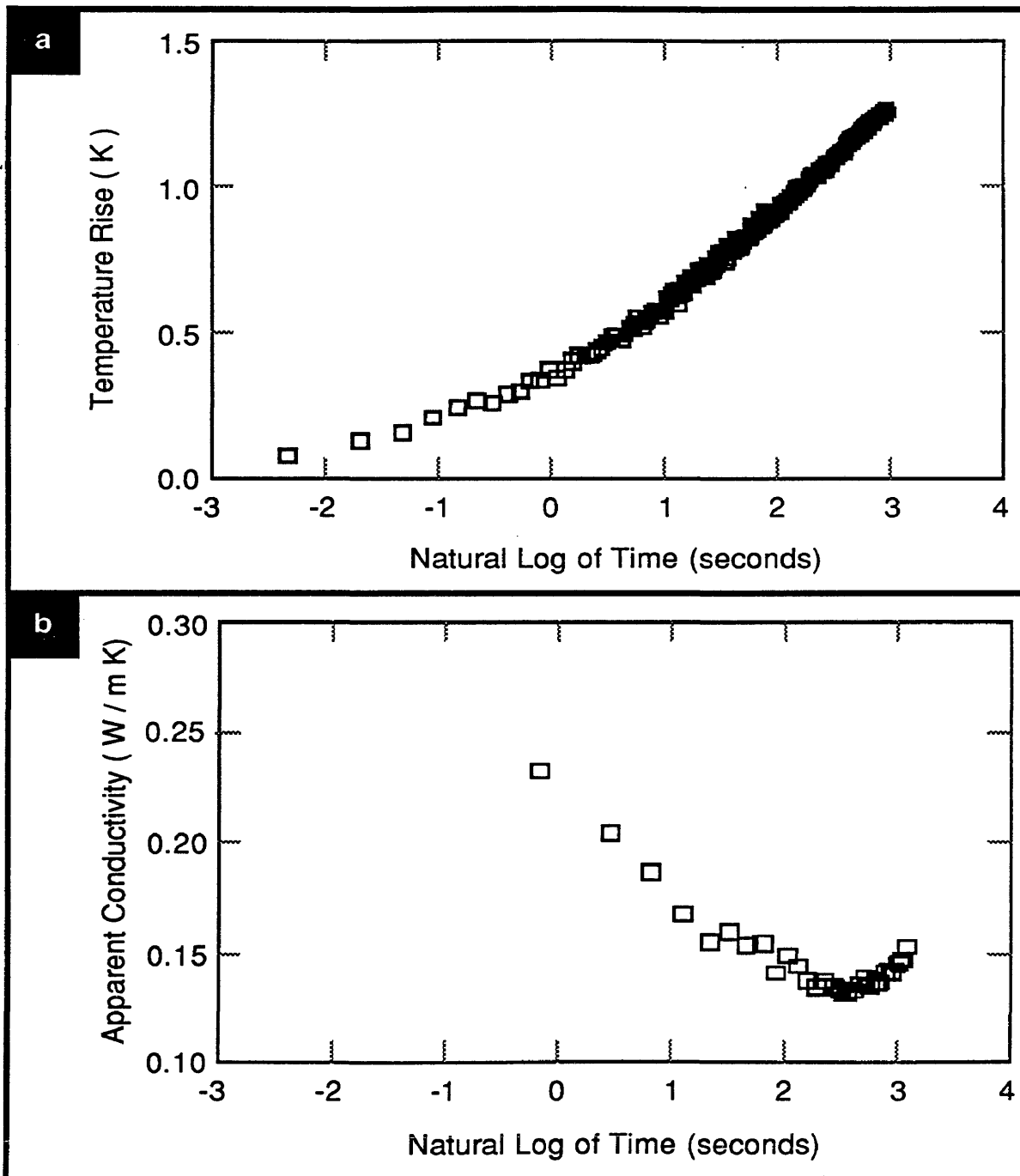
$$i_{\min} \approx \exp(x_{\min} \ln N - 1 + f \ln f / (f-1)) \quad (3.8a)$$

$$i_{\max} \approx \exp(x_{\max} \ln N - 1 + \ln f / (f-1)) \quad (3.8b)$$

Where  $x_{\min}$  is the fraction of the initial experimental data being ignored, and  $x_{\max}$  is the fraction of the final experimental data being ignored. In this work, the complete set of point estimates extend linearly from  $i_{\min}$  to  $i_{\max}$ .

Note in the analysis algorithm, the data analyzed is for a data set extending from  $i = 1, 2, \dots, n$ . This refers to successive points in the solution region, and  $n$  is the total number of data points in the region.

Figure 3.3

Acquisition and Analysis on 1-Methylnaphthalene,  $T = 296 \text{ K}$ ,  $Q = 0.6 \text{ W}\cdot\text{m}^{-1}$ 



### 3.2.2 REGRESSION AND LAGRANGE MULTIPLIERS

The long and short time solutions for the needle probe can be solved by a modified least squares analysis. Rewritten in the format of least squares regression, the equations are:

- Long Time Solution,

$$\bar{T}_i = \beta_0 + \beta_1 \ln t_i + u_{1,i} \quad (3.9a)$$

- Short Time Solution,

$$\bar{T}_i = \beta_0 + \beta_1 \ln t_i + (\beta_2 + \beta_3 \ln t_i) t_i^{-1} + u_{2,i} \quad (3.9b)$$

Let  $\varepsilon_i$  be the random measurement error, then the error terms are described by:

$$u_{p,i} = \varepsilon_i + R_{p,i} \quad (3.10)$$

$$R_{p,i} = \sum_{l=p}^{\infty} \sum_{k=0}^l \left( \beta_{\frac{1}{2}l(l+1)+k+1} \ln^k t_i \right) t_i^{-l} \quad (3.11a)$$

$$| R_{p,i+1} | < | R_{p,i} | \quad (3.11b)$$

$$\lim_{i \rightarrow \infty} | R_{p,i} | = 0 \quad (3.11c)$$

The time dependency of the error terms violates some assumptions of standard linear regression, namely: 1)  $\varepsilon_i$  are independent random variables, and 2)  $E(\varepsilon_i) = 0$ . Any errors induced by assuming independent error terms is minimized by properly selecting the region for data analysis. This region is:

- Long time solution,  $R_{1,i} \ll \beta_0 + \beta_1 \ln t_i$
- Short time solution,  $R_{2,i} \ll (\beta_2 + \beta_3 \ln t_i) t_i^{-1}$

When these statements are true, there exists a high degree of confidence that the  $b_k$ 's determined by least squares analysis are the best estimates for the  $\beta_k$ 's.

Another problem with using a general least squares analysis is that the  $\beta_k$ 's are not all independent. This problem is solved by modifying the linear regression by the method of Lagrangian multipliers.

Given the equation:

$$Y_i = \beta_0 x_{0,i} + \beta_1 x_{1,i} + \dots + \beta_{m-1} x_{m-1,i} + \beta_m x_{m,i} \quad (3.12)$$

Under the following set of constraints:

$$g_j(\beta_0, \beta_1, \dots, \beta_{m-1}, \beta_m) = 0 ; \quad j = 0, 1, \dots, l \quad (3.13)$$

And the following data set:

$$(x_0, x_1, \dots, x_{m-1}, x_m, Y)_i \quad i = 1, 2, \dots, n$$

The best estimates for the coefficients are determined by minimizing:

$$F = \sum_{i=1}^n \left( Y_i - \sum_{j=0}^m \beta_j x_{j,i} \right)^2 \quad (3.14)$$

The standard procedure for minimizing a function of several variables subject to one or more constraints is the method of Lagrange multipliers. The equations that minimize F are:

$$\Phi_k = \frac{\partial F}{\partial \beta_k} - \sum_{j=0}^l \lambda_j \frac{\partial g_j}{\partial \beta_k} = 0 \quad ; \quad k = 0, 1, \dots, m \quad (3.15)$$

Where the  $\lambda_j$ 's are the Lagrangian multipliers. The multipliers are solved for through the constraints  $g_j$ . To solve for the  $m$  coefficients,  $\beta_i$ , a set of  $(m+l+2)$  equations with  $(m+l+2)$  unknowns is solved.

There are two unknowns in the heat transfer model for the needle probe, namely the thermal conductivity and the volumetric heat capacity. For the  $m+1$  coefficients there are only two independent coefficients. Let these coefficients be  $\beta_{j'}$  and  $\beta_{j''}$ . The  $m-1$  constraining equations for this model are:

$$g_j = \beta_j - G_j(\beta_{j'}, \beta_{j''}) = 0 \quad j = 0, 1, \dots, m \text{ and } \neq j', j'' \quad (3.16)$$

Under these constraints the solution for the Lagrangian multipliers is:

$$\lambda_k = \frac{\partial F}{\partial \beta_k} \quad k = 0, 1, \dots, m \text{ and } \neq j', j'' \quad (3.17)$$

Substitute the partial derivative of  $g_j$  with respect to  $j'$  and  $j''$  and the solutions for the Lagrangian multipliers into the expressions for  $\Phi_{j'}$  and  $\Phi_{j''}$  yields:

$$\Phi_{j''} = \frac{\partial F}{\partial \beta_{j''}} + \sum_{\substack{j=0 \\ \neq j', j''}}^1 \frac{\partial F}{\partial \beta_j} \frac{\partial \beta_j}{\partial \beta_{j''}} = 0 \quad (3.18a)$$

$$\Phi_{j'} = \frac{\partial F}{\partial \beta_{j'}} + \sum_{\substack{j=0 \\ \neq j', j''}}^1 \frac{\partial F}{\partial \beta_j} \frac{\partial \beta_j}{\partial \beta_{j'}} = 0 \quad (3.18b)$$

$$\beta_j = G_j(\beta_{j'}, \beta_{j''}) \quad (3.19)$$

The solutions for the best estimates,  $b_{j'}$  and  $b_{j''}$ , of the coefficients,  $\beta_{j'}$  and  $\beta_{j''}$ , are found by solving this set of equations with two unknowns.

---

### 3.3 ALGORITHMS FOR UNKNOWN SAMPLE

---

In this section algorithms are presented for determining the unknown sample thermal conductivity by employing the long time and short time solutions. Complete equations for these models are presented in the data analysis algorithm development. Solutions for smaller times than these two solutions can be developed, but they would not increase the accuracy in the measured thermal conductivity. The contribution to the temperature by the smaller times is the same order of magnitude as the accuracy of the temperature measurement. It is possible that solutions for these times will give inaccurate results.

Both the long and short time algorithms are programmed into the thermal conductivity system. The program listings are presented in the appendices.

#### 3.3.1 LONG TIME SOLUTION FOR SAMPLE

The long time solution for the sample thermal conductivity is obtained directly by least squares regression. A method is presented for estimating the applicability of the long time solution.

The long time solution equation is:

$$\bar{T}_i = \beta_0 + \beta_1 \ln t_i + u_{1,i} \quad (3.20)$$

The physical meaning of parameters  $\beta_0$  and  $\beta_1$  is given in Table 3.2. The best estimates for  $\beta_0$  and  $\beta_1$  are  $b_0$  and  $b_1$ , respectively, which are determined by

least squares regression. The solution that minimizes the sum of squared error is (all summations for  $i = 1, 2, \dots, n$ ):

$$b_0 = \frac{1}{n} \sum \ln t_i - b_1 \frac{1}{n} \sum \bar{T}_i \quad (3.21a)$$

$$b_1 = \frac{\sum \bar{T}_i \ln t_i - \frac{1}{n} \sum \ln t_i \sum \bar{T}_i}{\sum \ln^2 t_i - \frac{1}{n} (\sum \ln t_i)^2} \quad (3.21b)$$

An estimate of the apparent thermal conductivity is:

$$k = Q / (4\pi b_1) \quad (3.22)$$

An estimate of the variance in the measured apparent thermal conductivity is determined from the estimate of the standard deviation of the coefficient  $\beta_1$ . The confidence in the apparent thermal conductivity,  $\Delta k$ , is:

$$\Delta k = \left( \left| k - \frac{Q}{4\pi (b_1 - 2 s(b_1))} \right| + \left| k - \frac{Q}{4\pi (b_1 + 2 s(b_1))} \right| \right) \quad (3.23)$$

Where  $s(b_1)$  is the standard deviation of  $b_1$ , and its solution is:

$$s^2(b_1) = \frac{1}{n-2} \frac{\sum (\bar{T}_i - (b_0 + b_1 \ln t_i))^2}{\sum \ln^2 t_i - \frac{1}{n} (\sum \ln t_i)^2} \quad (3.24)$$

All summations for  $i = 1, 2, \dots, n$ .

Estimating the applicability of the long time solution determines the confidence in estimating the true thermal conductivity by the apparent thermal conductivity. One method for determining the applicability is to estimate the temperature contribution of  $R_{1,j}$ . If its contribution is not significant, then there exists a high degree of confidence in the apparent conductivity, else the thermal conductivity should be estimated from the short time solution.

In estimating  $R_{1,i}$  only the first term of the infinite series is calculated.

$$R_{1,i} \approx (\beta_2 + \beta_3 \ln t_i) t_i^{-1} \quad (3.25)$$

Estimating  $R_{1,i}$  requires estimates for the coefficients  $\beta_2$  and  $\beta_3$ . The parameters  $b_0$  and  $b_1$  determined by the long time solution include the effects of  $R_{1,i}$ . To estimate values for  $\beta_2$  and  $\beta_3$ , these effects must be removed, that is:

$$\bar{T}_i' = \beta_0 + \beta_1 \ln t_i + u_{1,i} - R_{1,i} \quad (3.26)$$

Simultaneous estimates for the  $\beta_i$ 's are determined by successive substitution.

$$b_i = G_i (b_0, b_1) \quad i = 2, 3 \quad (3.27a - b)$$

$$b_1' = b_1 - [ (R_{1,n} - R_{1,1}) / (\ln t_n - \ln t_1) ] \quad (3.27c)$$

$$b_0' = b_0 - [ R_{1,1} + (b_1' - b_1) \ln t_1 ] \quad (3.27d)$$

Where  $G_2$  and  $G_3$  are solved by substituting the following expressions into the expressions for  $\beta_2$  and  $\beta_3$  given in Table 3.1 (given in Equation 3.31):

$$Q / (4\pi k) = \beta_1 \quad (3.28a)$$

$$\ln (4\alpha / Ca^2) = \beta_\chi \quad (3.28b)$$

$$a^2/2\alpha = 2C^{-1} \exp(-\beta_\chi) \quad (3.28c)$$

$$\omega = 2 (B\beta_1)^{-1} \exp(-\beta_\chi) \quad (3.28d)$$

$$\beta_\chi = \frac{1}{\beta_1} \left( \beta_0 - \frac{Q}{4\pi k_1} \right) \quad (3.29a)$$

$$B = \frac{4\pi k_1}{Q} \frac{Ca^2}{4\alpha_1} \quad (3.29a)$$

The new estimates  $b_0'$  and  $b_1'$  are compared to the previous values  $b_0$  and  $b_1$ , and the steps are repeated until the values converge.  $R_{1,i}$  is then estimated from the values of  $b_2$  and  $b_3$  for a given experimental point  $i$ .

### 3.3.2 SHORT TIME SOLUTION FOR SAMPLE

The short time solution for the sample thermal conductivity is obtained by least squares regression modified with Lagrange multipliers. A method is presented for estimating the applicability of the short time solution.

The short time solution equation is:

$$\bar{T}_i = \beta_0 + \beta_1 \ln t_i + (\beta_2 + \beta_3 \ln t_i) t_i^{-1} + u_{2,i} \quad (3.30)$$

The physical meaning of parameters  $\beta_0$  and  $\beta_1$  is given in Table 3.1.  $\beta_2$  and  $\beta_3$  explicitly in terms of  $\beta_0$  and  $\beta_1$  are:

$$\beta_2 = G_2(\beta_0, \beta_1) = \frac{2}{C} \beta_1 \left[ \left(1 + \beta_\chi\right) e^{-\beta_\chi} - B \left( \beta_1 \beta_\chi + \frac{3}{4} \frac{Q}{4\pi k_1} \right) \right] \quad (3.31a)$$

$$\beta_3 = G_3(\beta_0, \beta_1) = \frac{2}{C} \beta_1 \left[ e^{-\beta_\chi} - B \beta_1 \right] \quad (3.31b)$$

$\beta_\chi$  and  $B$  are defined in Equation 3.29. The best estimates for  $\beta_0$  and  $\beta_1$  are  $b_0$  and  $b_1$ , respectively. The sum of squared error function to minimize is:

$$F = \sum_{i=1}^n \left( \bar{T}_i - \beta_0 - \beta_1 \ln t_i - \beta_2 \frac{1}{t_i} - \beta_3 \frac{1}{t_i} \ln t_i \right)^2 \quad (3.32)$$

From the discussion on Lagrange multipliers and regression the solution is:

$$\Phi_0 = \frac{\partial F}{\partial b_0} + \frac{\partial F}{\partial b_2} \frac{\partial b_2}{\partial b_0} + \frac{\partial F}{\partial b_3} \frac{\partial b_3}{\partial b_0} = 0 \quad (3.33a)$$

$$\Phi_1 = \frac{\partial F}{\partial b_1} + \frac{\partial F}{\partial b_2} \frac{\partial b_2}{\partial b_1} + \frac{\partial F}{\partial b_3} \frac{\partial b_3}{\partial b_1} = 0 \quad (3.33b)$$

This is a nonlinear set of equations with two unknowns,  $b_0$  and  $b_1$ . In this work, the Newton-Raphson technique is used to solve for the unknowns. The first

This is a nonlinear set of equations with two unknowns,  $b_0$  and  $b_1$ . In this work, the Newton-Raphson technique is used to solve for the unknowns. The first guess at the solution is the values of  $b_0$  and  $b_1$  from the long time solution. The iterative equations are:

$$b_{0,k+1} = b_{0,k} + \delta_{0,k} \quad (3.34a)$$

$$b_{1,k+1} = b_{1,k} + \delta_{1,k} \quad (3.34b)$$

$$\delta_{0,k} = \frac{1}{D} \left( \Phi_1 \frac{\partial \Phi_0}{\partial b_1} - \Phi_0 \frac{\partial \Phi_1}{\partial b_1} \right) \Big|_k \quad (3.35a)$$

$$\delta_{1,k} = \frac{1}{D} \left( \Phi_0 \frac{\partial \Phi_1}{\partial b_0} - \Phi_1 \frac{\partial \Phi_0}{\partial b_0} \right) \Big|_k \quad (3.35b)$$

$$D = \frac{\partial \Phi_0}{\partial b_0} \frac{\partial \Phi_1}{\partial b_1} - \frac{\partial \Phi_0}{\partial b_1} \frac{\partial \Phi_1}{\partial b_0}$$

The new  $b_0$  and  $b_1$  are compared with the previous values, and the steps are repeated until the values converge. An estimate of the apparent thermal conductivity is:

$$k = Q / (4\pi b_1) \quad (3.36)$$

Complete definitions of all partials for the error function and Newton-Raphson technique are presented in the appendices.

An estimate of the variance in the measured apparent thermal conductivity is determined from the estimate of the standard deviation of the coefficient  $\beta_1$ . The confidence in the apparent thermal conductivity,  $\Delta k$ , is determined by Equation 3.23. Where  $s(b_1)$  is the standard deviation of  $b_1$  for the short time solution, and an estimate of the standard deviation is:



$$s^2(b_1) = \frac{1}{n-4} \frac{\sum (\bar{T}_i - (b_0 + b_1 \ln t_i + b_2 t_i^{-1} + b_3 t_i^{-1} \ln t_i))^2}{\sum \ln^2 t_i - \frac{1}{n} (\sum \ln t_i)^2} \quad (3.37)$$

All summations for  $i = 1, 2, \dots, n$ .

Estimating the applicability of the short time solution determines the confidence in estimating the true thermal conductivity by the apparent thermal conductivity. One method for determining the applicability is to estimate the temperature contribution of  $R_{2,i}$ . If its contribution is not significant, then there exists a high degree of confidence in the apparent conductivity, else the thermal conductivity should be estimated from the short time solution.

$R_{2,i}$  is estimated indirectly by estimating  $R_{1,i}$ , where the first two terms of the infinite series are calculated.

$$R_{1,i} \approx (\beta_2 + \beta_3 \ln t_i) t_i^{-1} + (\beta_4 + \beta_5 \ln t_i + \beta_6 \ln^2 t_i) t_i^{-2} \quad (3.38)$$

Simultaneous estimates for the  $\beta_i$ 's are determined by successive substitution in the same manner as for the long time solution.

$$b_i = G_i(b_0, b_1) \quad i = 2, 3, 4, 5, 6 \quad (3.39a - e)$$

$$b_1' = b_1 - [ (R_{1,n} - R_{1,1}) / (\ln t_n - \ln t_1) ] \quad (3.39f)$$

$$b_0' = b_0 - [ R_{1,1} + (b_1' - b_1) \ln t_1 ] \quad (3.39g)$$

Where  $G_2$  thru  $G_6$  are solved by substituting the expressions in Equation 3.28 into the expressions for  $\beta_2$  thru  $\beta_6$  given in Table 3.2. The new estimates  $b_0'$  and  $b_1'$  are compared to the previous values  $b_0$  and  $b_1$ , and the steps are repeated until the values converge.  $R_{2,i}$  is then estimated from the values of  $b_4$ ,  $b_5$ , and  $b_6$  for a given experimental point  $i$ .

---

### 3.4 ALGORITHM FOR UNKNOWN PROBE

---

Both the long and short time solutions for a unknown sample require an estimate of the probe thermal conductivity and volumetric heat capacity. The short time solution for the probe properties is obtained by least squares regression modified with Lagrange multipliers.

The algorithm is programmed into the thermal conductivity operating system. The program listings are presented in the appendices.

The short time solution equation is:

$$\bar{T}_i = \beta_0 + \beta_1 \ln t_i + (\beta_2 + \beta_3 \ln t_i) t_i^{-1} + u_{2,i} \quad (3.30)$$

$\beta_0$  contains the probe thermal conductivity as an unknown, therefore it is still used as an independent coefficient.  $\beta_1$  is not a function of any probe property, therefore in this solution it is a constant not a coefficient. The choice for the second independent coefficient is between  $\beta_2$  and  $\beta_3$ , and this choice is arbitrary. The parameter selected will affect the form of the algorithm, not the final solution for the probe properties.  $\beta_2$  depends on the probe thermal conductivity and volumetric heat capacity, and  $\beta_3$  depends only on the probe volumetric heat capacity. For this reason  $\beta_3$  was selected as the second

independent coefficient. The physical meaning of parameters  $\beta_0$  and  $\beta_3$  is given in Table 3.2.  $\beta_1$  and  $\beta_2$  explicitly in terms of  $\beta_0$  and  $\beta_3$  are:

$$b_1 = \frac{Q}{4\pi k} \quad (3.40a)$$

$$b_2 = -\frac{3}{4} \frac{a^2}{2\alpha} b_0 + \frac{3}{4} \frac{4\pi k}{Q} b_0 b_3 + \frac{1}{4} b_3 \ln \left( \frac{4\alpha}{Ca^2} \right) \quad (3.40b)$$

$$+ \frac{Q}{4\pi k} \frac{a^2}{2\alpha} \left( 1 + \frac{3}{4} \ln \left( \frac{4\alpha}{Ca^2} \right) \right)$$

The best estimates for  $\beta_0$  and  $\beta_3$  are  $b_0$  and  $b_3$ , respectively. The sum of squared error function to minimize is:

$$F = \sum_{i=1}^n \left( \bar{T}_i - \beta_0 - \beta_1 \ln t_i - \beta_2 \frac{1}{t_i} - \beta_3 \frac{1}{t_i} \ln t_i \right)^2 \quad (3.41)$$

From the discussion on Lagrange multipliers and regression the solution is:

$$\Phi_0 = \frac{\partial F}{\partial b_0} + \frac{\partial F}{\partial b_2} \frac{\partial b_2}{\partial b_0} = 0 \quad (3.42a)$$

$$\Phi_3 = \frac{\partial F}{\partial b_3} + \frac{\partial F}{\partial b_2} \frac{\partial b_2}{\partial b_3} = 0 \quad (3.42b)$$

This is a nonlinear set of equations with two unknowns,  $b_0$  and  $b_3$ . In this work, the Newton-Raphson technique is used to solve for the unknowns. The first guess at the solution is twofold: 1) let the probe volumetric heat capacity equal

the sample volumetric heat capacity, and 2) assume the probe is a perfect conductor. The iterative equations are:

$$b_{0,k+1} = b_{0,k} + \delta_{0,k} \quad (3.43a)$$

$$b_{3,k+1} = b_{3,k} + \delta_{3,k} \quad (3.43b)$$

$$\delta_{0,k} = \frac{1}{D} \left( \Phi_3 \frac{\partial \Phi_0}{\partial b_3} - \Phi_0 \frac{\partial \Phi_3}{\partial b_3} \right) \Big|_k \quad (3.44a)$$

$$\delta_{3,k} = \frac{1}{D} \left( \Phi_0 \frac{\partial \Phi_3}{\partial b_0} - \Phi_3 \frac{\partial \Phi_0}{\partial b_0} \right) \Big|_k \quad (3.44b)$$

$$D = \frac{\partial \Phi_0}{\partial b_0} \frac{\partial \Phi_3}{\partial b_3} - \frac{\partial \Phi_0}{\partial b_3} \frac{\partial \Phi_3}{\partial b_0}$$

The new  $b_0$  and  $b_3$  are compared with the previous values, and the steps are repeated until the values converge. Estimates for the probe thermal conductivity and volumetric heat capacity are:

$$k_1 = \frac{Q}{4\pi} \left( b_0 - \frac{Q}{4\pi k} \ln \left( \frac{4\alpha}{Ca^2} \right) \right)^{-1} \quad (3.45a)$$

$$(\rho C_p)_1 = (\rho C_p) \left( 1 - \frac{4\pi k}{Q} \frac{2\alpha}{a^2} b_3 \right) \quad (3.45b)$$

Complete definitions of all partials for the error function and Newton-Raphson technique are presented in the appendices.

---

### 3.5 CONCLUSION

---

In this chapter an algorithm for data acquisition and analysis was presented. The procedure for determining the thermal conductivity of a selected sample by the transient needle probe technique is:

- 1) Confidence estimates on the long and short time solution require the probe thermal conductivity and volumetric heat capacity to be known. Therefore, an experiment is conducted on a sample of known thermal conductivity and volumetric heat capacity. From this experiment, the probe properties are estimated by the algorithm for an unknown probe. A calibration of this type, unlike calibrations in the literature, does not require that the probe test only samples similar to the calibration sample. If it is known that an experiment on a sample will reach long times, then absolute conductivities are measured and calibration is not required.
- 2) On an unknown sample, perform multiple experiments and average these experiments into one composite experiment. The three operating parameters,  $Q$ ,  $\Delta t$ , and  $N\Delta t$ , are adjusted to properly locate the optimum solution region. After the experiment is completed, determine the conductivity by the long time solution for an unknown sample. If the confidence estimates show that long times were not reached, then determine conductivity by the short time solution for an unknown sample.

Implementation of the solution algorithms is presented in the chapter on experimental results.

# CHAPTER 4

## **THERMAL CONDUCTIVITY MEASUREMENT SYSTEM**

---

## 4.0 INTRODUCTION

---

In this chapter the thermal conductivity measurement system employing the transient needle probe is presented. The mathematical modeling and data acquisition and analysis presented earlier are incorporated into this system.

The thermal conductivity system is a flexible multifunctional software and hardware package designed for automatic thermal conductivity measurements on solids and viscous liquids. Experimental control, data acquisition, and data analysis for a thermal conductivity needle probe are accomplished via an IBM Personal Computer. A Keithley Series 500 System is the interface between the probe and the computer. A software operating system was developed to control the hardware.

Advantages of the thermal conductivity system design are: 1) all components of the system have off-the-shelf availability and are relatively inexpensive, and 2) a variety of probes can be used without requiring an update in the system hardware. In addition to performing thermal conductivity measurements, the system offers personal computer and analog / digital interfacing capabilities.

The presentation of the thermal conductivity system is in three parts:

- 1) System hardware specifications,
- 2) System hardware installation, and
- 3) System software.

Operation and documentation of the software is presented in the appendices.

---

## **4.1 SYSTEM HARDWARE SPECIFICATIONS**

---

The thermal conductivity system hardware requirements are minimal. A diagram of the system is given in Figure 4.1. Table 4.1 lists all of the hardware in the developmental thermal conductivity system. Also given in this table are the modifications possible in creating a duplicate system. Further hardware specifications are presented in two parts:

- 1) Thermal conductivity needle probe, and
- 2) Personal computer and interfacing.

### **4.1.1 THERMAL CONDUCTIVITY NEEDLE PROBE**

The thermal conductivity system will accept a variety of transient needle probes. Any needle probe selected must comply with certain system operating specifications concerning the heater wire and thermistor. These specifications arise from the inherent characteristics of the needle probe and Keithley Series 500 System. The probes used in this work were purchased as off-the-shelf items from Fluid Dynamics Corporation (operated by Warren Conner), Boulder, Colorado. The complete schematic for the needle probe is given in Figure 4.1. These probes are of a similar design as originally used by Von Herzen and Maxwell (1959).

The physical properties of the probe determine the required sample size. For the probes in this work, the sample should be a right cylindrical sample 30 times the probe diameter and the same length as the probe (refer to Chapter 2).



Figure 4.1  
Thermal Conductivity System Hardware

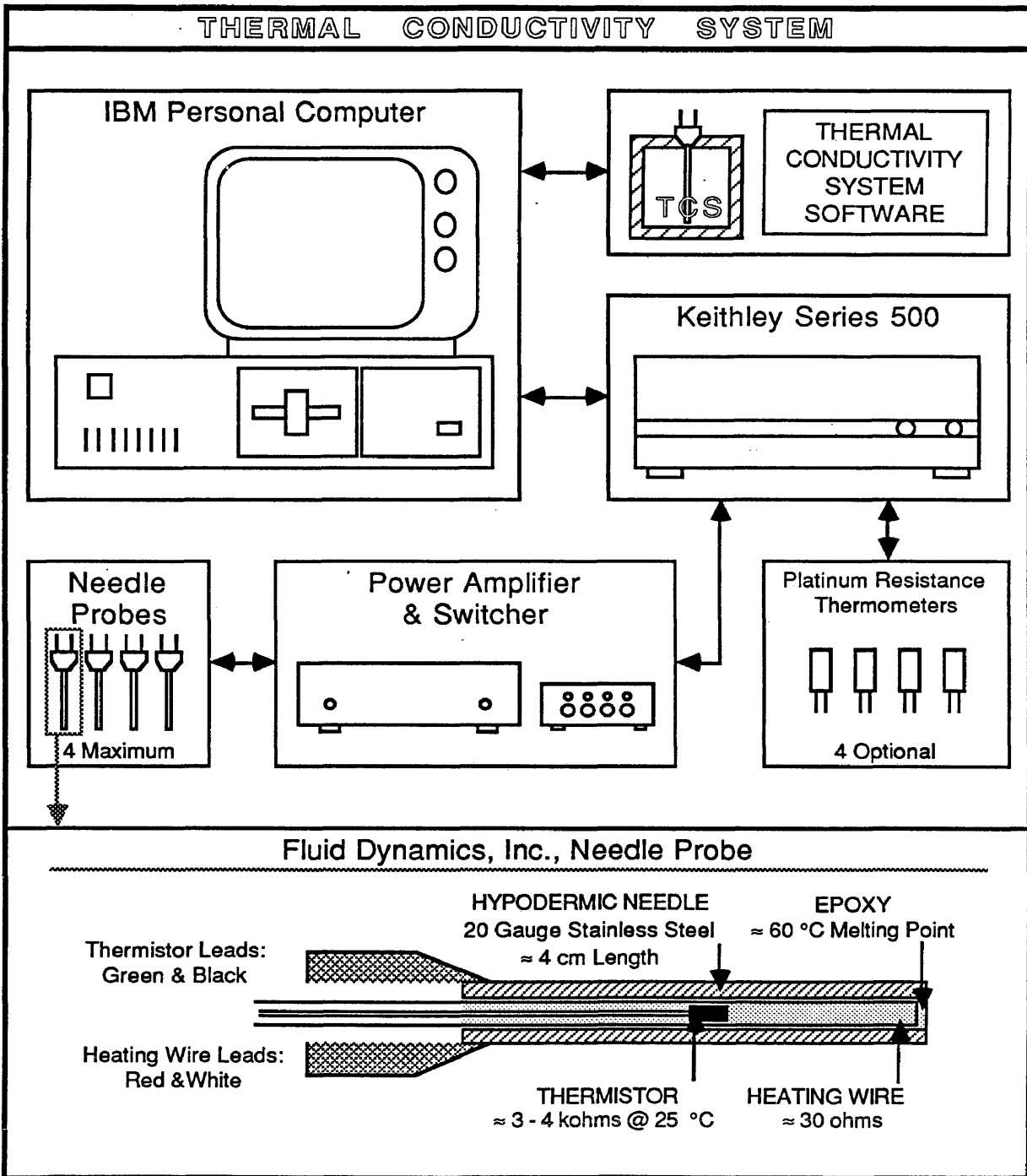


Table 4.1

## Developmental and Required Thermal Conductivity System Hardware

	<b>DEVELOPMENTAL</b>	<b>REQUIRED</b>
<b>COMPUTER SYSTEM</b>	IBM Personal Computer 2 Floppy Disk Drives, IBM and Tandem Apparat, Inc., 15 Mbyte Hard Disk 512 kbytes Internal Memory IBM Color Graphics Card Quadram Quadboard NEC 12" Monochrome Monitor Epson MX80/FT Printer  MS-DOS, Version 3.00 IBM Advanced Basic, Version 3.0	IBM Personal Computer, PC or XT 2 Floppy Disk Drives or Hard Disk 320 kbytes Internal Memory IBM Compatible Color Graphics Card Printer Port Monitor Printer  MS-DOS, Version 3.00 or Higher IBM Advanced Basic, Version 3.0
<b>INTERFACING SYSTEM</b>	Keithley Data Acquisition & Control, Inc. System 500 - Modular System AIM1, Analog Input ADM2, 14-bit Analog/Digital AOM1/5 12-bit Digital/Analog AIM6, RTD and Strain Gauge Keithley Soft500, Versions up to 4.0.  CSM Physics Dept., Electronics Shop Precision D.C. Power Amp Switcher, Manual	Keithley Data Acquisition & Control, Inc. System 500 - Modular System AIM1, Analog Input ADM2, 14-bit Analog/Digital AOM1/5, 12-bit Digital/Analog AIM6, RTD and Strain Gauge, optional Keithley Soft500, Versions up to 4.0.  Power Amplifier, > 5 kohm load, upgrade current for > 1 ohm load Switcher, controls amp output to probe
<b>MEASUREMENT SYSTEM</b>	Fluid Dynamics Corporation, Needle Probes P/N 2-204  Omega Engineering, Platinum Resistance Thermometers  Sample Cell, CSM CEPR Dept., Technicians Shop  Neslab, Inc., Temperature Bath	Needle Probes, Any that comply with specifications  Platinum Resistance Thermometers, For measuring bath, optional  Sample Cell  Temperature Bath Controls sample temperature

Power is supplied to the heater wire by a constant d.c. voltage source ( $P = V \cdot I = V^2 \cdot R^{-1} = I^2 \cdot R$ ;  $P$ =power,  $V$ =volts,  $I$ =current,  $R$ =resistance). Currently, the digital to analog power supply in the Keithley Series 500 is set to a maximum of 5 volts. The maximum power input to the probe is:

$$Q_{\max} = 25 \cdot R_{\text{htr}}^{-1} \cdot L_{\text{htr}}^{-1} \quad (4.1)$$

Where  $Q_{\max}$  is the power input per unit length in  $W \cdot m^{-1}$ ,  $R_{\text{htr}}$  is the heater resistance in ohms, and  $L_{\text{htr}}$  is the length of the heated section of the probe in meters. From this equation, it appears that maximum power input is obtained by forcing the length and resistance to be infinitesimal, but this may require currents in excess of the heater wire current limitations. The heater wire specifications for maximum current and voltage must not be exceeded for any power input.

The temperature of the thermistor is determined by its resistance. Resistance measurements are obtained by a series comparison to a known resistance. Several specifications exist for the probe thermistor resistance,  $R_{\text{therm}}$ , and standard resistance,  $R_{\text{std}}$ :

- For maximum accuracy the standard resistance should be matched to the thermistor resistance. Due to current limitations of the Keithley Series 500 digital to analog converter:

$$R_{\text{std}} + R_{\text{therm}} > 5 \text{ kohms} \quad (4.2)$$

- The voltage supplied to the standard resistor and the thermistor is limited to 1 volt each, and the current supplied to the thermistors will never exceed 100  $\mu$ amps. The total voltage supplied to both resistances is determined by a short algorithmic program as follows:

$$\begin{aligned}
 &\text{If } (R_{\text{std}} > 10 \text{ kohms}) \text{ or } (R_{\text{therm}} > 10 \text{ kohms}) \text{ then} && (4.3) \\
 &\quad ( \text{ If } (R_{\text{therm}} > R_{\text{std}}) \text{ then} \\
 &\quad\quad \text{Volts} = 0.95 \cdot (R_{\text{therm}} + R_{\text{std}}) \cdot R_{\text{therm}}^{-1} \\
 &\quad \text{Else} \\
 &\quad\quad \text{Volts} = 0.95 \cdot (R_{\text{therm}} + R_{\text{std}}) \cdot R_{\text{std}}^{-1} ). \\
 &\text{Else} \\
 &\quad \text{Volts} = 0.095 \cdot (R_{\text{therm}} + R_{\text{std}})
 \end{aligned}$$

#### 4.1.2 PERSONAL COMPUTER AND INTERFACING

The IBM Personal Computer is a industry standard, with operational information widely available. The interface between the probe and the computer, the Keithley Series 500 System, is operated from interpreted Microsoft Advanced BASIC.

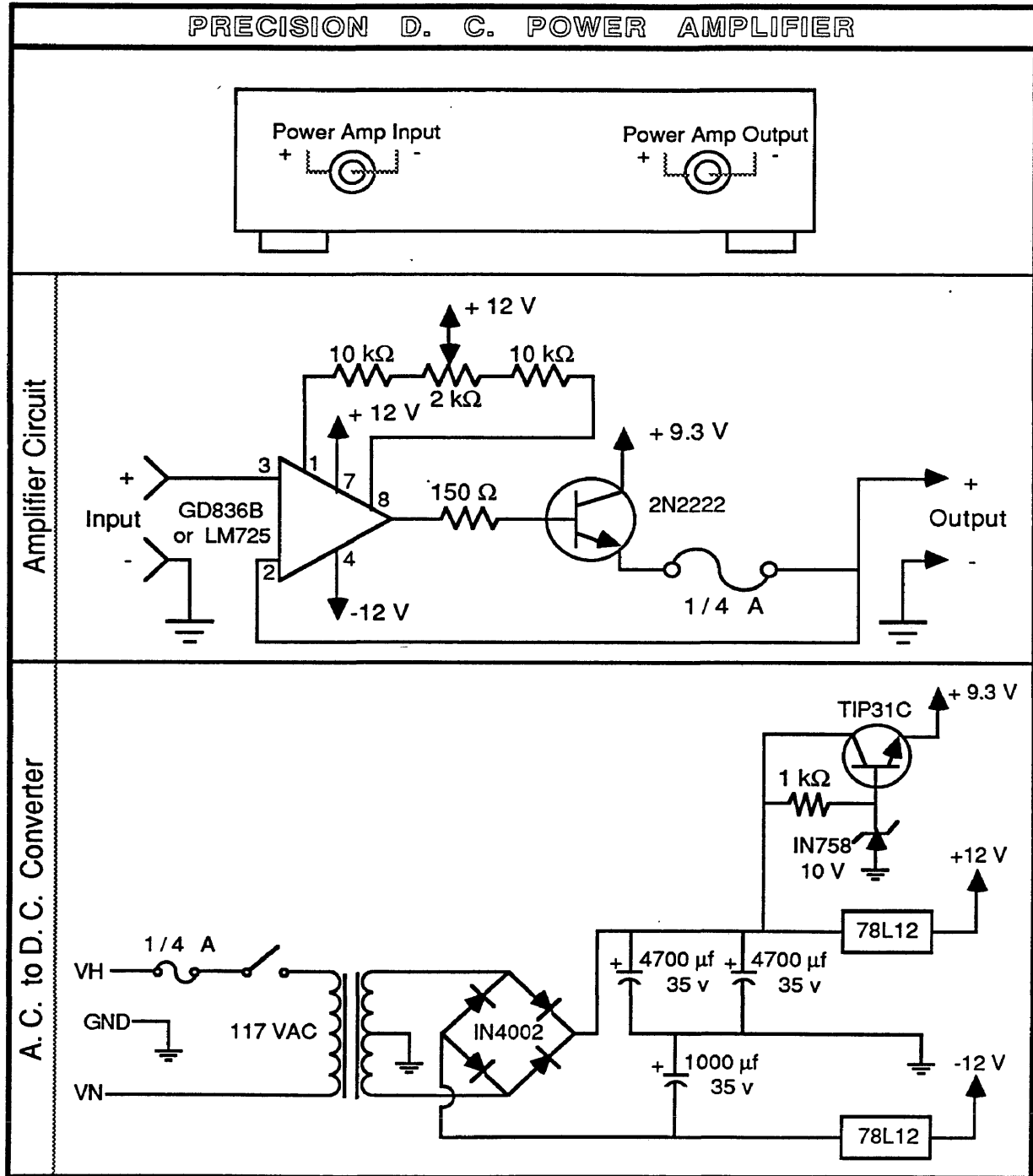
The Keithley Series 500 System is a state of the art analog / digital interfacing machine. The System 500 is capable of analog to digital input, digital to analog output, and several other features. The essential features of the Keithley system as equipped are:

- 8 channels of differential 14-bit analog to digital.
- 5 channels of 12-bit digital to analog.
- 4 channels for 100 ohm platinum resistance thermometers.
- Sampling rate to 15 kHz.
- Programmable interval timers.
- Internal power supplies.
- Comprehensive software package.

The use of the Keithley Series 500 System requires first loading their Soft500 system into the computer, and then writing a MS-BASICA program that includes Soft500 commands. Direct interaction with the Series 500 hardware is performed by Soft500, which supports all available hardware features in any configuration. The thermal conductivity system software supplies the necessary MS-BASICA programs for thermal conductivity measurements using a needle probe.

A precision direct current power amplifier, designed by the Electronics Shop in the Physics Department at the Colorado School of Mines, corrects for deficiencies the Keithley System 500 has in supplying power to the needle probe heater wire. The voltage source of the System requires a 5 kohm load resistance, and since the probe heater wires are less than 100 ohms the power amplifier is necessary. The schematic for the amplifier is presented in Figure 4.2.

Figure 4.2  
Schematic for Precision D.C. Power Amplifier



---

## 4.2 SYSTEM HARDWARE INSTALLATION

---

Installation of the thermal conductivity system is completed in three steps:

- 1) Computer system installation,
- 2) Interfacing system installation, and
- 3) Measurement system installation.

Install the computer system with all required components (listed in Table 4.1) as per their manuals.

There are three parts to the interfacing system installation: 1) the Keithley Series 500, 2) the power amplifier, and 3) the switcher.

The thermal conductivity system software assumes that the modules of the Keithley System 500 are arranged as:

AIM1,	Slot 1,	Gain X10, Differential Input
ADM2,	Slot 2,	Range -10/10v
AIM6,	Slot 4,	Gain X1
AOM1/5,	Slot 5,	Range 0/5v on All Channels

Other arrangements require modification of the thermal conductivity software.

The power amplifier is wired into channel 4 on the AOM1. Wiring details are presented in the Keithley Series 500 manuals. This channel is used as the power supply for all probe heater wires. The software assumes that the user switches the heater wire connections. All probe thermistors are wired into the other four channels on the AOM1, and the software will automatically switch to different probes.

The thermal conductivity needle probes are interfaced to the Series 500 through the switcher. The switcher completes every part of the thermistor and heating wire circuitry, except for the thermistor and heater wire themselves. It is recommended not to directly hard wire the probes into the Series 500. Power surges from the AOM1 channels may occur when the Series 500 is turned on. These surges can damage the needle probe electronics. Complete wiring diagrams for the switcher are presented in Figure 4.3.

There are three parts to the measurement system installation: 1) the sample cell and temperature bath, 2) the platinum resistance thermometers, and 3) the thermal conductivity needle probes.

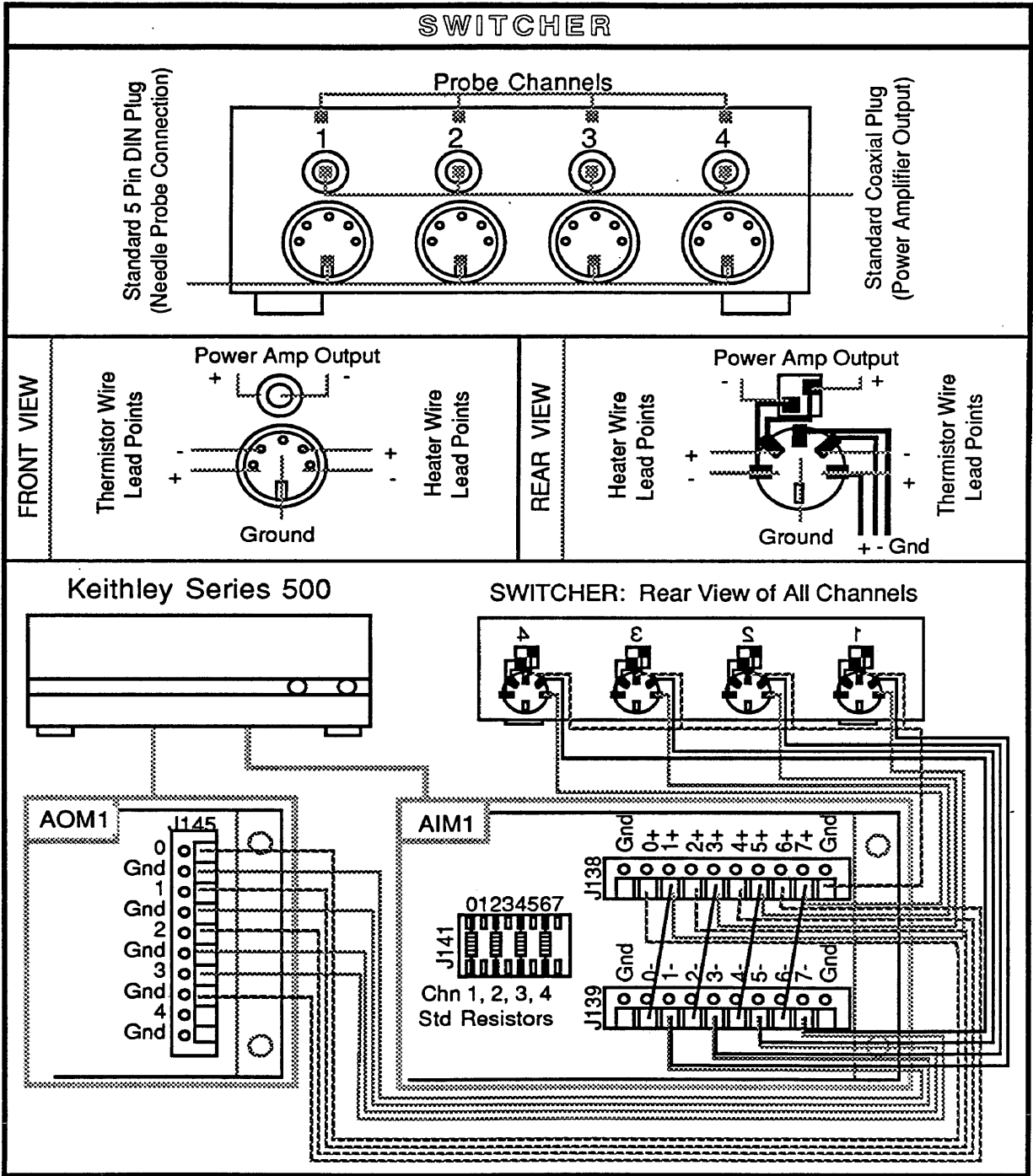
An acceptable sample cell and temperature bath arrangement satisfies two criteria: 1) the probe is inserted into the sample, and 2) the probe and sample are kept at a constant uniform temperature.

For each needle probe there is an optional platinum resistance thermometer (measures the bath temperature). The platinum resistance thermometer, corresponding to the  $i^{\text{th}}$  probe, is inserted into the  $i-1$  channel on the AIM6. Consult Keithley's System 500 manual for the installation procedure.

The final step (of installing the thermal conductivity system), is the installation of the thermal conductivity needle probes. The thermistor and heating wire leads are connected to a standard 5 pin DIN plug. The DIN plug is connected into the switcher. Figure 4.3 shows the configuration of all pins in the plug. Note, the needle probe is removed from the switcher whenever turning the Series 500 on or off. This prevents a power surge from destroying the thermistor or heating wire.



Figure 4.3  
Switcher Installation Diagram



---

### 4.3 SYSTEM SOFTWARE

---

The thermal conductivity system software has three functions:

- Series 500 System Configuration,
- Temperature Response Calibration, and
- Thermal Conductivity Measurement.

The operating procedure for this software is presented in the Appendices.

Series 500 System Configuration establishes the configuration of the needle probes and platinum resistance thermometers. Thermal Conductivity Apparatus informs the thermal conductivity system of the configuration of the Series 500 and the thermal conductivity needle probes.

Temperature Response Calibration determines the temperature characteristics of the needle probes and platinum resistance thermometers, and it has two parts. First is Data Set Acquisition, which acquires the temperature response data sets for the selected probes and thermometers. Second is Analysis and Plotter, which analyzes and plots two types of data: 1) the temperature versus resistance characteristics for the probe, and 2) the actual temperature versus measured temperature for the thermometers.

Thermal Conductivity Measurement determines the thermal conductivity of a given solid or viscous liquid, and it has two parts. First is Acquisition and Analysis, which performs the experiment and determines the sample thermal conductivity. Also, it determines the probe thermal conductivity and volumetric heat capacity from an experiment on a known sample. Second is File Search

and Plotter, which displays an experiment, two experiments, or the thermal conductivities from all experiments for a given material. Also, it locates past experiments according to a given set of specifications.

The IBM, Keithley, and thermal conductivity system software necessary to run the system are given in Figure 4.4. This table also lists how the software is stored on two diskettes. In this table, " DIR "Default\" " refers to the default directory, and all other directory references are defined from the default directory. There are three subdirectories which must be defined, but require no initial information. These directories are used by the thermal conductivity system for data storage during system operation. The interaction of these programs is shown in Figure 4.5.

Figure 4.4

Thermal Conductivity System Software Installation Requirements

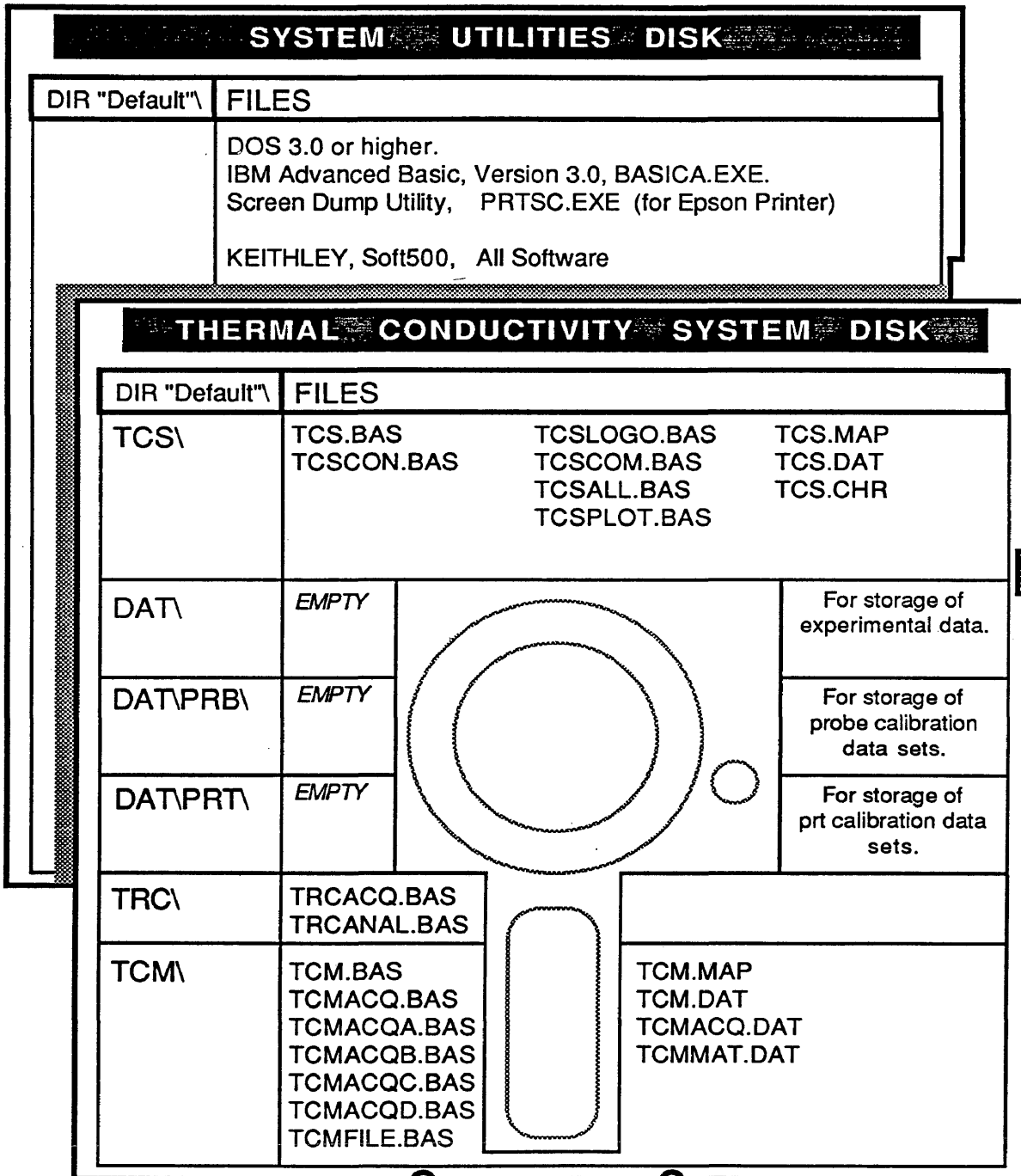
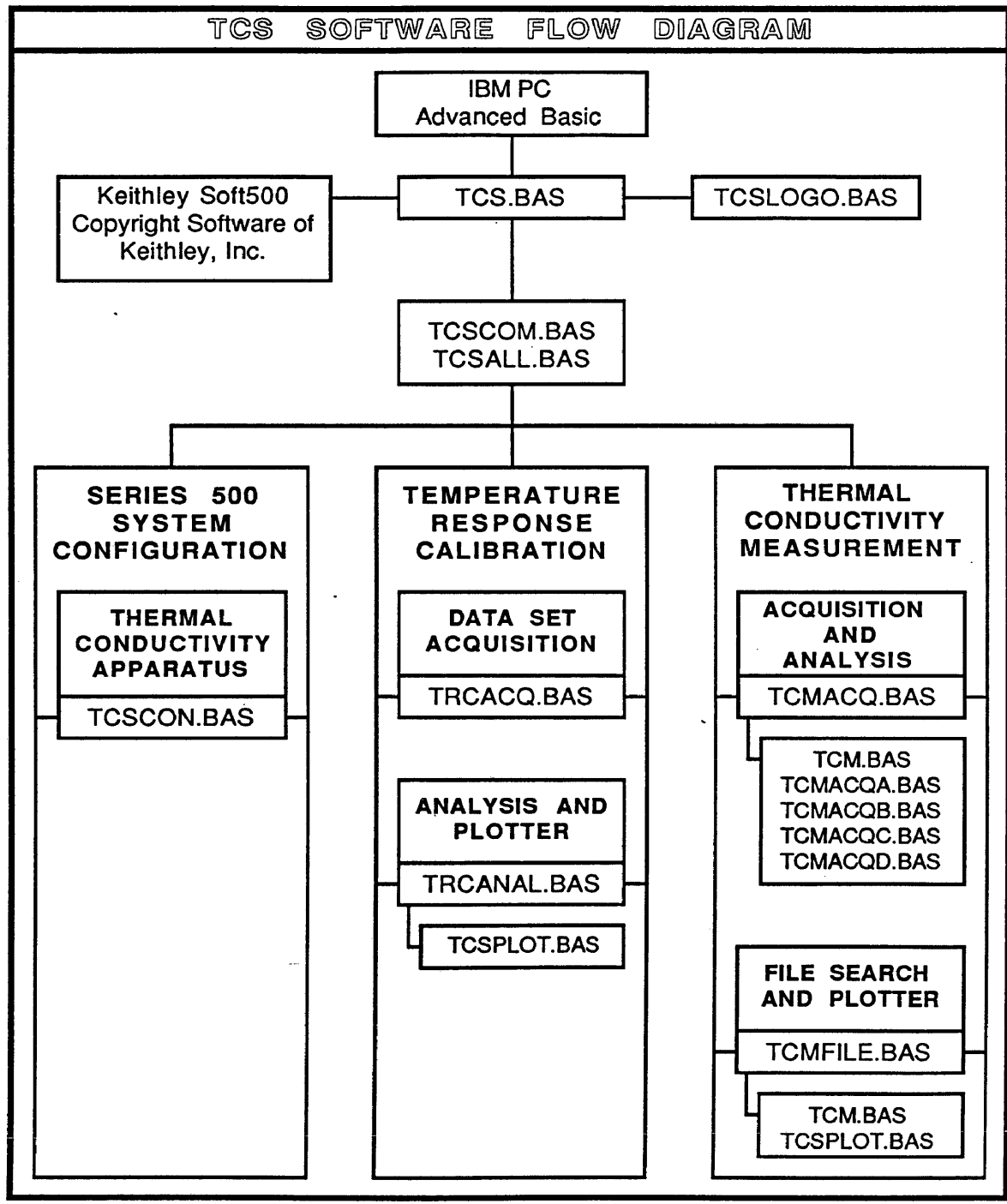


Figure 4.5  
Thermal Conductivity System Program Flow Diagram



---

## 4.4 CONCLUSION

---

In this chapter the thermal conductivity measurement system employing the transient needle probe was presented. Experimental control, data acquisition, and data analysis for a thermal conductivity needle probe are accomplished via an IBM Personal Computer. A Keithley Series 500 System is the interface between the probe and the computer.

The system is designed to handle a variety of needle probes. In this work only one type of needle probe is employed. The probe is similar to that of Von Herzen and Maxwell (1959), and is fabricated by Fluid Dynamics.

All aspects of the experimental procedure are computerized and under software control. Successful conductivity measurements require only knowledge of the system software. Detailed knowledge of the transport phenomena involved is not required. In this software, absolute thermal conductivities are measured by the probe heat transfer model presented earlier.

# CHAPTER 5

## SYSTEM VERIFICATION ON SOLIDS AND LIQUIDS

---

## 5.0 INTRODUCTION

---

In this chapter the correct operation of the thermal conductivity measurement system is verified. Materials selected for this study are those with known conductivities.

Conductivity measurements were performed on several solids: 1) tertiary butyl alcohol, 2) tetrahydrofuran hydrate, and 3) water ice. The thermal conductivity of solid and liquid tertiary butyl alcohol differ by approximately ten percent, and it is a good substance for comparing the difference between axial conduction and liquid convection. Tetrahydrofuran hydrate has been measured previously (Ross and Andersson, 1981), and its conductivity should be similar to methane and propane hydrate (presented in the next chapter). All solid measurements are within five percent of accepted literature values.

Conductivity measurements were performed on several liquids: 1) tertiary butyl alcohol, 2) glycerin, 3) 1 - methylnaphthalene, 4) water, and 5) toluene. The long time solution adequately models experiments on the first three samples. Accurate measurements on water and toluene require the short time solution. All liquid measurements, with the exception of toluene, are within fourpercent of accepted literature values.

The presentation of the system verification is in six parts:

- 1) Prior to any measurements there are two calibration steps. First, the analog to digital and digital to analog responses of the Keithley Series 500 System are calibrated. Second, the resistance versus temperature



characteristics of the probe thermistor are calibrated. Both of these steps are independent of the model used for data analysis.

- 2) The initial measurements on solids are described. All of these measurements employ the long time solution with no error analysis, therefore no probe properties are required. These tests demonstrate the overall validity of the model.
- 3) The initial measurements on liquids are described. All of these measurements employ the long time solution with no error analysis, therefore no probe properties are required. These tests demonstrate the use of the needle probe on viscous liquids.
- 4) Full utilization of the long and short time solutions requires the probe thermal conductivity and volumetric heat capacity. The calibration of the probe properties is dependent on the heat transfer model employed. For this reason, the measurement of the properties is after the initial measurements on solids and liquids that verify the validity of the model.
- 5) Measurements employing the long and short time solutions are presented for various liquids. These measurements require the probe properties. The short time solution improves the accuracy of the measurements. In fact, the results show that the needle probe can measure the thermal conductivity of a liquid far less viscous than glycerin, which is opposite of the statement by Stoll and Bryan (1979).
- 6) Guidelines are presented for the selection of model, the long or short time solution, employed for data analysis. These guidelines are used in the selection of the model for the application to hydrates in porous media.

---

## 5.1 THERMAL CONDUCTIVITY SYSTEM CALIBRATION

---

The thermal conductivity system is calibrated prior to any thermal conductivity measurements. First, the analog to digital and digital to analog responses of the Keithley Series 500 are calibrated. Second, the resistance versus temperature characteristics of the probe thermistor are calibrated.

### 5.1.1 COMPUTER AND INTERFACING CALIBRATION

The accuracy to which the Keithley Series 500 is calibrated affects the accuracy of the probe resistance measurements and the power supplied to the probe heating wire. The Series 500 modules to calibrate are:

AIM1,	Slot 1,	Gain X10, Differential Input
ADM2,	Slot 2,	Range -10/10v
AIM6,	Slot 4,	Gain X1
AOM1/5,	Slot 5,	Range 0/5v on All Channels

The Keithley Series 500 manuals completely described the steps required to calibrate these modules. The power supplies, volt meters, and resistors used to calibrate these modules were all of greater accuracy than the accuracy of the modules.

All modules were calibrated within the accuracy claimed by Keithley. For the paired combination of the AIM1 and ADM2, the analog input is accurate to  $\pm 1/2$  least significant bits with 14 bits in the voltage range of -1/+1 volt. For the AOM1, the analog output is accurate to  $\pm 1/2$  least significant bits with 12 bits in the voltage range of 0/+5 volt.

### **5.1.2 PROBE THERMISTOR CALIBRATION**

The accuracy in the calibration of the probe thermistor directly affects the accuracy of the thermal conductivity measurement. The accuracy in determining the thermistor temperature is affected by: 1) the inherent characteristics of the thermistor, 2) the methodology of measuring the temperature of the thermistor, and 3) the accuracy of the calibration process for the resistance versus temperature characteristics of the thermistor.

In this work, the needle probes purchased from Fluid Dynamics used thermistors made by Fenwal Electronics. These thermistors are rated for a maximum current of 100  $\mu$ amps and have platinum lead wires that are 0.001 inch in diameter.

The temperature of the thermistor is determined from its resistance. The methodology of determining the resistance is presented in the previous chapter. The accuracy of the resistance measurement is in part determined by the accuracy of the Keithley Series 500. All connections between the probe and the interfacing used shielded wire to minimize electrical interference.

For all probes used in this work, the resistance versus temperature characteristics were determined. This determination, or calibration, employed a bath that maintains temperature stability to an accuracy of 0.03 °C. The temperature of the bath was set at several temperatures from -20 to 30 °C. At each temperature set point the resistance of the thermistor(s) and the temperature of the bath were measured. The reported thermistor resistance is an average of several resistance measurements (averaging reduces the variance of the resistance measurement). The reference temperature of the

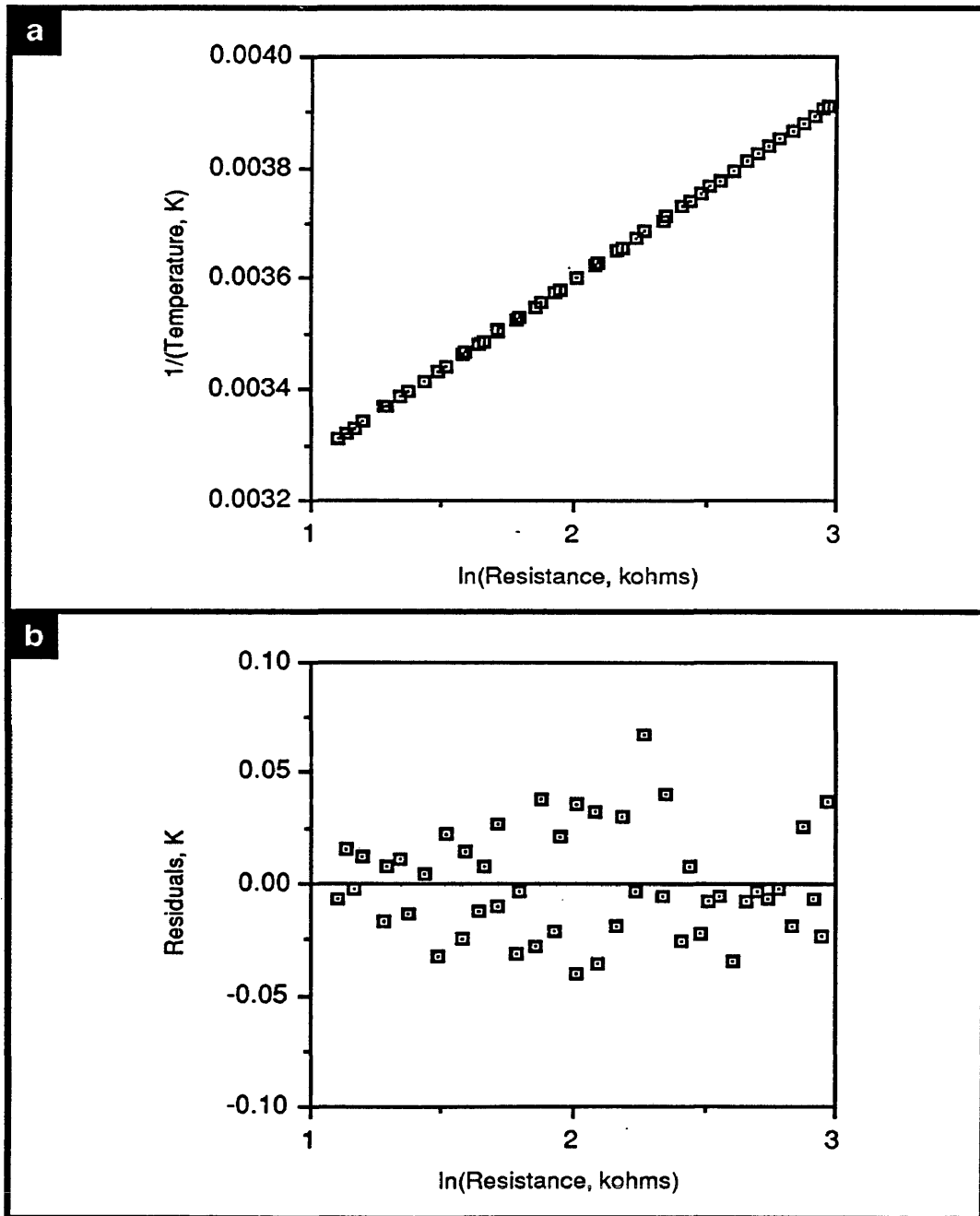
bath was measured from a platinum resistance thermometer with a Mueller bridge. The calibration of this platinum resistance thermometer is traceable to the National Bureau of Standards and is accurate to 0.001 °C. A typical thermistor resistance plot and residual plot are given in Figures 5.1 a and b (the residual is the difference between experimental data and the linear regression curve fit of the data).

Note, the variance of the temperature rise measurement, discussed in the data acquisition algorithm in Chapter 3, is not the same as the variance of the absolute temperature measurement. If each experiment of a multiple experiment were conducted under identical conditions, then the variance of the temperature rise measurement is twice the variance of the absolute temperature measurement, under the following assumptions: 1) the temperature measurement is characterized by a normal distribution, and 2) the temperature measurement at any time during an experiment is independent of the temperature measurement at the beginning of the experiment. The variance of the temperature rise measurement is also affected by the temperature stability of the sample during the course of the multiple experiments.

The variance of the temperature rise measurement affects the number of multiple experiments required. The magnitude of the variance is a factor of the specific probe thermistor and its calibration. A different probe may have a different variance for the same number of multiple experiments. The variance in the temperature measurement is the determining factor for how many runs must be made in a multiple experiment.

Figure 5.1

Thermistor Resistance and Residuals for the Needle Probe TCP111



---

## 5.2 INITIAL MEASUREMENTS ON SOLIDS

---

Thermal conductivity measurements were conducted on three solids: 1) tertiary butyl alcohol, 2) tetrahydrofuran hydrates, and 3) water ice. For the needle probes employed in this work, conductivity ratio effects are not significant on tertiary butyl alcohol, are fairly significant on tetrahydrofuran hydrate, and are significant on ice.

Complete results for these compounds are given in Table 5.1. In this table,  $k$  is the best estimate of the thermal conductivity using the long time solution,  $s_k$  is the standard deviation of the data, and  $M$  is the number of experiments performed. All conductivities are reported at the temperature corresponding to half the experimental temperature increase (typically 1 to 2 K). The responses of typical experiments are given in Figure 5.2.

### 5.2.1 SOLID TERTIARY BUTYL ALCOHOL

The system was initially evaluated by performing experiments on solid tertiary butyl alcohol. The thermal conductivity was determined to be  $0.122 \pm 0.006 \text{ W}\cdot\text{m}^{-1}\cdot\text{K}^{-1}$  at 293 K. A literature value of  $0.123 \text{ W}\cdot\text{m}^{-1}\cdot\text{K}^{-1}$  (Perkins,1983) is in excellent agreement with this system's value. Tertiary butyl alcohol has a relatively high melting point (297.6 K) and is easily formed as a solid around the probe. This is necessary to negate thermal resistance between the probe and sample. Figure 5.3 presents a typical experiment with the apparent conductivities and the solution region.

Table 5.1  
Measured Thermal Conductivities of Various Solids

Tertiary Butyl Alcohol	T (K)	M	k (W.m <sup>-1</sup> K <sup>-1</sup> )	s <sub>k</sub> (W.m <sup>-1</sup> K <sup>-1</sup> )
	263	6	0.117	0.003
	271	3	0.121	0.008
	276	4	0.125	0.003
	288	5	0.119	0.002
	293	6	0.122	0.006

Tetrahydrofuran Hydrate †	T (K)	M	k (W.m <sup>-1</sup> K <sup>-1</sup> )	s <sub>k</sub> (W.m <sup>-1</sup> K <sup>-1</sup> )
	254	7	0.473	0.013
	259	5	0.474	0.009
	264	5	0.476	0.008
	270	5	0.480	0.007
	273	6	0.482	0.008
	271	6	0.477	0.004
	267	6	0.473	0.006
	262	5	0.476	0.004
	257	4	0.477	0.005
	253	4	0.477	0.005
	250	4	0.475	0.008

Water Ice	T (K)	M	k (W.m <sup>-1</sup> K <sup>-1</sup> )	s <sub>k</sub> (W.m <sup>-1</sup> K <sup>-1</sup> )
	268	2	2.28	0.01
	269	14	2.29	0.03
270	2	2.32	0.03	

- o m = 1, each experiment represents only one experiment, not an average of multiple experiments.  
o long time solution for all conductivities, no error estimation.

†, o temperatures listed in experimental order.

Figure 5.2

Experimental Response Behavior of Various Solids

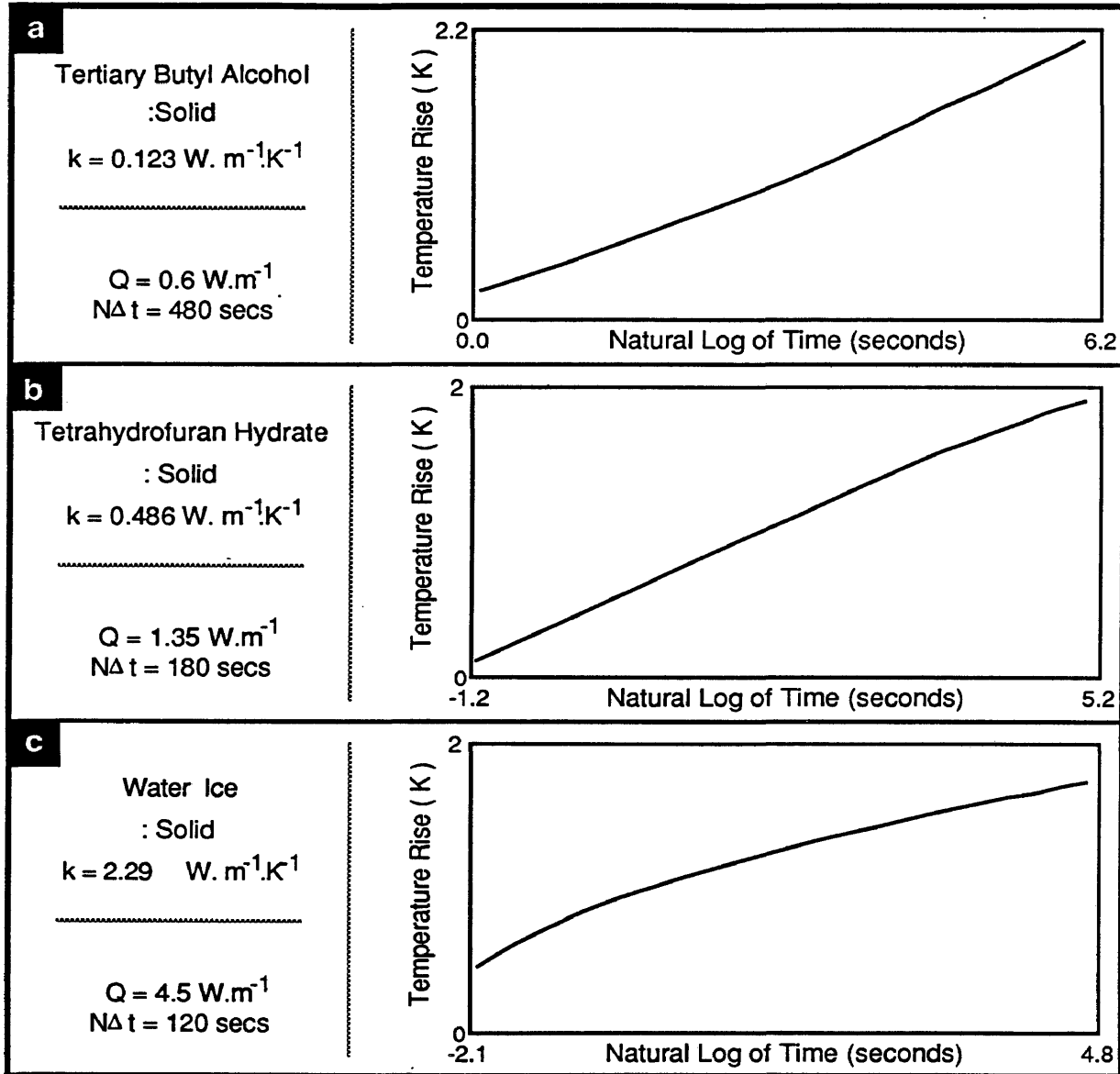
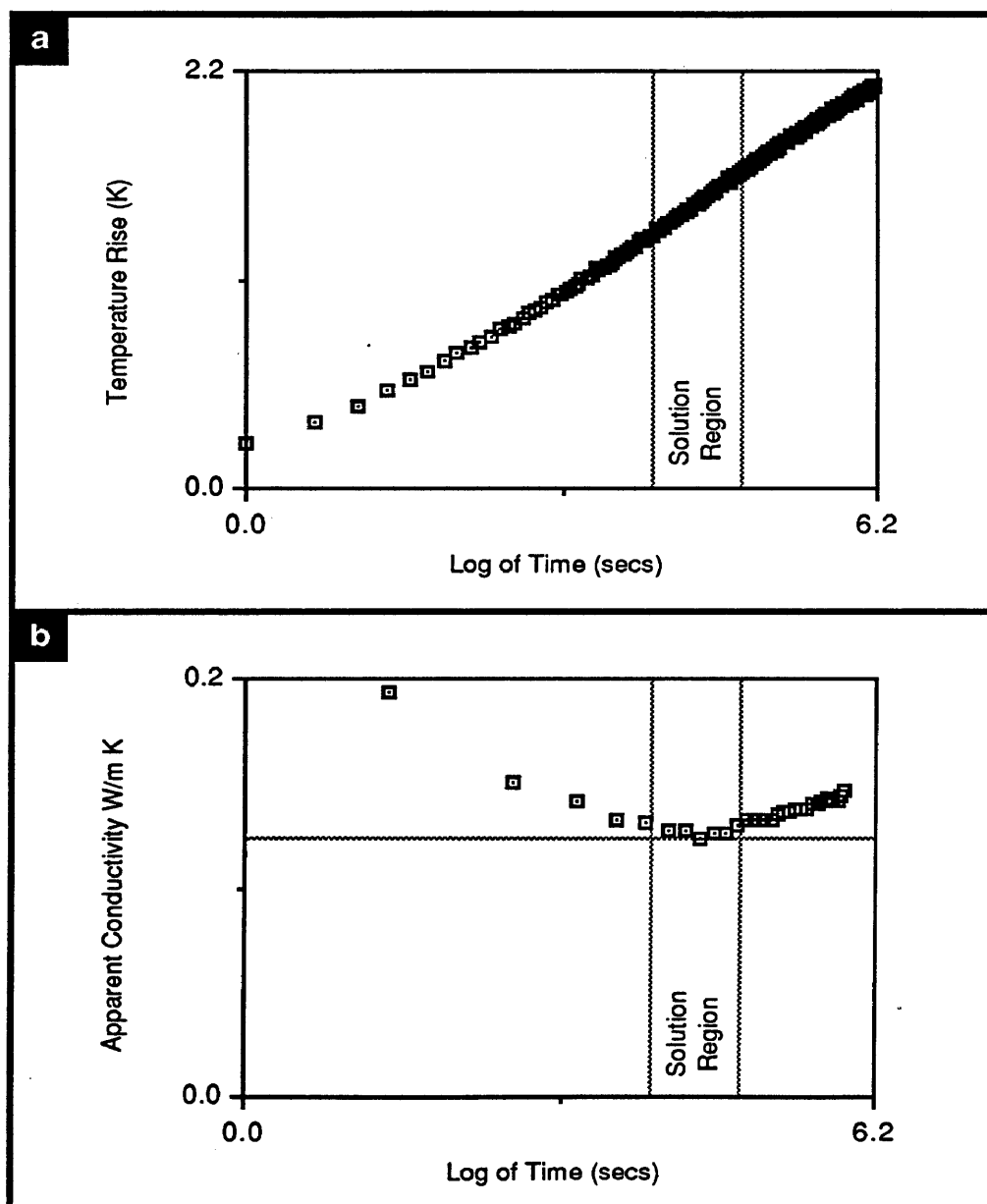




Figure 5.3

Acquisition and Analysis on Solid Tertiary Butyl Alcohol



### 5.2.2 TETRAHYDROFURAN HYDRATE

Liquid tetrahydrofuran rich hydrates were formed. The molar ratio of water to tetrahydrofuran was 16.88 to 1, and pure structure II hydrates have a molar ratio of 17 to 1. The thermal conductivity was determined to be  $0.486 \pm 0.008 \text{ W}\cdot\text{m}^{-1}\cdot\text{K}^{-1}$ . A literature value of  $0.5 \text{ W}\cdot\text{m}^{-1}\cdot\text{K}^{-1}$  for slightly ice rich hydrates is reported by Cook and Laubitz. The very early time portion of an experiment exhibited slight conductivity effects, and this time was ignored in finding the optimum solution region. Figure 5.4 presents a typical experiment with the apparent conductivities and the solution region.

### 5.2.3 WATER ICE

Ice measurements (structure Ih) were the most difficult to determine from an experiment. The thermal conductivity was determined to be  $2.29 \pm 0.03 \text{ W}\cdot\text{m}^{-1}\cdot\text{K}^{-1}$  at 269 K, which compares favorably with a literature value of  $2.21 \text{ W}\cdot\text{m}^{-1}\cdot\text{K}^{-1}$  (Ross, Andersson, and Backstrom, 1977). The early time portion of an experiment exhibited significant conductivity effects, and this time was ignored in finding the solution region. Figure 5.5 presents a typical experiment with the apparent conductivities and the solution region.

Figure 5.2c shows that conductivity ratio effects are so significant that the slope at the beginning of an experiment is reversed from normal. Figure 5.2 shows that the slope reversal increases as the conductivity ratio increases. At some conductivity ratios the initial slope will match the slope during the long time portion of the experiment. The entire experiment then appears to be at long time, and it is possible that none of the experiment is at long time.

Figure 5.4  
Acquisition and Analysis on Tetrahydrofuran Hydrate

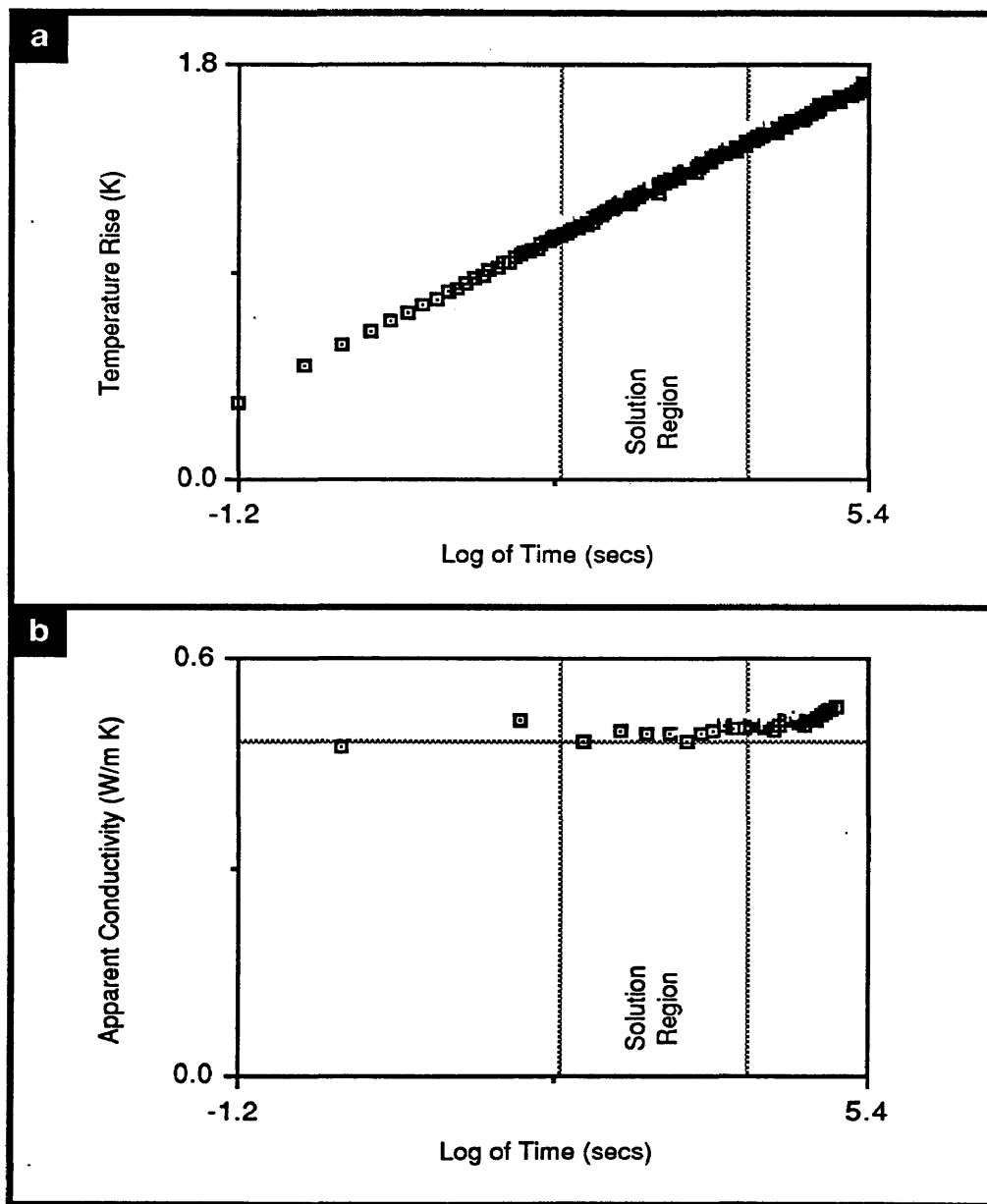
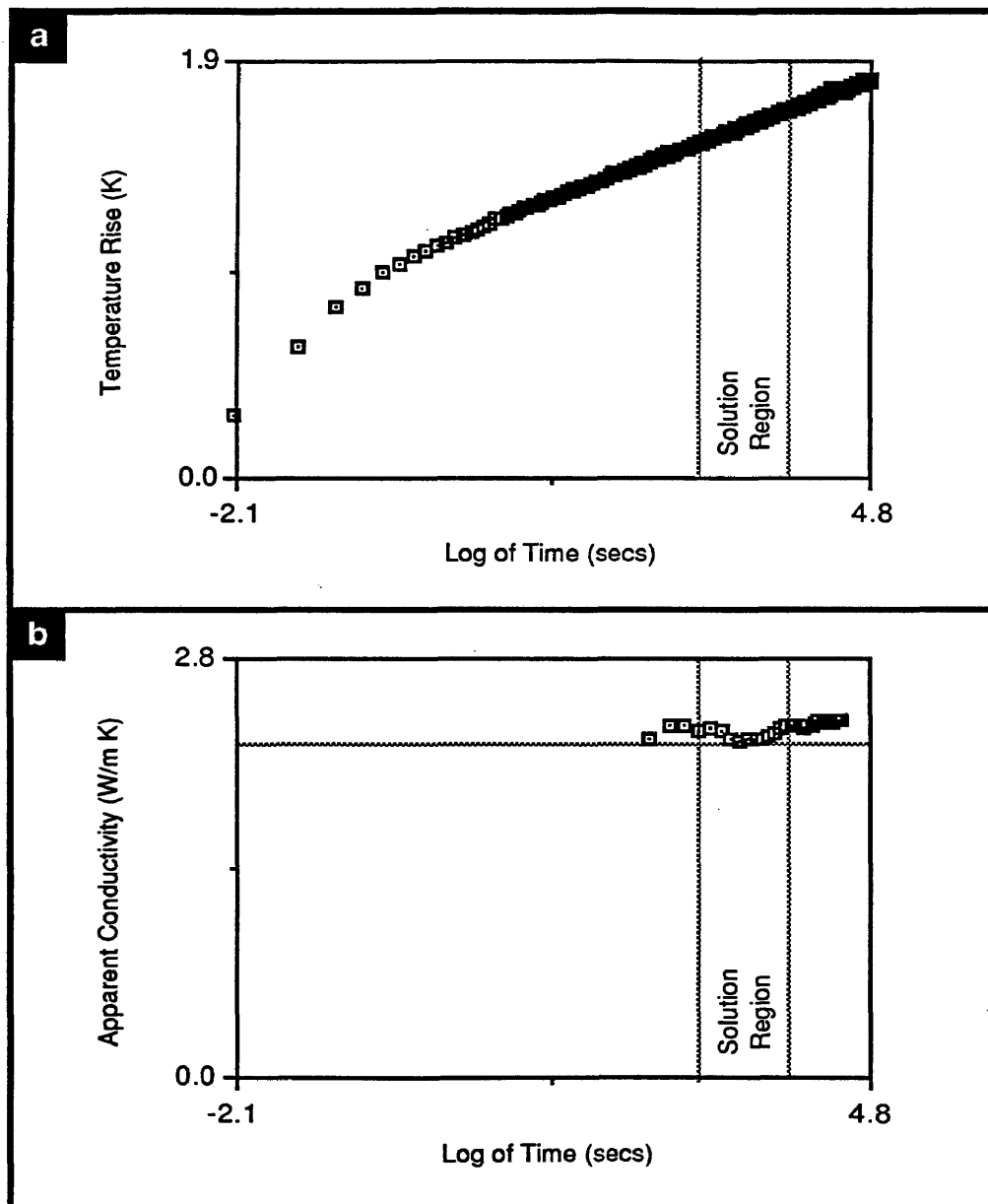


Figure 5.5  
Acquisition and Analysis on Water Ice



---

## 5.3 INITIAL MEASUREMENTS ON LIQUIDS

---

Three liquids, tertiary butyl alcohol, 1-methylnaphthalene, and glycerin, were analyzed at room temperature using the thermal conductivity needle probe. No elaborate safeguards were taken to minimize the effect of liquid convection. A technique for building cells to minimize convection for the transient hot-wire technique is described by Graham (1985) and Perkins (1983). A cell to minimize convection effects could also be built for the needle probe.

Table 5.2 summarizes the results of all liquid measurements. All thermal conductivities are reported at the temperature corresponding to half the experimental temperature increase (typically 1 to 2 K). Figure 5.6 shows the responses of typical experiments for the liquids.

For the compounds presented, the corrections due to heat capacity effects (short time solution) are within the stated experimental accuracy. This result was determined by using the actual fluid properties and the theory for all times presented by Carslaw and Jaeger (1959).

### 5.3.1 LIQUID TERTIARY BUTYL ALCOHOL

Experiments were conducted on 99.9% pure liquid tertiary butyl alcohol (viscosity, 6 cP) at room temperature. A thermal conductivity of  $0.110 \pm 0.006$   $\text{W}\cdot\text{m}^{-1}\cdot\text{K}^{-1}$  at 301 K was determined, which is in excellent agreement with that of  $0.109$   $\text{W}\cdot\text{m}^{-1}\cdot\text{K}^{-1}$  reported by Perkins (1983). Figure 5.7 presents a typical experiment with the apparent conductivities and the optimum solution region.

Table 5.2

## Measured Thermal Conductivities of Various Liquids

Tertiary Butyl Alcohol	T (K)	M	$k$ (W.m <sup>-1</sup> K <sup>-1</sup> )	$s_k$ (W.m <sup>-1</sup> K <sup>-1</sup> )	Q (W.m <sup>-1</sup> )
	300	7	0.122	0.006	0.8
	300	5	0.119	0.005	0.6
	300	3	0.113	0.005	0.5
	301	4	0.110	0.006	0.4

1-Methyl- naphthalene	T (K)	M	$k$ (W.m <sup>-1</sup> K <sup>-1</sup> )	$s_k$ (W.m <sup>-1</sup> K <sup>-1</sup> )	Q (W.m <sup>-1</sup> )
	297	4	0.135	0.002	1.0
	297	4	0.134	0.002	0.9
	297	2	0.136	0.001	0.8
	296	4	0.133	0.002	0.7
	296	4	0.136	0.003	0.6

Glycerin	T (K)	M	$k$ (W.m <sup>-1</sup> K <sup>-1</sup> )	$s_k$ (W.m <sup>-1</sup> K <sup>-1</sup> )	Q (W.m <sup>-1</sup> )
	297	1	0.298	-	1.3
	301	2	0.292	0.005	1.1
	298	4	0.296	0.004	1.0
	298	4	0.287	0.005	0.9
	297	3	0.289	0.004	0.8

- 
- o  $m = 1$ , each experiment represents only one experiment, not an average of multiple experiments.
  - o long time solution for all conductivities, no error estimation.

Figure 5.6

## Experimental Response Behavior of Various Liquids

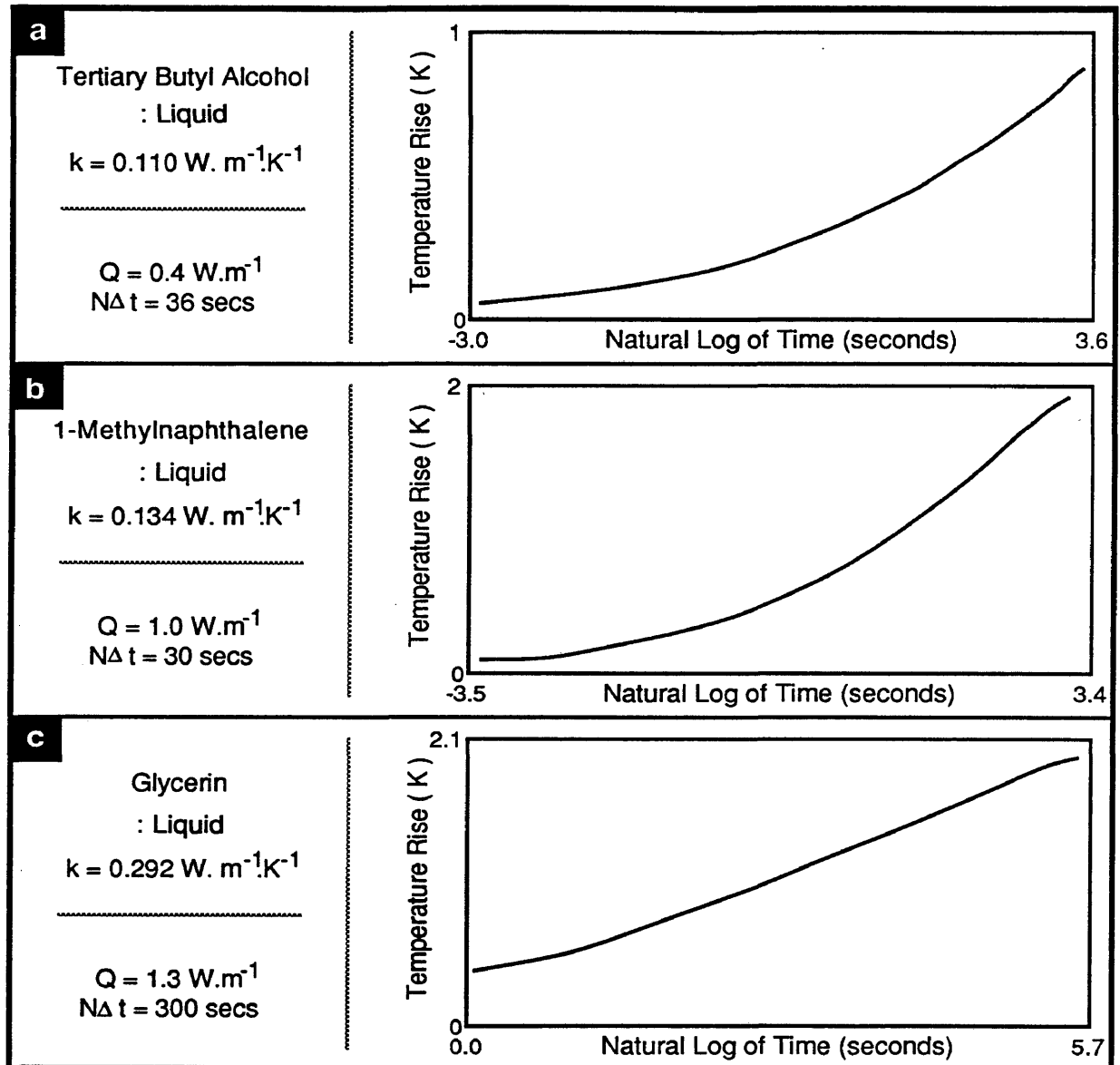
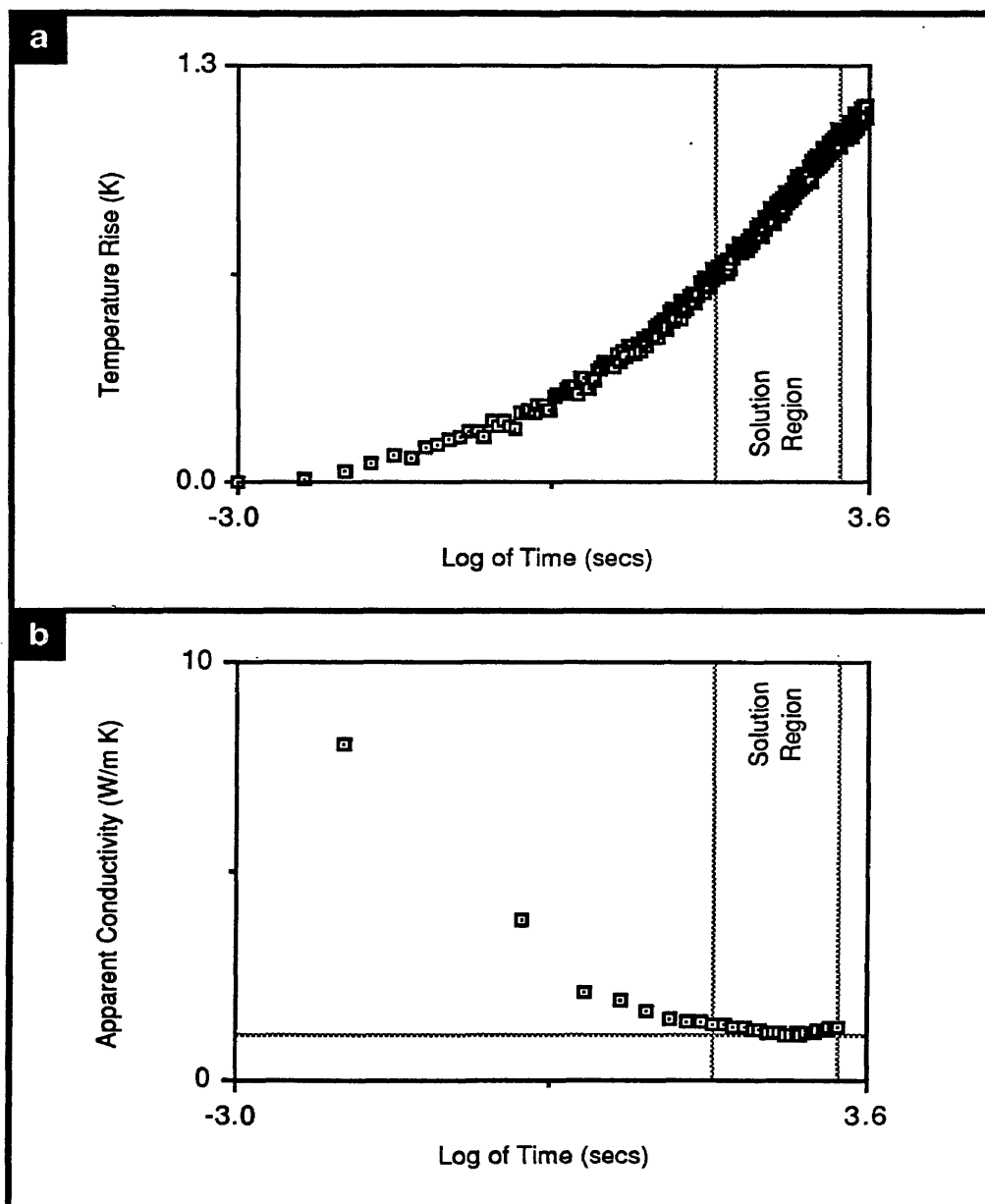


Figure 5.7

Acquisition and Analysis on Liquid Tertiary Butyl Alcohol





At first consideration of the raw data in Table 5.2, it appears that the measured thermal conductivity varies with the heat supplied to the medium. Further analysis showed that this effect was due to convection instabilities. The occurrence of this phenomenon is delayed by decreasing the supplied heat. Therefore, the maximum confidence in the measured thermal conductivity occurs at minimum heat input.

Heat inputs lower than those shown in Table 5.2 were not feasible. As the heat input decreases, the temperature rise of the probe decreases. The relative discretization error in the temperature measurement then increases. This causes a large error associated with fitting the temperature rise versus log of time plot.

Both liquid convection and probe finite length have the same effect on the experimental temperature response in that both cause a temperature rollover. Experiments on solid tertiary butyl alcohol were performed in order to distinguish between convection effects and axial effects.

As theoretically predicted by the model of Kierkus, Mani, and Venart (1973) and experimentally observed, the time when axial effects dominate is not related to the heat input to the probe. In liquids, the onset of convection is directly related to the probe power input. Minimizing the power input lengthens the time period until convection, then the long time infinite line source solution yields a more accurate fit.

### 5.3.2 LIQUID 1-METHYLNAPHTHALENE

Experiments were conducted on 1-methylnaphthalene (viscosity, 3 cP) at room temperature. A thermal conductivity of  $0.135 \pm 0.002 \text{ W}\cdot\text{m}^{-1}\cdot\text{K}^{-1}$  at 296 K was determined, which is in excellent agreement with that of  $0.134 \text{ W}\cdot\text{m}^{-1}\cdot\text{K}^{-1}$  reported by Graham (1985). Convection did not appear significant in any of the measurements. Figure 3.3 presents a typical experiment with the apparent conductivities and the optimum solution region.

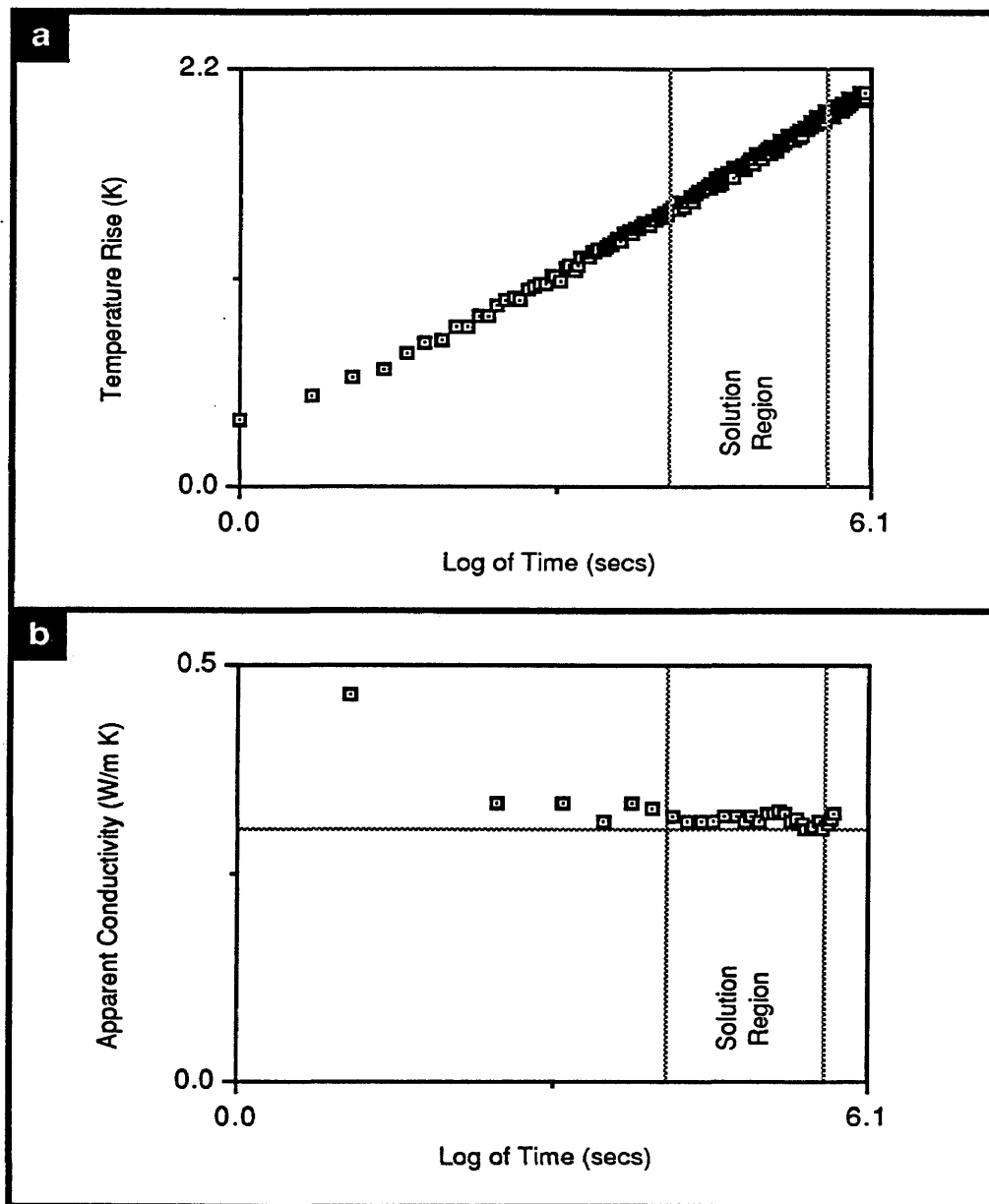
More results are presented for this liquid in the rest of this chapter.

### 5.3.3 LIQUID GLYCERIN

Experiments were conducted on pure liquid glycerin (viscosity, 3800 cP) at room temperature. A thermal conductivity of  $0.292 \pm 0.004 \text{ W}\cdot\text{m}^{-1}\cdot\text{K}^{-1}$  at 298 K was determined, which is in agreement with a literature value of  $0.288 \text{ W}\cdot\text{m}^{-1}\cdot\text{K}^{-1}$  (Thermal Properties of Matter, 1970). Figure 5.8 presents a typical experiment with the apparent conductivities and the optimum solution region.

Stoll and Bryan (1979) recommended using needle probes on liquids only as viscous as glycerin. In this research, no convective instabilities occurred with any level of power input. Experimental temperature increases were observed in excess of 2 K without causing convection. Temperature increases of this magnitude cause convection in tertiary butyl alcohol and 1-methylnaphthalene. Through accurate data analysis it becomes possible to use the probe on liquids far less viscous than glycerin.

Figure 5.8  
Acquisition and Analysis on Liquid Glycerin



---

## 5.4 MEASUREMENT OF PROBE PROPERTIES

---

The measurements on solids and liquids verified the correct operation of the system. In all cases, the long time solution was employed, and it was not necessary to employ the short time solution. The applicability of the long time solution was determined by comparison to literature. Solving the short time solution or estimating the applicability of the long or short time solution requires the probe thermal conductivity and volumetric heat capacity.

All probes used in this work are of the same design and construction. In the following discussion the physical properties for a particular probe (Fluid Dynamics P/N 2-204, P/N 111, referred by TCP111) are determined. The process is the same for all probes, and the thermal conductivity and volumetric heat capacity of other Fluid Dynamic probes are similar.

1-Methylnaphthalene was selected as the standard for determining the probe properties. Graham (1985) measured the thermal conductivity and volumetric heat capacity of this fluid by the transient hot-wire technique. At room temperature (297 K), the values are:  $k = 0.134 \text{ W}\cdot\text{m}^{-1}\cdot\text{K}^{-1}$ , and  $(\rho C_p) = 1.66 \times 10^6 \text{ J}\cdot\text{m}^{-3}\cdot\text{K}^{-1}$ .

The process for determining the probe properties was:

- 1) Three multiple experiments,  $m = 2, 4, \text{ and } 9$ , were performed on 1-methylnaphthalene with  $Q = 1.0 \text{ W}\cdot\text{m}^{-1}$ ,  $\Delta t = 0.03 \text{ secs}$ ,  $N\Delta t = 30 \text{ secs}$ .

- 2) The optimum solution region was located for each experiment (refer to selection on optimum solution region in Chapter 3). For  $\delta = 0.10$  the region for all experiments extended from  $\ln t = 2.17$  to  $\ln t = 2.87$ .
- 3) For 1-methylnaphthalene the optimum solution region was adequately described by the long time solution. The unknown probe algorithm is a short time solution. Therefore, the region selected to measure properties should include shorter times, but should not be short enough that the short time solution is not applicable. The region selected extended from  $\ln t = 2.00$  to  $\ln t = 2.70$ .
- 4) The algorithm for unknown probe properties (consult Chapter 3) was then used to determine  $k_1$  and  $(\rho C_p)_1$ . The results are:
- $m = 2, N = 1000$   
 $\rightarrow k_1 = 0.383 \text{ W}\cdot\text{m}^{-1}\cdot\text{K}^{-1}, (\rho C_p)_1 = 2.214 \times 10^6 \text{ J}\cdot\text{m}^{-3}\cdot\text{K}^{-1}$
  - $m = 4, N = 1000$   
 $\rightarrow k_1 = 0.380 \text{ W}\cdot\text{m}^{-1}\cdot\text{K}^{-1}, (\rho C_p)_1 = 2.232 \times 10^6 \text{ J}\cdot\text{m}^{-3}\cdot\text{K}^{-1}$
  - $m = 9, N = 1000$   
 $\rightarrow k_1 = 0.384 \text{ W}\cdot\text{m}^{-1}\cdot\text{K}^{-1}, (\rho C_p)_1 = 2.208 \times 10^6 \text{ J}\cdot\text{m}^{-3}\cdot\text{K}^{-1}$
- 5) The best estimates for the probe properties are then:
- $$k_1 = 0.382 \text{ W}\cdot\text{m}^{-1}\cdot\text{K}^{-1}, (\rho C_p)_1 = 2.22 \times 10^6 \text{ J}\cdot\text{m}^{-3}\cdot\text{K}^{-1}$$

The estimation of the volumetric heat capacity by this method is reasonable. Rueff (1985,1) measured the heat capacity of a different probe and estimated a value of  $2.6 \times 10^6 \text{ J}\cdot\text{m}^{-3}\cdot\text{K}^{-1}$ . The method employed by Rueff (1985,2) to measure the heat capacity required the destruction of the probe and is not a viable means of measuring the heat capacity of a good probe.

The estimate of the thermal conductivity by this method is reasonable. First, the conductivity is reasonable for an epoxy. Second, the conductivity effects shown in the earlier time of the ice measurements require that the thermal conductivity of the sample be significantly greater than the probe. In another estimation technique, the heat capacity for this probe was fixed to the value measured by Rueff (1985,1) for another probe. Then the thermal conductivity was determined by the long and short time solutions. In both cases the thermal conductivity estimates were the same and they were slightly lower than the estimated value given above.

---

## 5.5 MEASUREMENTS WITH SOLUTION ANALYSIS

---

The long time solution with remainder analysis,  $R_{1,j}$ , and the short time solution with remainder analysis,  $R_{2,j}$ , are determined with the probe properties. Measurements, with solution analysis are presented for three liquid compound: 1) 1-methylnaphthalene, the calibration compound, 2) water, and 3) toluene.

### 5.5.1 1-METHYLNAPHTHALENE LIQUID

A set of measurements on 1-methylnaphthalene are presented in Tables 5.3 and 5.4. When estimating the probe properties, it was assumed that measurements on this liquid reach long times. As expected, the long and short time solution yield thermal conductivities that are not statistically different.

The sample standard deviation of the temperature measurement,  $s$ , decreases with the square root of  $m$ . By the central limit theorem for statistics, normality of the temperature rise measurements is assumed. Past the average of 16 experiments the small decrease in  $s$  does not warrant the increase in experimental time. To calculate  $s$  the number of averaged experiments,  $m$ , must be greater than one. Therefore, an optimal range for  $m$  is  $2 \leq m \leq 16$ .

The remainder terms for the long time solution,  $R_{1,j}$ , are greater (in most cases) than than standard deviation of the temperature rise measurement,  $s$ , but they are not significantly greater. The remainder terms for the short time solution,  $R_{2,j}$ , did not converge for all cases. For 1-methylnaphthalene a large number of multiple experiments are necessary to justify the short time solution.

Table 5.3

## Thermal Conductivity Measurements on Liquid 1-Methylnaphthalene

m	N	LONG TIME SOLUTION , k $\pm$ $\Delta$ k	SHORT TIME SOLUTION , k $\pm$ $\Delta$ k
2	300	0.136 $\pm$ 0.003	0.137 $\pm$ 0.003
	600	0.138 $\pm$ 0.002	†
	1000	0.137 $\pm$ 0.001	0.137 $\pm$ 0.001
4	300	0.136 $\pm$ 0.002	0.136 $\pm$ 0.002
	600	0.136 $\pm$ 0.001	0.134 $\pm$ 0.001
	1000	0.136 $\pm$ 0.001	0.136 $\pm$ 0.001
9	300	0.137 $\pm$ 0.002	0.136 $\pm$ 0.002
	600	0.136 $\pm$ 0.001	0.135 $\pm$ 0.001
	1000	0.137 $\pm$ 0.001	0.136 $\pm$ 0.001
16	300	0.136 $\pm$ 0.001	0.134 $\pm$ 0.001
	600	0.137 $\pm$ 0.001	0.133 $\pm$ 0.001
	1000	0.137 $\pm$ 0.000	0.137 $\pm$ 0.001
25	300	0.136 $\pm$ 0.001	0.134 $\pm$ 0.001
	600	0.137 $\pm$ 0.000	0.136 $\pm$ 0.001
	1000	0.137 $\pm$ 0.000	0.137 $\pm$ 0.001
30	300	0.138 $\pm$ 0.000	0.132 $\pm$ 0.001
	600	0.135 $\pm$ 0.002	0.137 $\pm$ 0.001
	1000	0.137 $\pm$ 0.001	0.137 $\pm$ 0.001

o All conductivities  $W \cdot m^{-1} \cdot K^{-1}$

o All experiments at 297 K, with probe TCP111, and  $Q = 1.0 W \cdot m^{-1}$ ,  $N\Delta t = 30$  secs.

†, o Short time solution converged for all cases except  $m = 2$ ,  $N = 600$ .



Table 5.4

## Solution Analysis for Measurements on Liquid 1-Methylnaphthalene

m	N	s	$T_1$ { $\hat{R}_{1,1}$ }, $T_n$ { $\hat{R}_{1,n}$ }
2	300	0.012	1.443 { 0.014 }, 1.783 { 0.017 }
	600	0.009	1.395 { 0.048 }, 1.749 { 0.039 }
	1000	0.015	1.412 { 0.012 }, 1.814 { 0.017 }
4	300	0.007	1.424 { 0.005 }, 1.748 { 0.007 }
	600	0.008	1.418 { 0.012 }, 1.827 { 0.003 }
	1000	0.007	1.424 { 0.008 }, 1.822 { 0.015 }
9	300	0.006	1.418 { 0.011 }, 1.768 { 0.016 }
	600	0.006	1.407 { 0.002 }, 1.749 { 0.011 }
	1000	0.004	1.411 { 0.020 }, 1.809 { 0.021 }
16	300	0.004	1.408 { 0.013 }, 1.807 { 0.002 }
	600	0.004	1.374 { 0.029 }, 1.742 { 0.007 }
	1000	0.004	1.412 { 0.012 }, 1.814 { 0.017 }
25	300	0.003	1.448 { 0.001 }, 1.773 { 0.010 }
	600	0.003	1.438 { 0.005 }, 1.804 { 0.012 }
	1000	0.003	1.376 { 0.011 }, 1.777 { 0.017 }
30	300	0.003	1.407 { 0.006 }, 1.738 { 0.013 }
	600	0.003	1.445 { 0.012 }, 1.804 { 0.016 }
	1000	0.003	1.376 { 0.010 }, 1.776 { 0.016 }

o s,  $T_i$  and  $R_{1,i}$  are in Kelvin.

o All experiments at 297 K, with probe TCP111, and  $Q = 1.0 \text{ W}\cdot\text{m}^{-1}$ ,  $N\Delta t = 30$  secs.

o Optimum solution region,  $i = 1, 2, \dots, n$ .

o Short time solution converged for all cases except  $m = 2$ ,  $N = 600$ .

o  $R_{2,i}$  did not converge for all cases.

### 5.5.2 WATER LIQUID

An estimate of the thermal conductivity of water at 298 K (viscosity 1 cP) from the long time solution,  $0.663 \pm 0.07 \text{ W}\cdot\text{m}^{-1}\cdot\text{K}^{-1}$ , is ten percent in excess of the literature,  $0.605 \text{ W}\cdot\text{m}^{-1}\cdot\text{K}^{-1}$  (Venart, Prasad, and Stocher, 1979). The short time solution reduces the difference to three percent,  $0.623 \pm 0.13 \text{ W}\cdot\text{m}^{-1}\cdot\text{K}^{-1}$ . Tables 5.5 and 5.6 summarize the measurements on liquid water.

Employing the short time solution is justifiable since the remainder terms for the long time solution,  $R_{1,i}$ , are significantly greater than than standard deviation of the temperature rise measurement,  $s$ . The remainder terms for the short time solution,  $R_{2,i}$ , are the same order of magnitude as  $s$ . Therefore, the short time solution determines the best estimate of the thermal conductivity.

### 5.5.3 TOLUENE LIQUID

An estimate of the thermal conductivity of toluene at 298 K (viscosity 0.6 cP) from the long time solution,  $0.147 \text{ W}\cdot\text{m}^{-1}\cdot\text{K}^{-1}$ , is 12.2% in excess of the literature,  $0.131 \text{ W}\cdot\text{m}^{-1}\cdot\text{K}^{-1}$  (Graham, 1985). The short time solution reduces the difference to 7.6 %,  $0.141 \text{ W}\cdot\text{m}^{-1}\cdot\text{K}^{-1}$ . Tables 5.7 and 5.8 summarize the measurements on liquid toluene.

The remainder for the short time solution,  $R_{2,i}$ , did not converge for any measurement.  $R_{2,i}$  did not converge for 1-methylnaphthalene either, but unlike these measurements a *short* short time solution is necessary for toluene. Due to the accuracy of the temperature measurements, this is not possible. The thermal conductivity value determined from the short time solution is the best estimate for the thermal conductivity of toluene.

Table 5.5

## Thermal Conductivity Measurements on Liquid Water

m	N	LONG TIME SOLUTION , k $\pm$ $\Delta$ k	SHORT TIME SOLUTION , k $\pm$ $\Delta$ k
2	300	0.632 $\pm$ 0.021	0.569 $\pm$ 0.017
	600	0.670 $\pm$ 0.012	0.643 $\pm$ 0.011
	1000	0.666 $\pm$ 0.011	0.618 $\pm$ 0.009
4	300	0.654 $\pm$ 0.017	0.603 $\pm$ 0.014
	600	0.664 $\pm$ 0.010	0.626 $\pm$ 0.009
	1000	0.667 $\pm$ 0.006	0.634 $\pm$ 0.005
9	300	0.655 $\pm$ 0.013	0.612 $\pm$ 0.011
	600	0.664 $\pm$ 0.007	0.624 $\pm$ 0.006
	1000	0.662 $\pm$ 0.005	0.622 $\pm$ 0.005
16	300	0.653 $\pm$ 0.011	0.604 $\pm$ 0.009
	600	0.665 $\pm$ 0.007	0.633 $\pm$ 0.006
	1000	0.673 $\pm$ 0.005	0.637 $\pm$ 0.004

o All conductivities  $W \cdot m^{-1} \cdot K^{-1}$

o All experiments at 298 K, with probe TCP111, and  $Q = 3.0 W \cdot m^{-1}$ ,  $N\Delta t = 30$  secs.

o Due to excessive remainder terms the experiment for  $m = 2$  and  $N = 300$  was disregarded in determining the average thermal conductivity.

Table 5.6

## Solution Analysis for Measurements on Liquid Water

m	N	s	$T_1$	$\{\hat{R}_{1,1}, \hat{R}_{2,1}\}$	$T_n$	$\{\hat{R}_{1,n}, \hat{R}_{2,n}\}$
2	300	0.007	1.721	{ 0.072, 1.721 }	1.937	{ 0.048, 1.937 }
	600	0.009	1.722	{ 0.027, 0.006 }	1.928	{ 0.017, 0.003 }
	1000	0.009	1.544	{ 0.055, 0.007 }	1.812	{ 0.034, 0.003 }
4	300	0.010	1.670	{ 0.054, 0.023 }	1.879	{ 0.035, 0.012 }
	600	0.006	1.643	{ 0.039, 0.014 }	1.870	{ 0.025, 0.006 }
	1000	0.014	1.702	{ 0.032, 0.009 }	1.937	{ 0.020, 0.004 }
9	300	0.005	1.695	{ 0.045, 0.016 }	1.915	{ 0.029, 0.008 }
	600	0.006	1.684	{ 0.042, 0.014 }	1.922	{ 0.026, 0.006 }
	1000	0.004	1.630	{ 0.043, 0.016 }	1.873	{ 0.026, 0.007 }
16	300	0.003	1.679	{ 0.053, 0.021 }	1.907	{ 0.035, 0.011 }
	600	0.005	1.693	{ 0.034, 0.010 }	1.916	{ 0.021, 0.004 }
	1000	0.004	1.591	{ 0.039, 0.014 }	1.836	{ 0.024, 0.006 }

o  $s$ ,  $T_i$ ,  $R_{1,i}$  and  $R_{2,i}$  are in Kelvin.

o All experiments at 298 K, with probe TCP111, and  $Q = 3.0 \text{ W}\cdot\text{m}^{-1}$ ,  $N\Delta t = 30 \text{ secs}$ .

o Optimum solution region,  $i = 1, 2, \dots, n$ .

o If  $R_{j,i} = T_i$ , then no convergence for  $R_{j,i}$ .

Table 5.7

## Thermal Conductivity Measurements on Liquid Toluene

m	N	LONG TIME SOLUTION , $k \pm \Delta k$	SHORT TIME SOLUTION , $k \pm \Delta k$	
A	300	0.146 $\pm$ 0.002	0.141 $\pm$ 0.002	
		600	0.145 $\pm$ 0.002	
	4	300	0.145 $\pm$ 0.002	0.141 $\pm$ 0.002
		600	0.146 $\pm$ 0.001	0.141 $\pm$ 0.001
	9	300	0.145 $\pm$ 0.001	0.139 $\pm$ 0.001
		600	0.145 $\pm$ 0.001	0.138 $\pm$ 0.001
B	1000	0.147 $\pm$ 0.001	0.141 $\pm$ 0.001	
		1000	0.145 $\pm$ 0.001	0.141 $\pm$ 0.001
	4	1000	0.147 $\pm$ 0.001	0.140 $\pm$ 0.001
		1000	0.146 $\pm$ 0.001	0.141 $\pm$ 0.001
	9	1000	0.146 $\pm$ 0.001	0.141 $\pm$ 0.001

o All conductivities  $W \cdot m^{-1} \cdot K^{-1}$

o A, experiments at 298 K, with probe TCP111, and  $Q = 1.2 W \cdot m^{-1}$ ,  $N\Delta t = 18$  secs.

o B, experiments at 297 K, with probe TCP111, and  $Q = 1.2 W \cdot m^{-1}$ ,  $N\Delta t = 20$  secs.

Table 5.8

## Solution Analysis for Measurements on Liquid Toluene

m	N	s	$T_1$	$\{\hat{R}_{1,1}, \hat{R}_{2,1}\}$	$T_n$	$\{\hat{R}_{1,n}, \hat{R}_{2,n}\}$
A	2	300	0.007	1.412 {†, †}	1.787 {†, †}	
		600	0.009	1.334 {†, †}	1.727 {†, †}	
	4	300	0.010	1.361 {†, †}	1.735 {†, †}	
		600	0.006	1.337 {†, †}	1.735 {†, †}	
	9	300	0.005	1.365 {†, †}	1.745 {†, †}	
		600	0.006	1.364 {†, †}	1.784 {†, †}	
B	2	1000	0.005	1.308 {†, †}	1.767 {†, †}	
		1000	0.006	1.316 {†, †}	1.760 {†, †}	
	4	1000	0.005	1.318 {†, †}	1.758 {†, †}	
		1000	0.006	1.311 {†, †}	1.754 {†, †}	
	9	1000	0.005	1.316 {†, †}	1.759 {†, †}	

o s,  $T_i$ ,  $R_{1,i}$  and  $R_{2,i}$  are in Kelvin.

o A, experiments at 298 K, with probe TCP111, and  $Q = 1.2 \text{ W}\cdot\text{m}^{-1}$ ,  $N\Delta t = 18$  secs.

o B, experiments at 297 K, with probe TCP111, and  $Q = 1.2 \text{ W}\cdot\text{m}^{-1}$ ,  $N\Delta t = 20$  secs.

†, Estimates of remainders did not converge for all cases.

---

## 5.6 SELECTION OF LONG OR SHORT TIME SOLUTION

---

The long time solution with remainder analysis,  $R_{1,i}$ , and the short time solution with remainder analysis,  $R_{2,i}$ , are determined with the calibrated probe properties. With these parameters and the standard deviation of the temperature rise measurement,  $s$ , guidelines are established for the selection of when the long or short time solution is appropriate. The number of multiple experiments required is also presented in the guidelines.

The sample standard deviation of the temperature measurement,  $s$ , decreases with the square root of the multiple experiment number,  $m$ . A better estimate of the thermal conductivity is determined when  $s$  is minimized. Past multiple experiments of 16, the small decrease in the standard deviation does not warrant the increase in experimental time. To calculate  $s$ , the number of averaged experiments,  $m$ , must be greater than one. Ultimately, the standard deviation is sufficiently small that it does not come into consideration in the long or short time solution. But, this cannot be determined until after the experiment is complete and the data analyzed.

To achieve a reasonable value for the multiple experiment number, the following steps are recommended:

- 1) Perform an experiment and monitor  $s$  during the experiment, and when  $s$  becomes small terminate the experiment.
- 2) Analyze the data by the long and/or short time solution.

- 3) If more information can be gained from the experiment by decreasing  $s$ , then return to the first step.

As presented in the probe thermistor calibration, different probes may require different multiple experiment numbers to achieve the same value for the standard deviation,  $s$ . For the probes employed in this work, a suitable range for  $m$  is  $2 \leq m \leq 16$ .

If the estimate for the remainder of the long time solution,  $R_{1,i}$ , is less than one percent of the temperature rise,  $T_i$ , then there is a high degree of confidence that the long time solution is valid. Convergence is not possible on the estimate for  $R_{1,i}$  when: 1) the true value of  $R_{1,i}$  is significantly lower than  $s$ , or 2)  $R_{2,i}$  is comparable in value to  $R_{1,i}$ . For the first case,  $m$  should be increased to decrease  $s$ . If the problem still occurs, then the population standard deviation of the thermistor is excessive (refer to the data acquisition algorithm section of Chapter 3). In the second case, the short time solution is applied.

If the remainder terms for the long time solution are approximately the same as the standard deviation of the temperature rise, then the long time solution determines the best estimate of the thermal conductivity. In this case the short time solution may converge, but its estimate of the thermal conductivity may or may not be valid. The short time solution cannot distinguish between error in the fit of the long time solution and the accuracy of the experimental data.



If the estimate for the remainder of the short time solution,  $R_{2,i}$ , is less than one percent of the temperature rise,  $T_i$ , then there is a high degree of confidence that the short time solution is valid. Convergence is not possible on the estimate for  $R_{2,i}$  when: 1) the true value of  $R_{2,i}$  is significantly lower than  $s$ , or 2)  $R_{3,i}$  is comparable in value to  $R_{2,i}$ . In the first case, the long time solution determines the best estimate of the thermal conductivity. In the second case, the best estimate of the thermal conductivity cannot be determined by the long or short time solution.

Solutions for times smaller than in the short time solution cannot be determined for the probes used in this work. At these very short times the additional terms in the solution are too close in value to the temperature rise standard deviation.

---

## 5.7 CONCLUSION

---

In this chapter, the correct operation of the thermal conductivity measurement system was verified. Materials selected for this study are those with known conductivities. Conductivity measurements on solids are threefold: 1) tertiary butyl alcohol, 2) tetrahydrofuran hydrate, and 3) water ice. Conductivity measurements on liquids are fivefold: 1) tertiary butyl alcohol, 2) glycerin, 3) 1 - Methyl-naphthalene, 4) water, and 5) toluene. All measurements are within 5 % of accepted literature values, except for toluene which is within 8 % . Table 5.9 summarizes the results on the compounds.

The needle probe, in this work, exhibits limitations on liquids of viscosities less than 1 cP. But, it does not exhibit the limitation of no accurately measuring liquids less viscous than glycerin (Stoll and Bryan, 1979).

The long time solution will generally predict accurate thermal conductivities for solids and viscous liquids. For low viscosity liquids, the short time solution is required to predict the conductivity. If neither method is applicable, then the conductivity cannot be determined on an absolute basis.

It is necessary to account for the probe thermal conductivity for the compounds and probe employed in this work. Assuming the probe thermal conductivity is infinite causes several errors. First, estimates for  $R_{1,i}$  are incorrect and the applicability of the long time solution cannot be determined. Second, the short time solution does not converge, because the inner probe temperature profiles are assumed flat when they are highly curved.

Table 5.9  
Summary of Thermal Conductivity Measurements

		LITERATURE k	LONG TIME k      %		SHORT TIME k      %	
SOLIDS	Tertiary Butyl Alcohol	0.123 †	0.122	0.8	<i>Not Used</i>	
	THF Hydrate	0.5 §	0.486	5		
	Water Ice	2.21 Δ	2.29	3.6		
LIQUIDS	Tertiary Butyl Alcohol	0.109 †	0.110	0.9	<i>Not Used</i>	
	1-Methylnaphthalene	0.134 ‡	0.135	0.8		
	Glycerin	0.288 *	0.292	1.4		
LIQUIDS	1-Methylnaphthalene	0.134 ‡	0.135	0.8	0.134	Calibration Fluid
	Water	0.605 •	0.663	9.6	0.623	3.0
	Toluene	0.131 ‡	0.147	12.2	0.141	7.6

- o All conductivities  $W \cdot m^{-1} \cdot K^{-1}$ .
- o % is percent difference from literature.

- † Perkins (1983)
- § Cook and Laubitz
- Δ Ross, Andersson, and Backstrom (1977)
- \* Thermal Properties of Matter (1970)
- ‡ Graham (1985)
- Venart, Prasad, and Stocher (1979)

# CHAPTER 6

**AN APPLICATION TO HYDRATES IN POROUS MEDIA**

---

## 6.0 INTRODUCTION

---

In this chapter, the thermal conductivity measurement system is applied to hydrates in porous media. The hydrates tested in this chapter were formed in conjunction with A. Ouar, and complete details of the formation process are documented in his thesis (1987).

Tremendous quantities of natural gas exist in hydrated form. These hydrates represent a substantial natural gas resource. Determining the economic feasibility of producing these reservoirs is crucial. Estimates of natural gas existing in hydrated form range from 5 to 12,000 % of the proven United States gas reserves (Zielinski and McIver, 1982). Production rates can be estimated by mathematically modeling the recovery of natural gas from a hydrate reservoir. Several physical properties are necessary for hydrates in a reservoir: 1) heat capacity, 2) heat of dissociation, and 3) thermal conductivity, 4) density.

Thermal conductivity measurements of hydrates in sediments are presented herein. The presentation is in three parts:

- Factors influencing effective thermal conductivities,
- Hydrate formation around the probe, and
- Measurements on hydrates on porous media.

---

## 6.1 EFFECTIVE THERMAL CONDUCTIVITY

---

A great deal of work has been conducted on the thermal conductivity of porous sediments. The porous sediment is considered to consist of a continuous and discontinuous phase. An interest in the thermal conductivity of oil-bearing sand and rock has existed for many years (Woodside and Messmer, 1961). Many applications (refer to Chapter 1) have employed the needle probe in determining conductivities of porous sediments.

When experimentally determining thermal conductivities on porous media, neither the conductivity of the continuous or discontinuous phase is measured. The effective thermal conductivity is measured. The conductivities of the continuous and discontinuous phase along with the shape and packing arrangement of the continuous phase determine the effective thermal conductivity. Crane, Vachon, and Khader (1977) reviewed the major published correlations of thermal conductivity of granular materials. Such thermal conductivity correlations are limited in accuracy, typically to within twenty percent. Maxwell (1881) presented the initial correlation for effective conductivities, and work still continues today (Davis, 1986) in search of the best correlation. Whenever possible, it is more desirable to experimentally determine the effective thermal conductivity of sediments.

### 6.1.1 THE CONTINUOUS PHASE

The continuous phase is the sediment. The thermal conductivity of rocks reflect the constitution of the rocks in terms of their principal minerals and of the conductivities of aggregates of these minerals. An example of this is rock samples collected by Birch (1954) near Calumet, Michigan:

<u>Core Sample</u>	<u>Conductivity, <math>W \cdot m^{-1} \cdot K^{-1}</math></u>		
	<u>Range</u>	<u>Average</u>	<u>Standard Deviation</u>
Copper Harbor Conglomerate •	0.9 to 3.3	2.1	0.6
Jacobsville Sandstone •	2.1 to 10.6	2.8	0.8
Nonesuch Shale •	2.6 to 2.9	2.8	0.2
Freda Sandstone •	2.2 to 3.6	2.9	0.4

These measurements show the differences between rocks of differing mineralogy, and demonstrate that the reservoir conductivity may vary greatly.

The purpose of measuring hydrates in sediments is to determine the effective thermal conductivity for reservoir modeling. Ottawa sands (20-30 mesh) were chosen for the unconsolidated sediments. This is the same sediment as used by Stoll and Bryan (1979) for their propane hydrate in sediment measurements.

Unconsolidated sediments were chosen because of the difficulty of forming hydrates in consolidated sediments. Makogon (1981) gave various factors influencing hydrate formation in porous rock: 1) the degree of moisture saturation of the rock, 2) the gas/water contact area, and 3) the capillary radii of the pores. Ouar (1987) also discusses the difficulties of forming hydrates in consolidated sediments.

### 6.1.2 THE DISCONTINUOUS PHASE

The discontinuous phase is water, ice, hydrocarbon gas, and hydrates. Thermal conductivities of water and ice were determined previously (refer to Chapter 5). It is not possible to determine the thermal conductivity of only a gas phase with a needle probe. The gas convects readily and nullifies the pure conduction heat transfer model used for experimental data analysis in this work. But gas trapped in porous sediment cannot convect as readily. For sediments of low porosities the heat transferred by gas convection is not significant, and the conduction model is still a valid approximation.

Methane was selected as the guest species for the hydrate. This compound forms structure I hydrates. Propane hydrates, structure II, in Ottawa sands were formed and tested by Stoll and Bryan (1979). Gas hydrates of methane, structure I, in Ottawa Sand were made by Ouar (1987).

The formation of propane hydrates in sediment was also attempted by Ouar (1987). In these experiments the hydrates formed above the sediment by denuding the sediment of water, and, therefore, were not useful for thermal conductivity measurements. Stoll and Bryan (1979) formed propane hydrates while mixing and compacting the sample. In contrast, in the batch method of Ouar (1987) the sample was not disturbed during formation, and the sample did not form homogeneously.



---

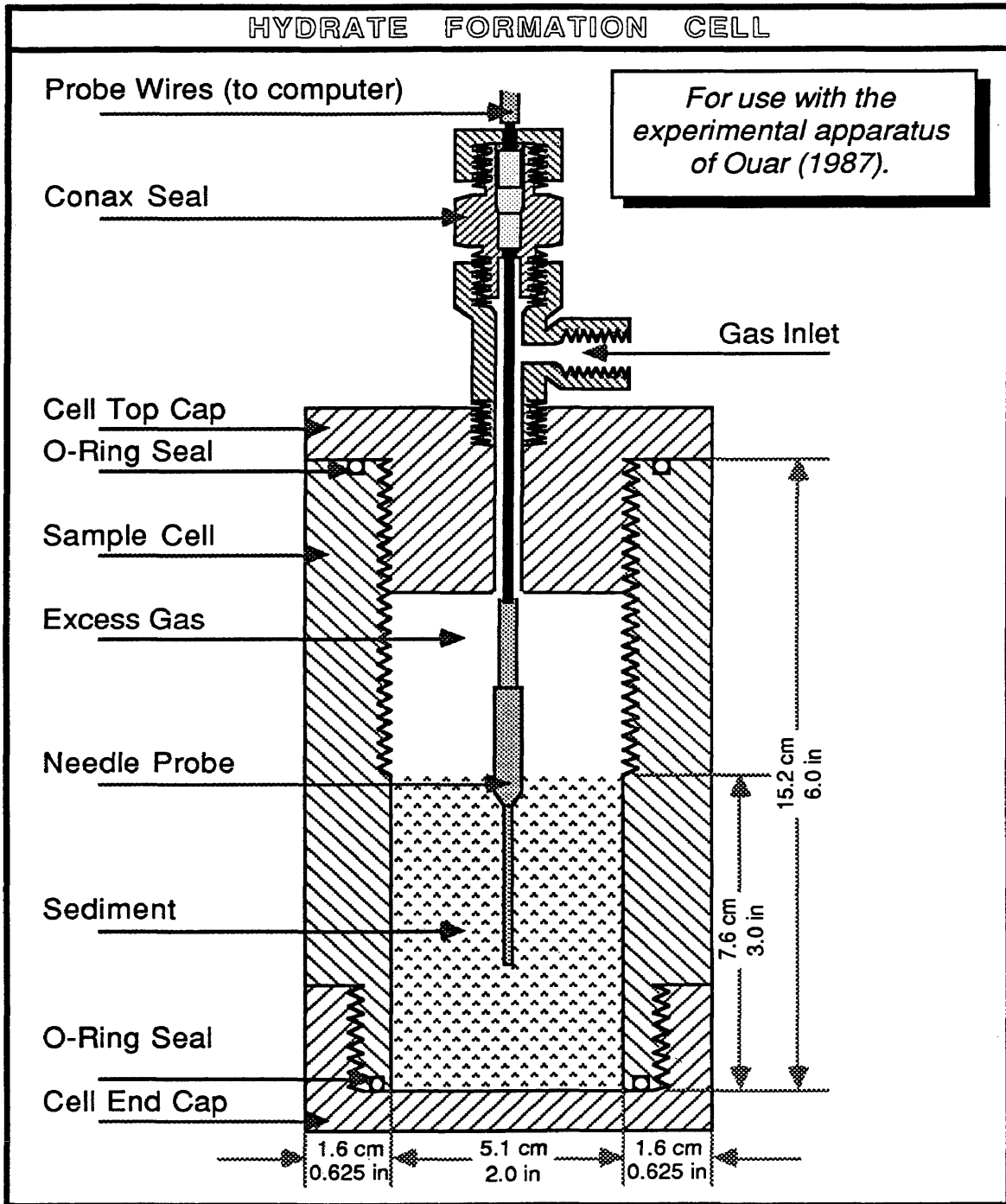
## 6.2 HYDRATE FORMATION AROUND THE PROBE

---

The experimental procedure for the formation of hydrates in sediments is given by Ouar (1987). The following procedure was modified for the formation of hydrates around the probe in conjunction with Ouar (1987). The hydrates in sediment were formed around the probe to insure thermal contact between the probe and hydrates. An abbreviated summary of the method is presented in this section.

A known volume of the hydrate formation cell (Figure 6.1) is packed with a known mass of sediment. The porosity of the packed sediment and thus the pore volume are determined, allowing the evaluation of the amount of water required to saturate the sediment. The hydrate formation cell is then sealed with the needle probe placed in the sediment, connected to the system piping ("Gas Inlet" in Figure 6.1), and placed in a temperature bath maintained between 10 and 16 °C. The system is evacuated for five minutes, and then pressurized with methane up to 11.7 MPa (1700 psia). After temperature and pressure stabilization the temperature of the bath is decreased progressively to 1 °C, where the hydrates start forming. As the hydrates form the pressure of the system declines, and the hydrate formation is assumed complete when the rate of change of the pressure drop approaches zero. The duration of a run varies between 3 to 7 days.

Figure 6.1  
Schematic of the Hydrate Formation Cell



In the case of unconsolidated sediments, the probe was in intimate contact with the sediment and water before forming the hydrates. After the formation and the thermal conductivity measurements on the first sample, the needle probe broke when attempting to remove it from the sample. The hydrates had formed around the needle probe, and upon removal of the probe the hypodermic needle separated from the epoxy housing. In subsequent experiments the hydrates at the surface of the needle probe were dissociated before the removal of the probe. From such occurrences, it was determined that there was no thermal contact resistance between the probe and the sample being tested.

In the case of consolidated sediments, it was required to drill a hole in the sediment, thus there is no simple means of eliminating the thermal contact resistance. To minimize this resistance the hole was drilled closely to the diameter of the probe. From the discussion presented in Chapter 2, it was determined that the contact resistance would not add any appreciable error if the long time solution is applicable.

In all measurements, except for the sediment saturated with methane gas, the long time solution determined the best estimate for the thermal conductivity. The estimates of the remainder terms for the long time solution were equivalent to the error in the temperature rise measurements, therefore the short time solution was not applicable. The measurements of the gas saturated sediments were determined best from the short time solution. All errors in the temperature rise measurement were estimated to be less than 0.01°C.

---

## 6.3 MEASUREMENTS ON HYDRATES IN SEDIMENTS

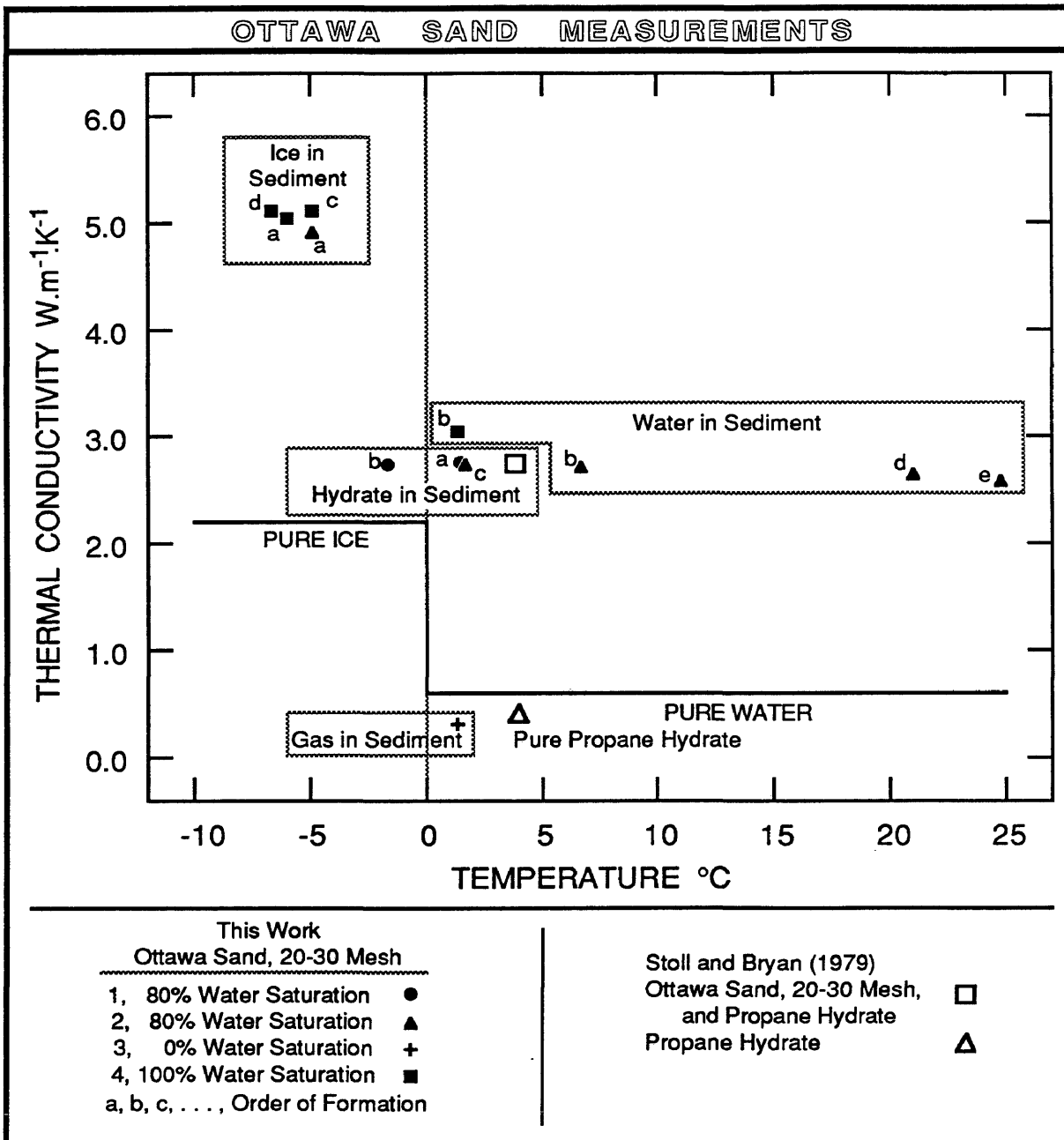
---

The results for this work's methane hydrate in sediment study are similar to the measurement on propane hydrate in sediment reported by Stoll and Bryan (1979). From this it is concluded that the thermal conductivity of a hydrate is not a function of either the structure, I or II, or the guest molecule.

Figure 6.2 shows the results of the present measurements of the methane hydrate in sediment study (sediment porosity of 0.38). Also, presented are measurements of the present work on water, ice, and methane gas in sediments. These substances were measured to determine the extent that the conductivity changes for hydrates in sediments. In this figure, the numbers, 1, 2, 3, and 4 (with their corresponding symbols), refer to the order of fabricating the samples and the letters, a, b, c, and d, refer to the order of thermal conductivity measurements on these samples during the hydrate formation process.

In these experiments, it was necessary to verify that the thermal conductivity of methane hydrate, and not of ice, was measured. To accomplish this, the conductivity was measured above and below the ice point. The conductivity of ice is more than three and a half times that of water. If the sediment was saturated only with hydrate (no excess water phase), then the thermal conductivity must be the same above and below the ice point.

Figure 6.2  
 Thermal Conductivities of  
 Water, Ice, Methane Gas, and Methane Hydrate in Ottawa Sand



In case number 1 the thermal conductivity measurement did not change above and below the ice point (a and b). Therefore it is likely that the sediment was methane hydrate. For cases 1 and 2 hydrate conversion tests via mass loss by Ouar (1987) indicated that these samples were hydrated. In case 2 ice (a) was first formed in sediment and then melted (b), then gas was added for the formation of hydrates and the conductivity measured (c). The gas was subsequently released on melting of the hydrates and the conductivity measured (d and e) Case 3 put the gas in sediment to determine the difference in hydrate and gas in sediment conductivity measurements. In case 4 the conductivity changed appreciably above (b) and below (a, c, and d) the ice point; therefore, it is likely the sediment consisted mostly of water with a few hydrates.

In Figure 6.2, the substance in experiment 4 was thought to have been hydrate according to the pressure drop exhibited during formation. But, from the thermal conductivity measurements this hypothesis was not verified. Visual inspection of the hydrates revealed that the hydrates did not form in the sediment, but instead the hydrates formed on above the sediment and on the cell wall. In this experiment the sediment was completely saturated with water.

Several explanations are hypothesized why hydrates did not form in the sediment for this experiment. First, by completely saturating the sediment the gas water interface was dramatically reduced in the sediment. Past experimental research (Holder, 1983), indicates that hydrates form at the gas water interface. In partially saturated sediments the gas water interface is greater, and hence the chances of forming hydrates in the sediments is greater. Second, hydrates

may have formed above the sediment in the water that was displaced from the sediment by pressurizing the formation cell. These hydrates above the sediment inhibited the mass transfer of gas into the sediments. It is possible for a hydrate layer to form an impermeable barrier to the flow of gas.

There are several important results of this study, in addition to the thermal conductivity of a hydrate reservoir will not depend upon the structure or guests of hydrates in the reservoir, as shown in Figure 6.2.

First, thermal conductivity measurements provide a tool to determine the integrity of the hydrate sample. The existence of the hydrates may be inferred from the pressure drop during formation, but the quality of the hydrates cannot. However, the tests of the present work only indicate the presence of hydrates around the thermal conductivity probe. Moving out radially from the probe into the sample, the effect of the local sediment composition decreases in significance for the thermal conductivity measurement (refer to Chapter 2).

Second, the thermal conductivity of methane hydrate in sediment is not statistically different from the conductivity of 80% water saturated sediment, as shown by samples 1 and 2 in Figure 6.2.

Attempts were also made at forming hydrates in consolidated sediment. The following discussion is a summary of this work from a thermal conductivity standpoint. Complete details of the formation are given in Ouar (1987).

Methane hydrate could not be formed in consolidated sediments, namely Berea Sandstone. All thermal conductivity tests indicated that it was largely ice that formed around the probe. It was hypothesized that there was a large mass transfer resistance for the gas to enter the sediment.

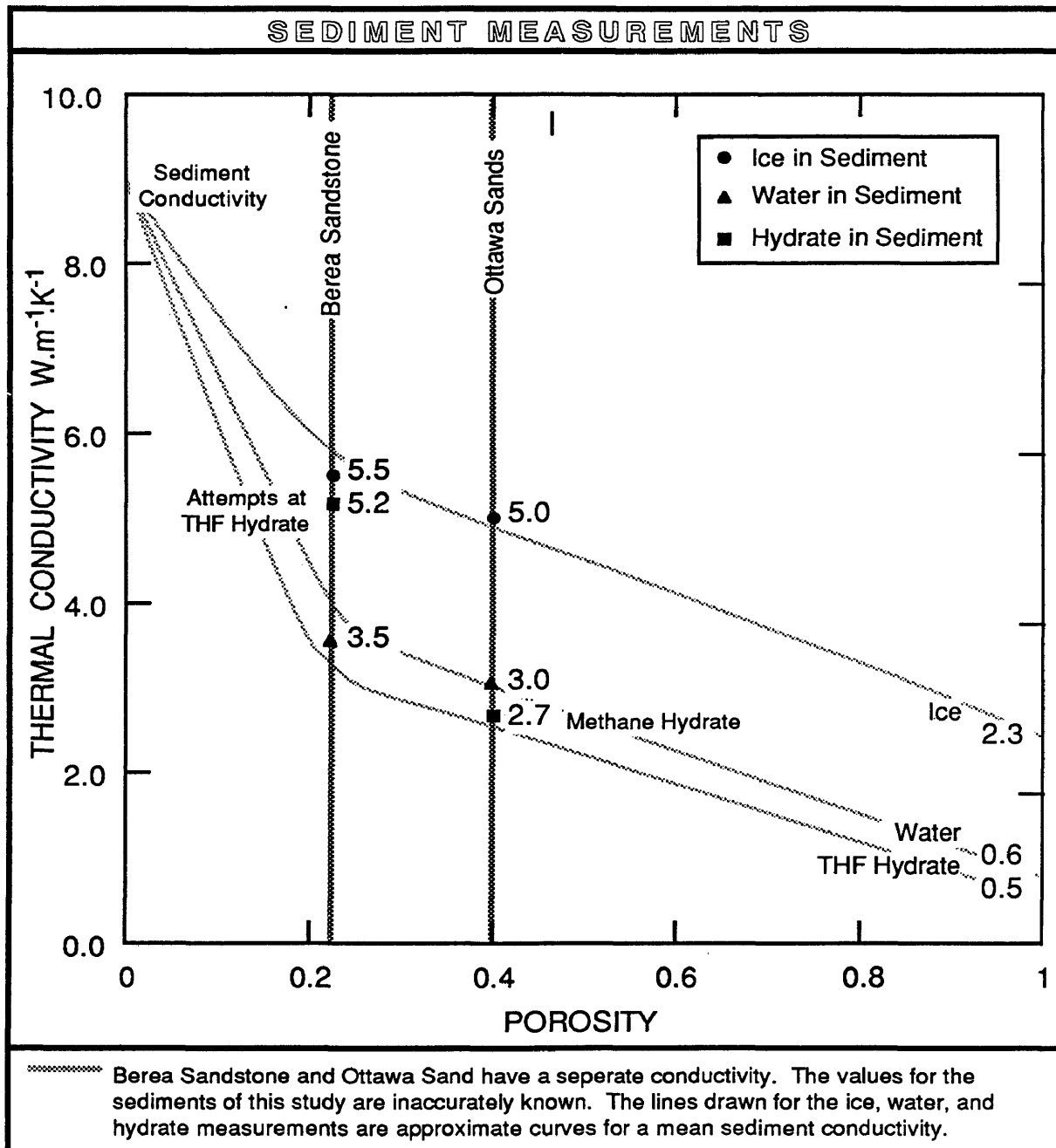
To investigate this problem attempts were made at forming hydrates from miscible hydrate formers, tetrahydrofuran and cyclobutanone. Measurements on pure tetrahydrofuran hydrate are presented in Chapter 5. Figure 6.3 summarizes the results of the unconsolidated and consolidated sediments. As can be seen by Figure 6.3, the thermal conductivity of the hydrate in consolidated sediment should be below that of water in sediment. But Berea Sandstone "hydrate" thermal conductivity tests indicated that mostly ice formed around the probe.

A hypothesis as to why hydrates did not form in Berea Sandstone is threefold. First, in the case of the methane hydrate, diffusion was the driving force for the methane to enter the core and it was not possible to get sufficient methane into the core. Secondly, in the case of the miscible hydrate formers, the the complete saturation of the sediment did not permit the formation of hydrate. A consolidated rock core is a fairly rigid structure. As ice or hydrate expand in the core, the rock must expand and the pressure will build up inside of the core. Under these circumstance the formation of ice may be more favored. Finally, preferential adsorption of either the guest or the host molecule on the sandstone surface may have changed the liquid composition such that hydrate formation was thermodynamically unfavorable.

Even though the hydrates did not form in consolidated sediment, it is premature to conclude that hydrates will not form in consolidated sediments. Future attempts at forming hydrates should be conducted in a flow system. The flow system would increase the amount of gas in the core and also partially saturate the core, and accomodate the adsorption phenomena.



Figure 6.3  
 Summary of Hydrate Measurements in Sediments



A hypothesis as to why the structure of the hydrate of the guest molecule does not affect the hydrate thermal conductivity follows: 1) Phonons are scattered by the guest molecule in the hydrate cavity. This scattering, rather than the solid structure, largely controls the thermal conductivity values. 2) In ice, phonons would pass through similar voids without scattering, due to the absence of guest molecules. 3) The phonon scattering by the guest molecule is insensitive to the molecular structure. The energy given to the guest molecule by the phonon is insufficient to change the translational, rotational, or vibrational energies of the molecule. Therefore the phonon is diffracted or deflected, and the thermal conductivity values are low.

---

## 6.4 CONCLUSION

---

Thermal conductivity measurements were presented for methane hydrates formed in Ottawa sands. Formation of methane hydrates in consolidated sediment were unsuccessful (refer to Ouar(1987) for complete details), and therefore conductivity measurements for hydrates in consolidated sediments were not obtained.

The thermal conductivity of methane hydrate, Structure I, in Ottawa Sands was determined to be similar to the propane hydrate, Structure II, in Ottawa Sands determined by Stoll and Bryan (1979). The thermal conductivity of a hydrate is not a function of either the structure, I or II, or the guest molecule. This is important in reservoir modeling, since the structure of the hydrate does not need to be considered to determine the reservoir thermal conductivity.

As expected, the sediment dominates the measured value for the thermal conductivity. The constitution of the sediment and whether it is consolidated or unconsolidated is important in determining the thermal conductivity of a hydrate reservoir.

The measurements of methane hydrate in porous sediment presented herein are currently the only available values. The data base should be expanded for several consolidated or unconsolidated sediments. These sediments should be similar to sediments found in naturally occurring hydrate reservoirs.

**CHAPTER 7**

**CONCLUSIONS AND RECOMMENDATIONS**

---

## 7.0 CONCLUSIONS

---

The development, verification, and application of a thermal conductivity measurement system have been presented. The three phases of this presentation are: 1) Development of a computerized thermal conductivity measurement system utilizing the transient needle probe technique, 2) Verification of the operation of the thermal conductivity system by testing various solids and liquids, and 3) Measurement of the unknown thermal conductivities of methane hydrates in porous media.

This work employs a heat transfer model for determining thermal conductivities from a transient needle probe experiment. While this model accounts for the probe volumetric heat capacity, it goes one step further than commonly used and accounts for the probe thermal conductivity. The model was broken down into a solution for both short and long times. If long times can be reached, then thermal conductivities can be measured without knowing the probe properties. But, the probe properties are required to determine whether the short or long time solutions are valid.

Thermal conductivities of solids and liquids with waterlike viscosities are determined with an accuracy of 4%. The solids tested and their conductivities are: 1) ice,  $2.29 \text{ W}\cdot\text{m}^{-1}\cdot\text{K}^{-1}$  at 269 K, 2) tetrahydrofuran hydrate,  $0.486 \text{ W}\cdot\text{m}^{-1}\cdot\text{K}^{-1}$  at 273 K, and 3) tertiary butyl alcohol,  $0.122 \text{ W}\cdot\text{m}^{-1}\cdot\text{K}^{-1}$  at 293 K. The liquids tested and their conductivities at 298 K are: 1) water,  $0.623 \text{ W}\cdot\text{m}^{-1}\cdot\text{K}^{-1}$ , 2) glycerin,  $0.292 \text{ W}\cdot\text{m}^{-1}\cdot\text{K}^{-1}$ , 3) 1-methylnaphthalene,  $0.135 \text{ W}\cdot\text{m}^{-1}\cdot\text{K}^{-1}$ , and

4) tertiary butyl alcohol,  $0.110 \text{ W}\cdot\text{m}^{-1}\cdot\text{K}^{-1}$ . The water measurements demonstrate that this system is also capable of measuring the conductivity of electrolytes.

When analyzing an experiment the solution region can be discerned to a better degree of accuracy for experiments with a low sample to probe thermal conductivity ratio. In the discussion of the system verification on solids and liquids the system was shown to have an inaccuracy of less than four percent up to a thermal conductivity ratio of six. In all cases for solids of high thermal conductivity ratios the long time solution was determined to be applicable. The inaccuracy for thermal conductivity ratios above six is also approximated to be less than four percent.

The work presented advances the state of the art in needle probe experimentation in several ways. These are: 1) Experimental data analysis is accomplished via a mathematical model, which employs both the probe thermal conductivity and volumetric heat capacity. 2) The needle probe can determine thermal conductivities for liquids with waterlike viscosities. 3) A system has been generated which automatically measures absolute thermal conductivities with an inaccuracy of four percent.

---

## 7.1 RECOMMENDATIONS

---

There are several recommendations on ways in which this work can be improved. These are:

**1** The needle probe exhibits limitations when measuring liquids, and attempts at reducing the limitations are beneficial. A cell to control convection would allow for liquids less viscous than 1cP.

**2** Due to the design of the needle probe electrolyte thermal conductivities can be measured by this technique. New work in this area utilizing the needle probe would be useful.

**3** Design a different thermal conductivity needle probe for the following reasons: 1) increase the thermal conductivity of the probe, thereby decreasing the conductivity ratio effect, and 2) increase the temperature range of the probe, thereby increasing the usefulness of the measurement system presented.

---

## REFERENCES

---

- Asher, G.B., Sloan, E.D., and Graboski, M.S., *A Computer Controlled Transient Needle-Probe Thermal Conductivity Instrument for Liquids*, **International Journal of Thermophysics**, **7**:285-294 (1986).
- Beck, A.E., *Measuring Heat Flow on Land*, in **Terrestrial Heat Flow**, W.H.K. Lee, Ed., Publication 1288 of the American Geophysical Union of the National Academy of Sciences - National Research Council, 36-40 (1965).
- Birch, F., *Thermal Conductivity, Climatic Variation, and Heat Flow Near Calumet, Michigan*, **American Journal of Science**, **252**:1-25 (1954).
- Blackwell, J.H., *The Axial-Flow Error in the Thermal Conductivity Probe*, **Canadian Journal of Physics**, **34**:412-417 (1956).
- Bloomer, J.R., and Ward, J., *A Semi-Automatic Field Apparatus for the Measurement of Thermal Conductivities of Sedimentary Rocks*, **Journal of Physics E: Scientific Instruments**, **12**:1033-1035 (1979).
- Carslaw, H.S., and Jaeger, J.C., **Conduction of Heat in Solids**, (2<sup>nd</sup> ed.), Oxford University Press, New York (1959).
- Cook, J.G., and Laubitz, M.J., *The Thermal Conductivity of Two Clathrate Hydrates*, National research Council of Canada, Ottawa, Canada.
- Corry, C., Dubois, C., and Vacquier, V., *Instrument for Measuring Terrestrial Heat Flow Trough the Ocean Floor*, **Journal of Marine Research**, **26**:265-277 (1968).
- Crane, R.A., Vachon, R.I., and Khader, M.S., *Thermal Conductivity of Granular Materials - A Review*, **Proceedings of the 7<sup>th</sup> Symposium on Thermophysical Properties**, 109-123 (1977).
- Davis, R.H., *The Effective Thermal Conductivity of a Composite Material with Spherical Inclusions*, **International Journal of Thermophysics**, **7**:609-620 (1986).
- Gerard, R., Langseth, M.G., and Ewing, M., *Thermal Gradient Measurements in the Water and Bottom Sediment of the Western Atlantic*, **Journal of Geophysical Research**, **67**:785-803 (1962).



- Goodman, M.A., and Giussani, A.P., *In Situ Gas Hydrates: Evaluation of Past Experience and Methods for Field Detection and Testing*, Final Report, Gas Research Institute, Contract No: 5014-321-0245 (1982).
- Graham, G., M.Sc. Thesis, Colorado School of Mines, Golden, Colorado (1985).
- Halleck, P.M., *In Situ Properties of Natural Gas Clathrate Deposits*, Methane Hydrate Workshop, Technical Proceedings, DOE, Morgantown, West Virginia (1982).
- Hitchon, B., *Occurrence of Natural Gas Hydrates in Sedimentary Basins, Natural Gases in Marine Sediments*, Edited by I.R. Kaplan, Plenum Press, 195-225 (1974).
- Holder, G.D., Angert, P.F., John, V.T., and Yen, S., *A Thermodynamic Evaluation of Thermal Recovery of Gas from Hydrates in the Earth*, **Journal of Petroleum Technology**, 1127-1132 (1982).
- Holder, G.D., *Laboratory Analysis of Gas Hydrate Cores for Evaluation of Reservoir Conditions*, Monthly Report No. 1, DOE Contract Number, DE-AC21-83MC20013 (1983).
- Jaeger, J.C., *The Measurement of Thermal Conductivity and Diffusivity with Cylindrical Probes*, **Transactions, American Geophysical Union**, 39:708-710 (1958).
- Judge, A., *Natural Gas Hydrates in Canada, Gas Hydrates and Permafrost*, 4<sup>th</sup> Canadian Permafrost Conference, 320-328 (1982).
- Katz, D.L., *Depths to Which Gas Fields (Gas Hydrates) May Be Expected*, **Journal of Petroleum Technology**, 23:419-423 (1971).
- Kierkus, W.T., Mani, N., and Venart, J.E.S., *Radial-Axial Transient Heat Conduction in a Region Bounded Internally by a Circular Cylinder of Finite Length and Appreciable Heat Capacity*, **Canadian Journal of Physics**, 51:1182-1186 (1973).
- Lachenbruch, A.H., and Marshall, B.V., *Heat Flow Through the Artic Ocean Floor: The Canadian Basin-Alpha Rise Boundary*, **Journal of Geophysical Research**, 71:1223-1248 (1966).
- Langseth, M.E., Grim, P.J., and Ewing, M., *Heat -Flow Measurements in the East Pacific Ocean*, **Journal of Geophysical Research**, 70:367-380 (1965).

- Macleod, M.K., *Gas Hydrates in Ocean Bottom Sediments*, **The American Association of Petroleum Geologists Bulletin**, **66**:2649-2662 (1982).
- Makogon, Y.F., *Hydrates of Natural Gas*, Trans. by W.J. Cieslewicz, Penwell Pub. Co. (1981).
- Maxwell, **A Treatise on Electricity and Magnetism**, Volume 1, Second Edition, Clarendon Press Series, Oxford (1881).
- McGuire, P.L., *Methane Hydrate Gas Production by Stimulation*, **Gas Hydrates and Permafrost**, 4<sup>th</sup> Canadian Permafrost Conference, 320-328 (1982).
- Mitchell, J.K., ASCE, F. and Kao, T.C., *Measurement of Soil Thermal Resistivity*, American Society of Civil Engineers, **Journal of Geotechnical Engineering Division**, **104**:1307-1320 (1978).
- Morrow, G.D., *Improved Hot Wire Thermal Conductivity Technique*, **American Ceramic Society Bulletin**, **58**:687-690 (1979).
- Nason, R.D., and Lee, W.H.K., *Heat Flow Measurements in the North Atlantic, Caribbean, and Mediterranean*, **Journal of Geophysical Research**, **69**:4875-4883 (1978).
- Ouar, A., M.Sc. Thesis, Colorado School of Mines, Golden, Colorado (1987).
- Pantaloni, J., Guyon, E., Velarde, M.G., Bailleux, R., and Finiels, G., **Rev. Phys. Appl.**, **12**:1849 (1977).
- Pearson, C.F., Halleck, P.M., McGuire, P.L., Hermes, R., and Matthews, M., *Natural Gas Hydrate Deposits: A Review of In Situ Properties*, **Journal of Physical Properties**, **87**:4180-4185 (1983).
- Perkins, R., Ph.D. Thesis, Colorado School of Mines, Golden, Colorado (1983).
- Ross, R.G., and Andersson, P., *Clathrate and Other Solid Phases in the Tetrahydrofuran-Water System: Thermal Conductivity and Heat Capacity Under Pressure*, **Canadian Journal of Chemistry**, **10**:881-892 (1982).
- Ross, R.G., Andersson, P., and Bäckström, G., *Thermal Conductivity of Nine Solids Phases of H<sub>2</sub>O, High Temperatures - High Pressures*, **9**:87-96 (1977).

- Ross, R.G., Andersson, P., and Bäckström, G., *Unusual PT Dependence of Thermal Conductivity for a Clathrate Hydrate*, **Nature**, **290**:322 (1981).
- Rueff, R., Personal Communication at Colorado School of Mines (1985,1).
- Rueff, R., Ph.D. Thesis, Colorado School of Mines, Golden, Colorado (1985,2).
- Selim, S., and Sloan, E.D., *Modeling of the Dissociation of an In-Situ Hydrate*, Society of Petroleum Engineers 1985 California Regional Meeting, Bakersfield, California (1985).
- Stoll, R.D., and Bryan, G.M., *Physical Properties of Sediment Containing Gas Hydrates*, **Journal of Geophysical Research**, **84**:1629-1634 (1979).
- Thermal Properties of Matter, Vol. 3, Thermal Conductivity, Nonmetallic Liquids and Gases**, IFI/Plenum Press, New York (1970).
- Venart, J.E.S., Prasad, R.S., and Stocher, D.G., *The Thermal Conductivity of Water and Heavy Water, Water and Steam, Their Properties and Current Industrial Application*, Straub and Scheffler, Ed., Pergamon Press, 392-406 (1979).
- Von Herzen, R.P., and Maxwell, A.E., *The Measurement of Thermal Conductivity Deep-Sea Sediment by a Needle Probe Method*, **Journal of Geophysical Research**, **64**:1557-1553 (1959).
- Von Herzen, R.P., and Uyeda, S., *Heat-Flow Through the Eastern Pacific Ocean Floor*, **Journal of Geophysical Research**, **69**:741-748 (1963).
- Weaver, J.S., and Stewart, J.M., *In Situ Hydrates Under the Beaufort Sea Shelf, Gas Hydrates and Permafrost, Proceedings 4<sup>th</sup> Canadian Permafrost Conference*, 312-319 (1982).
- Woodside, W., and Messmer, J.H., *Thermal Conductivity of Porous Media*, **Journal of Applied Physics**, **32**:1688-1706 (1961).
- Yamano, M., Uyeda, S., Aoki, Y., and Shipley, T.H., *Estimated of Heat Flow Derived from Gas Hydrates*, **Geology**, **10**:339-343 (1982).
- Zielinski, R.E., and McIver, R.D., *The Occurrence and Magnitude of Methane-Hydrate Accumulations*, SPE/DOE Unconventional Gas Recovery Symposium, Pittsburgh, PA (1982).

APPENDIX A

**MATHEMATICAL MODELING ADDENDUM**

---

## A.1 FINITE CONDUCTOR MODEL EXPANSION

---

The following is the solution for the expansion for the finite conductor model presented in Equation 2.7. Laplace's equation and appropriate boundary conditions are given in Equation 2.5. The solution for the temperature within the probe in the Laplace domain is (Carslaw and Jaeger (1959)):

$$\bar{T}_1 = \frac{Q}{4\pi k} \frac{2\alpha}{a^2} \frac{\omega}{s^2} \left[ 1 - \frac{\beta\chi I_0(r^*u/\chi) K_1(u)}{\beta\chi I_0(u/\chi) K_1(u) + I_1(u/\chi) K_0(u)} \right] \quad (\text{A.1})$$

$$u = (s a^2 / \alpha)^{1/2}$$

$$r^* = r / a$$

$\beta$ ,  $\omega$ , and  $\chi$  are defined in Chapter 2.  $I$  and  $K$  are the modified Bessel's function of the first and second kind, respectively.

The inversion theorem for the Laplace transformation is:

$$T_1(t) = \frac{1}{2\pi i} \int_{v-i\cdot\infty}^{v+i\cdot\infty} e^{\lambda t} \bar{T}_1(\lambda) d\lambda \quad (\text{A.2})$$

Where  $v$  is of large magnitude so that all singularities of the function line to the left of the line  $(v - i\cdot\infty, v + i\cdot\infty)$ . For the problem under consideration the inversion theorem is rewritten as (Carslaw and Jaeger (1959)):

$$T_1(t) = \frac{1}{2\pi i} \int_{-\infty}^{(0+)} e^{\lambda t} \bar{T}_1(\lambda) d\lambda \quad (\text{A.3})$$

A inversion valid for large times is solved by; 1) expand the Laplace equation for small values of  $s$ , and 2) apply the inversion theorem to the expansion. First, expand the modified Bessel's functions for the numerator and denominator of Equation A.2 and simplify.

$$\bar{T}_1 = \frac{Q}{4\pi k} \frac{1}{s} \left[ \frac{c_0 + c_1 s + c_2 s^2 + \dots}{1 + a_1 s + a_2 s^2 + \dots} \right] \quad (\text{A.4})$$

$$c_0 = \beta (1 - r^{*2}) - \ln \left( \frac{C^2 a^2 s}{4\alpha} \right)$$

$$c_1 = \left[ \left( 1 - \frac{1}{2} \beta (1 - r^{*2}) + \frac{1}{4} \frac{\beta^2}{\omega} (1 - r^{*4}) \right) - \frac{1}{2} \left( 1 + \frac{\beta}{\omega} + \beta (1 - r^{*2}) \right) \ln \left( \frac{C^2 a^2 s}{4\alpha} \right) \right] \frac{a^2}{2\alpha}$$

$$c_2 = \left[ \left( \frac{3}{16} + \frac{1}{2} \frac{\beta}{\omega} - \frac{5}{16} \beta (1 - r^{*2}) - \frac{1}{8} \frac{\beta^2}{\omega} (1 - r^{*4}) + \frac{1}{36} \frac{\beta^3}{\omega^2} (1 - r^{*6}) \right) - \left( \frac{1}{16} + \frac{1}{4} \frac{\beta}{\omega} - \frac{1}{12} \frac{\beta^2}{\omega^2} + \frac{1}{8} \beta (1 - r^{*2}) + \frac{1}{8} \frac{\beta^2}{\omega} (1 - r^{*4}) \right) \ln \left( \frac{C^2 a^2 s}{4\alpha} \right) \right] \left( \frac{a^2}{2\alpha} \right)^2$$

$$a_1 = \left[ \left( -\frac{1}{2} + \frac{\beta}{\omega} \right) + \left( \frac{1}{2} - \frac{1}{\omega} \right) \ln \left( \frac{C^2 a^2 s}{4\alpha} \right) \right] \frac{a^2}{2\alpha}$$

$$a_2 = \left[ \left( -\frac{5}{16} + \frac{1}{\omega} - \frac{1}{2} \frac{\beta}{\omega} + \frac{1}{4} \frac{\beta^2}{\omega^2} \right) + \left( \frac{1}{8} - \frac{1}{2} \frac{1}{\omega} + \frac{1}{2} \frac{\beta}{\omega} - \frac{1}{2} \frac{\beta}{\omega^2} \right) \ln \left( \frac{C^2 a^2 s}{4\alpha} \right) \right] \left( \frac{a^2}{2\alpha} \right)^2$$

Complete the long division and simplify. Only terms of  $s$  up to and including order 1 are saved. This corresponds to times of order 0 to -2.

$$\begin{aligned} \bar{T}_1 = \frac{Q}{4\pi k} & \left[ \left( f_0 + f_1 \ln \left( \frac{C^2 a^2 s}{4\alpha} \right) \right) \frac{1}{s} \right. \\ & + \left( f_2 + f_3 \ln \left( \frac{C^2 a^2 s}{4\alpha} \right) + f_4 \ln^2 \left( \frac{C^2 a^2 s}{4\alpha} \right) \right) \frac{a^2}{2\alpha} \\ & \left. + \left( f_5 + f_6 \ln \left( \frac{C^2 a^2 s}{4\alpha} \right) + f_7 \ln^2 \left( \frac{C^2 a^2 s}{4\alpha} \right) + f_8 \ln^3 \left( \frac{C^2 a^2 s}{4\alpha} \right) \right) \left( \frac{a^2}{2\alpha} \right)^2 s \right] \end{aligned} \quad (\text{A.5})$$

$$f_0 = \beta (1 - r^{*2})$$

$$f_1 = -1$$

$$f_2 = 1 - \frac{3\beta^2}{4\omega} (1 - r^{*2})$$

$$f_3 = -1 + \frac{\beta}{\omega} (1 - r^{*2}) + \frac{1}{2} \frac{\beta}{\omega}$$

$$f_4 = \frac{1}{2} \left( \frac{\omega - 2}{\omega} \right)$$

$$f_5 = \frac{11}{16} + \frac{\beta}{\omega} \left[ -\frac{1}{2} - (1 - r^{*2}) + \frac{\beta^2}{\omega} \left( \frac{3}{4} (1 - r^{*2}) - \frac{1}{4} (1 - r^{*4}) + \frac{1}{36} (1 - r^{*6}) \right) \right]$$

$$f_6 = -\frac{3}{8} - \left[ \left( \frac{\omega - 2}{\omega} \right) + \frac{\beta}{\omega} \frac{1}{2} - \frac{1}{3} \frac{\beta}{\omega} + \left( 1 - \frac{3\beta}{2\omega} \right) (1 - r^{*2}) + \frac{1}{4} \frac{\beta}{\omega} (1 - r^{*4}) \right]$$

$$f_7 = -\frac{1}{8} + \left( \frac{\omega - 2}{\omega} \right) + \frac{1}{2} \frac{\beta}{\omega} \left[ \frac{1}{2} - \left( \frac{\omega - 2}{\omega} \right) - \left( \frac{\omega - 2}{\omega} \right) (1 - r^{*2}) \right]$$

$$f_8 = -\frac{1}{4} \left( \frac{\omega - 2}{\omega} \right)^2$$

Second, substitute this expression into the inversion theorem and solve.

$$\begin{aligned}
 T_1 = \frac{Q}{4\pi k} \frac{1}{2\pi i} & \left[ f_0 \int_{-\infty}^{(0+)} \frac{1}{\lambda} e^{\lambda t} d\lambda + f_1 \int_{-\infty}^{(0+)} \frac{1}{\lambda} e^{\lambda t} \ln \left( \frac{C^2 a^2 s}{4\alpha} \right) d\lambda \right. \\
 & + \left( f_2 \int_{-\infty}^{(0+)} e^{\lambda t} d\lambda + f_3 \int_{-\infty}^{(0+)} e^{\lambda t} \ln \left( \frac{C^2 a^2 s}{4\alpha} \right) d\lambda \right. \\
 & \qquad \qquad \qquad \left. + f_4 \int_{-\infty}^{(0+)} e^{\lambda t} \ln^2 \left( \frac{C^2 a^2 s}{4\alpha} \right) d\lambda \right) \frac{a^2}{2\alpha} \\
 & + \left( f_5 \int_{-\infty}^{(0+)} \lambda e^{\lambda t} d\lambda + f_6 \int_{-\infty}^{(0+)} \lambda e^{\lambda t} \ln \left( \frac{C^2 a^2 s}{4\alpha} \right) d\lambda \right. \\
 & \left. + f_7 \int_{-\infty}^{(0+)} \lambda e^{\lambda t} \ln^2 \left( \frac{C^2 a^2 s}{4\alpha} \right) d\lambda + f_8 \int_{-\infty}^{(0+)} \lambda e^{\lambda t} \ln^3 \left( \frac{C^2 a^2 s}{4\alpha} \right) d\lambda \right) \left( \frac{a^2}{2\alpha} \right)^2 \Big]
 \end{aligned} \tag{A.6}$$

Each contour integral is evaluated separately.

$$\begin{aligned}
 T_1 = \frac{Q}{4\pi k} & \left[ f_0 - f_1 \ln \left( \frac{4\alpha t}{Ca^2} \right) + \left( -f_3 + 2f_4 \ln \left( \frac{4\alpha t}{Ca^2} \right) \right) \frac{a^2}{2\alpha t} \right. \\
 & \left. + \left( f_6 + 2f_7 \left( 1 - \ln \left( \frac{4\alpha t}{Ca^2} \right) \right) + f_8 \left( -\frac{\pi}{2} - 6 \ln \left( \frac{4\alpha t}{Ca^2} \right) + 3 \ln^2 \left( \frac{4\alpha t}{Ca^2} \right) \right) \right) \left( \frac{a^2}{2\alpha t} \right)^2 \right]
 \end{aligned} \tag{A.7}$$

This solution is for suitably large times. This equation rearranged and simplified yields the expansion for the finite conductor presented in Chapter 2, Equation 2.7.



---

## A.2 TERMS FOR SHORT TIME DATA ANALYSIS

---

### A.2.1 TERMS FOR UNKNOWN SAMPLE

All equations listed in this section are supplemental to the short time solution for an unknown sample (refer to Chapter 3).

$$\Phi_0 = \frac{\partial F}{\partial b_0} + \frac{\partial F}{\partial b_2} \frac{\partial b_2}{\partial b_0} + \frac{\partial F}{\partial b_3} \frac{\partial b_3}{\partial b_0} = 0 \quad (\text{A.8a})$$

$$\Phi_1 = \frac{\partial F}{\partial b_1} + \frac{\partial F}{\partial b_2} \frac{\partial b_2}{\partial b_1} + \frac{\partial F}{\partial b_3} \frac{\partial b_3}{\partial b_1} = 0 \quad (\text{A.8b})$$

$$\frac{\partial \Phi_0}{\partial b_0} = \frac{\partial^2 F}{\partial b_0^2} + \frac{\partial^2 F}{\partial b_0 \partial b_2} \frac{\partial b_2}{\partial b_0} + \frac{\partial^2 F}{\partial b_0 \partial b_3} \frac{\partial b_3}{\partial b_0} + \frac{\partial F}{\partial b_2} \frac{\partial^2 b_2}{\partial b_0^2} + \frac{\partial F}{\partial b_3} \frac{\partial^2 b_3}{\partial b_0^2} \quad (\text{A.9a})$$

$$\frac{\partial \Phi_0}{\partial b_1} = \frac{\partial^2 F}{\partial b_0 \partial b_1} + \frac{\partial^2 F}{\partial b_1 \partial b_2} \frac{\partial b_2}{\partial b_0} + \frac{\partial^2 F}{\partial b_1 \partial b_3} \frac{\partial b_3}{\partial b_0} + \frac{\partial F}{\partial b_2} \frac{\partial^2 b_2}{\partial b_0 \partial b_1} + \frac{\partial F}{\partial b_3} \frac{\partial^2 b_3}{\partial b_0 \partial b_1} \quad (\text{A.9b})$$

$$\frac{\partial \Phi_1}{\partial b_0} = \frac{\partial^2 F}{\partial b_0 \partial b_1} + \frac{\partial^2 F}{\partial b_0 \partial b_2} \frac{\partial b_2}{\partial b_1} + \frac{\partial^2 F}{\partial b_0 \partial b_3} \frac{\partial b_3}{\partial b_1} + \frac{\partial F}{\partial b_2} \frac{\partial^2 b_2}{\partial b_0 \partial b_1} + \frac{\partial F}{\partial b_3} \frac{\partial^2 b_3}{\partial b_0 \partial b_1} \quad (\text{A.9c})$$

$$\frac{\partial \Phi_1}{\partial b_1} = \frac{\partial^2 F}{\partial b_1^2} + \frac{\partial^2 F}{\partial b_1 \partial b_2} \frac{\partial b_2}{\partial b_1} + \frac{\partial^2 F}{\partial b_1 \partial b_3} \frac{\partial b_3}{\partial b_1} + \frac{\partial F}{\partial b_2} \frac{\partial^2 b_2}{\partial b_1^2} + \frac{\partial F}{\partial b_3} \frac{\partial^2 b_3}{\partial b_1^2} \quad (\text{A.9d})$$

The expressions for all first partials of F with respect to  $b_i$  are:

$$\frac{-1}{2} \frac{\partial F}{\partial b_0} = \sum \bar{T}_i - b_0 n - b_1 \sum \ln t_i - b_2 \sum t_i^{-1} - b_3 \sum t_i^{-1} \ln t_i \quad (\text{A.10a})$$

$$\frac{-1}{2} \frac{\partial F}{\partial b_1} = \sum \bar{T}_i \ln t_i - b_0 \sum \ln t_i - b_1 \sum \ln^2 t_i - b_2 \sum t_i^{-1} \ln t_i - b_3 \sum t_i^{-1} \ln^2 t_i \quad (\text{A.10b})$$

$$\frac{-1}{2} \frac{\partial F}{\partial b_2} = \sum \bar{T}_i t_i^{-1} - b_0 \sum t_i^{-1} - b_1 \sum t_i^{-1} \ln t_i - b_2 \sum t_i^{-2} - b_3 \sum t_i^{-2} \ln t_i \quad (\text{A.10c})$$

$$\frac{-1}{2} \frac{\partial F}{\partial b_3} = \sum \bar{T}_i t_i^{-1} \ln t_i - b_0 \sum t_i^{-1} \ln t_i - b_1 \sum t_i^{-1} \ln^2 t_i - b_2 \sum t_i^{-2} \ln t_i - b_3 \sum t_i^{-2} \ln^2 t_i \quad (\text{A.10d})$$

The expressions for all second partials of F with respect to  $b_i$  are:

$$\frac{-1}{2} \frac{\partial^2 F}{\partial b_0^2} = -n \quad (\text{A.11a})$$

$$\frac{-1}{2} \frac{\partial^2 F}{\partial b_0 \partial b_1} = -\sum \ln t_i \quad (\text{A.11b})$$

$$\frac{-1}{2} \frac{\partial^2 F}{\partial b_1^2} = -\sum \ln^2 t_i \quad (\text{A.11c})$$

$$\frac{-1}{2} \frac{\partial^2 F}{\partial b_0 \partial b_2} = -\sum t_i^{-1} \quad (\text{A.11d})$$

$$\frac{-1}{2} \frac{\partial^2 F}{\partial b_0 \partial b_3} = -\sum t_i^{-1} \ln t_i \quad (\text{A.11e})$$

$$\frac{-1}{2} \frac{\partial^2 F}{\partial b_1 \partial b_2} = -\sum t_i^{-1} \ln t_i \quad (\text{A.11f})$$

$$\frac{-1}{2} \frac{\partial^2 F}{\partial b_1 \partial b_3} = -\sum t_i^{-1} \ln^2 t_i \quad (\text{A.11g})$$

The expressions for all first partials of  $b_i$  with respect to  $b_j$  are:

$$\frac{\partial b_2}{\partial b_0} = -\frac{2}{C} \left[ b_\chi e^{-b_\chi} + B b_1 \right] \quad (\text{A.12a})$$

$$\frac{\partial b_2}{\partial b_1} = \frac{2}{C} \left[ \left( 1 + b_\chi + b_\chi^2 \right) e^{-b_\chi} - B b_1 b_\chi - \frac{3}{4} \frac{Q}{4\pi k_1} B \right] \quad (\text{A.12b})$$

$$\frac{\partial b_3}{\partial b_0} = -\frac{2}{C} e^{-b_\chi} \quad (\text{A.12c})$$

$$\frac{\partial b_3}{\partial b_1} = \frac{2}{C} \left[ \left( 1 + b_\chi \right) e^{-b_\chi} - 2B b_1 \right] \quad (\text{A.12d})$$

The expressions for all second partials of  $b_i$  with respect to  $b_i$  are:

$$\frac{\partial^2 b_2}{\partial b_0^2} = -\frac{2}{C} (1 - b_x) b_1^{-1} e^{-b_x} \quad (\text{A.13a})$$

$$\frac{\partial^2 b_2}{\partial b_0 \partial b_1} = \frac{2}{C} \left[ (1 - b_x) b_x b_1^{-1} e^{-b_x} - B \right] \quad (\text{A.13b})$$

$$\frac{\partial^2 b_2}{\partial b_1^2} = \frac{2}{C} (1 - b_x) b_x^2 b_1^{-1} e^{-b_x} \quad (\text{A.13c})$$

$$\frac{\partial^2 b_3}{\partial b_0^2} = \frac{2}{C} b_1^{-1} e^{-b_x} \quad (\text{A.13d})$$

$$\frac{\partial^2 b_3}{\partial b_0 \partial b_1} = -\frac{2}{C} b_x b_1^{-1} e^{-b_x} \quad (\text{A.13e})$$

$$\frac{\partial^2 b_3}{\partial b_1^2} = \frac{2}{C} \left[ b_x^2 b_1^{-1} e^{-b_x} - 2B \right] \quad (\text{A.13f})$$

## A.2.2 TERMS FOR UNKNOWN PROBE

All equations listed in this section are supplemental to the short time solution for an unknown probe (refer to Chapter 3).

$$\Phi_0 = \frac{\partial F}{\partial b_0} + \frac{\partial F}{\partial b_2} \frac{\partial b_2}{\partial b_0} = 0 \quad (\text{A.14a})$$

$$\Phi_3 = \frac{\partial F}{\partial b_3} + \frac{\partial F}{\partial b_2} \frac{\partial b_2}{\partial b_3} = 0 \quad (\text{A.14b})$$

$$\frac{\partial \Phi_0}{\partial b_0} = \frac{\partial^2 F}{\partial b_0^2} + \frac{\partial^2 F}{\partial b_0 \partial b_2} \frac{\partial b_2}{\partial b_0} \quad (\text{A.15a})$$

$$\frac{\partial \Phi_0}{\partial b_3} = \frac{\partial^2 F}{\partial b_0 \partial b_3} + \frac{\partial^2 F}{\partial b_2 \partial b_3} \frac{\partial b_2}{\partial b_0} + \frac{\partial F}{\partial b_2} \frac{\partial^2 b_2}{\partial b_0 \partial b_3} \quad (\text{A.15b})$$

$$\frac{\partial \Phi_3}{\partial b_0} = \frac{\partial^2 F}{\partial b_0 \partial b_3} + \frac{\partial^2 F}{\partial b_0 \partial b_2} \frac{\partial b_2}{\partial b_3} + \frac{\partial F}{\partial b_2} \frac{\partial^2 b_2}{\partial b_0 \partial b_3} \quad (\text{A.15c})$$

$$\frac{\partial \Phi_3}{\partial b_3} = \frac{\partial^2 F}{\partial b_3^2} + \frac{\partial^2 F}{\partial b_2 \partial b_3} \frac{\partial b_2}{\partial b_3} \quad (\text{A.15d})$$

The expressions for all first partials of F with respect to  $b_i$  are:

$$\frac{-1}{2} \frac{\partial F}{\partial b_0} = \sum \bar{T}_i - b_0 n - b_1 \sum \ln t_i - b_2 \sum t_i^{-1} - b_3 \sum t_i^{-1} \ln t_i \quad (\text{A.16a})$$

$$\frac{-1}{2} \frac{\partial F}{\partial b_2} = \sum \bar{T}_i t_i^{-1} - b_0 \sum t_i^{-1} - b_1 \sum t_i^{-1} \ln t_i - b_2 \sum t_i^{-2} - b_3 \sum t_i^{-2} \ln t_i \quad (\text{A.16b})$$

$$\frac{-1}{2} \frac{\partial F}{\partial b_3} = \sum \bar{T}_i t_i^{-1} \ln t_i - b_0 \sum t_i^{-1} \ln t_i - b_1 \sum t_i^{-1} \ln^2 t_i - b_2 \sum t_i^{-2} \ln t_i - b_3 \sum t_i^{-2} \ln^2 t_i \quad (\text{A.16c})$$

The expressions for all second partials of F with respect to  $b_i$  are:

$$\frac{-1}{2} \frac{\partial^2 F}{\partial b_0^2} = -n \quad (\text{A.17a})$$

$$\frac{-1}{2} \frac{\partial^2 F}{\partial b_0 \partial b_2} = -\sum t_i^{-1} \quad (\text{A.17b})$$

$$\frac{-1}{2} \frac{\partial^2 F}{\partial b_0 \partial b_3} = -\sum t_i^{-1} \ln t_i \quad (\text{A.17c})$$

$$\frac{-1}{2} \frac{\partial^2 F}{\partial b_2 \partial b_3} = -\sum t_i^{-2} \ln t_i \quad (\text{A.17d})$$

$$\frac{-1}{2} \frac{\partial^2 F}{\partial b_3^2} = -\sum t_i^{-2} \ln^2 t_i \quad (\text{A.17e})$$

The expressions for all first partials of  $b_i$  with respect to  $b_i$  are:

$$\frac{\partial b_2}{\partial b_0} = -\frac{3}{4} \frac{\alpha^2}{2\alpha} + \frac{3}{4} b_3 b_1^{-1} \quad (\text{A.18a})$$

$$\frac{\partial b_2}{\partial b_3} = \frac{3}{4} b_0 b_1^{-1} + \frac{1}{4} \ln \left( \frac{4\alpha}{Ca^2} \right) \quad (\text{A.18b})$$

The expressions for all second partials of  $b_i$  with respect to  $b_i$  are:

$$\frac{\partial^2 b_2}{\partial b_0 \partial b_3} = \frac{3}{4} b_1 \quad (\text{A.19})$$

APPENDIX B

**THERMAL CONDUCTIVITY SYSTEM SOFTWARE MANUAL**

---

## **B.0 INTRODUCTION**

---

To perform a thermal conductivity experiment with a needle probe two steps must be completed. First, the needle probe is inserted into the Keithley Series 500 and the characteristics of the probe are input to the software. Second, the resistance versus temperature characteristics of the probe are determined. Prior to an experiment it may also be necessary to determine the probe heat capacity and thermal conductivity.

This appendix contains the operating procedure and software description for the thermal conductivity system software. There are four basic procedures; 1) log in, 2) Series 500 system configuration, 3) temperature response calibration, and 4) thermal conductivity measurement. Before operating the system complete the details of Chapter 4.

This appendix also contains the program code for the software. It is written in Version 3.0 of IBM's interpreter BASICA for the IBM Personal Computer.

---

## B.1 LOG IN AND OPERATING PROCEDURES

---

In the following text all input and output for the IBM PC text is in Courier typeface (abcdefghijklmnopqrstuvwxyz1234567890). All Courier typeface grouped by < > refers to keys on the IBM PC keyboard. In all thermal conductivity system sections <Num Locks> must be off.

The thermal conductivity system follows a specific set of operating conventions. Each section of the software is controlled via a menu bar, and each item in the menu bar is controlled via a menu list. Additional input is via full-time and pop-up dialog boxes. All text and numeric input is via the data editor. Figures B.9, B.10, B.11, and B.12 detail the basic operating guidelines.

After logging into the thermal conductivity system there are three basic operating procedures; 1) Series 500 System Configuration, 2) Temperature Response Calibration, and 3) Thermal Conductivity Measurement. All of the tasks necessary are detailed in the remainder of this appendix. A summary is presented in Table B.1



Figure B.1

Menu Bar, Menu List, and System Control Guidelines

☐ MenuBar
MenuList
SystemControl

1234567890

### MENU BAR

- Located at top of screen.
- Symbol "☐" is a branch to the system menu.
- Selection changed by <←,→> .
- Menu List for selection activated by <Return>.
- Selection changed and the menu list activated by typing the number of the item in the menu bar. The main menu branch is item 0. Increment by 1 for the numbers of the remaining items.

### MENU LIST

- When activated the list is placed directly the menu bar selection.
- Selection changed by <↑,←,↓,→>.
- Selection is activated by <Return>.
- "..." at the end of a selection requires further information.
- "▶" at the beginning of a selection is an active item.
- "?" at the beginning of a selection is an altered item.
- A selection that is grayed cannot be activated.
- A grayed dash line is an inactive selection to divide the menu.
- Selection changed and activated by typing the item number.
- End the list by <End>.

☐

☐

☐

☐

☐

☐

☐

☐

☐

☐

☐

☐

☐

☐

☐

☐

☐

☐

☐

☐

☐

☐

☐

☐

☐

☐

☐

☐

☐

☐

☐

☐

☐

☐

☐

☐

☐

☐

☐

☐

☐

☐

☐

☐

☐

☐

☐

☐

☐

☐

☐

☐

☐

☐

☐

☐

☐

☐

☐

☐

☐

☐

☐

☐

☐

☐

☐

☐

☐

☐

☐

☐

☐

☐

☐

☐

☐

☐

☐

☐

☐

☐

☐

☐

☐

☐

☐

☐

☐

☐

☐

☐

☐

☐

☐

☐

☐

☐

☐

☐

☐

☐

☐

☐

☐

☐

☐

☐

☐

☐

☐

☐

☐

☐

☐

☐

☐

☐

☐

☐

☐

☐

☐

☐

☐

☐

☐

☐

☐

☐

☐

☐

☐

☐

☐

☐

☐

☐

☐

☐

☐

☐

☐

☐

☐

☐

☐

☐

☐

☐

☐

☐

☐

☐

☐

☐

☐

☐

☐

☐

☐

☐

☐

☐

☐

☐

☐

☐

☐

☐

☐

☐

☐

☐

☐

☐

☐

☐

☐

☐

☐

☐

☐

☐

☐

☐

☐

☐

☐

☐

☐

☐

☐

☐

☐

☐

☐

☐

☐

☐

☐

☐

☐

☐

☐

☐

☐

☐

☐

☐

☐

☐

☐

☐

☐

☐

☐

☐

☐

☐

☐

☐

☐

☐

☐

☐

☐

☐

☐

☐

☐

☐

☐

☐

☐

☐

☐

☐

☐

☐

☐

☐

☐

☐

☐

☐

☐

☐

☐

☐

☐

☐

☐

☐

☐

☐

☐

☐

☐

☐

☐

☐

☐

☐

☐

☐

☐

☐

☐

☐

☐

☐

☐

☐

☐

☐

☐

☐

☐

☐

☐

☐

☐

☐

☐

☐

☐

☐

☐

☐

☐

☐

☐

☐

☐

☐

☐

☐

☐

☐

☐

☐

☐

☐

☐

☐

☐

☐

☐

☐

☐

☐

☐

☐

☐

☐

☐

☐

☐

☐

☐

☐

☐

☐

☐

☐

☐

☐

☐

☐

☐

☐

☐

☐

☐

☐

☐

☐

☐

☐

☐

☐

☐

☐

☐

☐

☐

☐

☐

☐

☐

☐

☐

☐

☐

☐

☐

☐

☐

☐

☐

☐

☐

☐

Figure B.2  
Dialog Box Guidelines

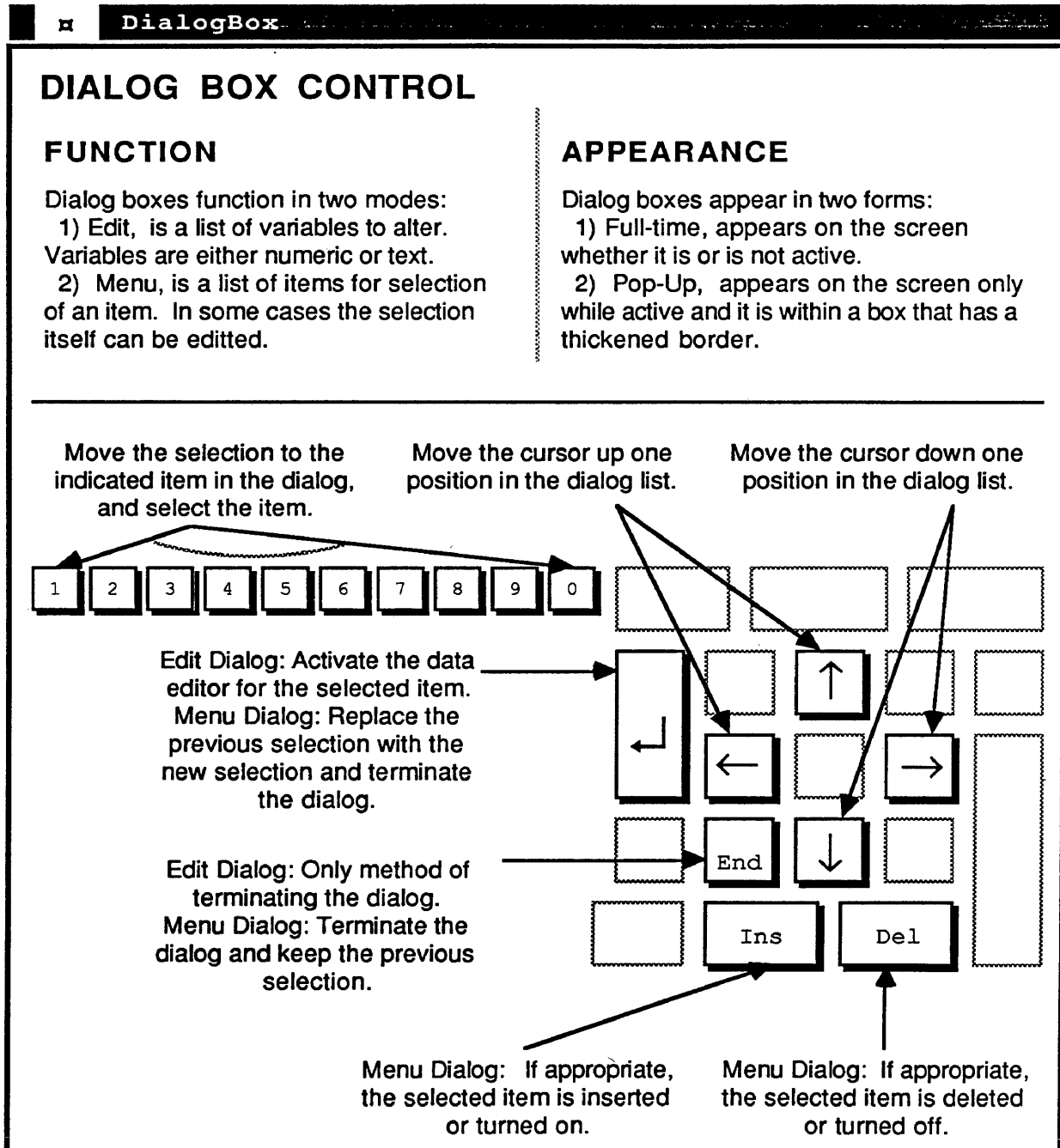


Figure B.3  
Data Editor Guidelines

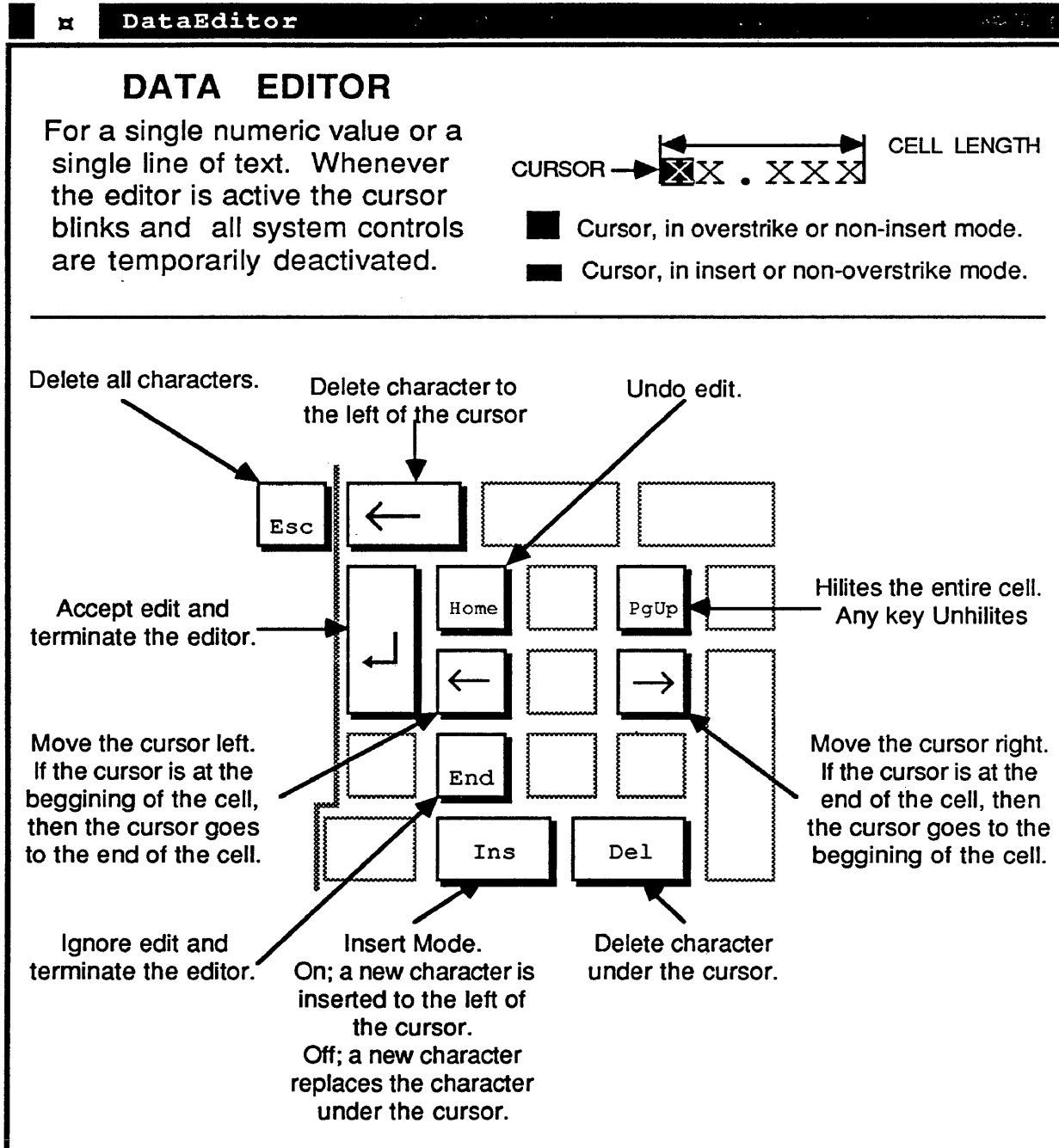
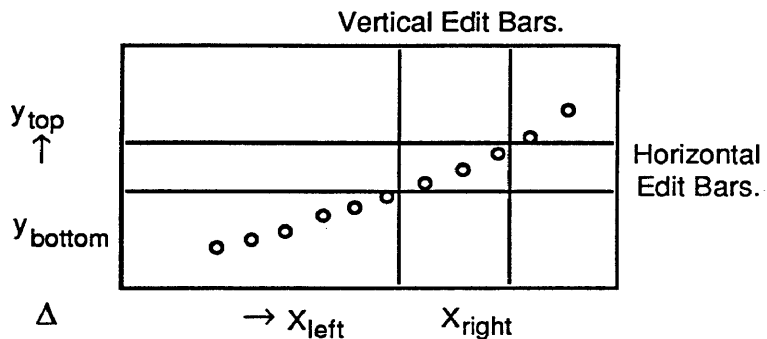


Figure B.4  
Graph Editor Guidelines

**GraphEditor**

### GRAPH EDITOR

For editing a file to remove inaccurate data, and for editing the experimental data for a thermal conductivity experiment.



Vertical Edit Bars.

Horizontal Edit Bars.

$y_{top}$


$y_{bottom}$

$\Delta$

$\rightarrow X_{left}$   $X_{right}$

---

Alter the increment that the edit bars move by; 1) 0.01, 2) 0.1, 3) 1.0, 4) 10.0, and 5) 100.0.



Return the edit bars and/or graph to the original settings.

Move the active horizontal cursor up.

Perform a special function on the data isolated by the edit bars.

Select the active horizontal edit bar.

Move the active vertical cursor left.

Terminating the editor.

Select the active vertical edit bar.

Rescale and redraw the graph according to the edit bars.

Move the active vertical cursor right.

Rescale and redraw the graph according to a previous setting.

Move the active horizontal cursor down.

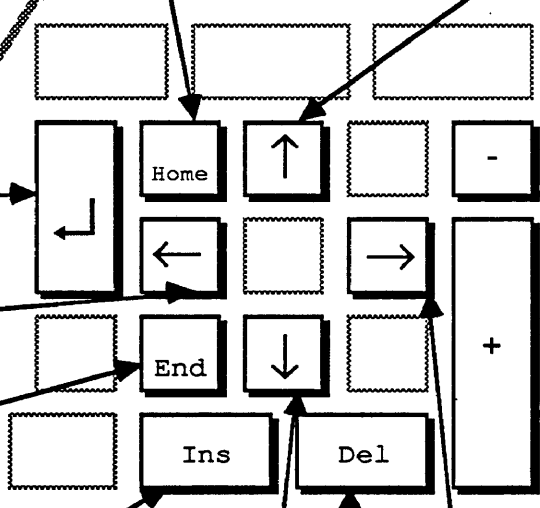


Table B.1  
Summary of the Operating Procedures

---

**Log In Procedure.**

Figure B.13.

**Series 500 System Configuration - Thermal Conductivity Apparatus.**

1. Install a needle probe and platinum resistance thermometer into one of four thermal conductivity system channels. Figure B.14.

**Temperature Response Calibration - Data Set Acquisition.**

2. Obtain a set of calibration points for the thermal conductivity needle probe and the platinum resistance thermometer. Figure B.15.

**Temperature Response Calibration - Analysis and Plotter.**

3. Determining a set of calibration coefficients and plotting the calibration data set for a needle probe or a platinum resistance thermometer. Figure B.16.

**Thermal Conductivity Measurement - Acquisition and Analysis.**

4. Selecting and setting up a probe for an experiment. Figure B.17.
5. Selecting a material for the selected probe and inserting, editing, or deleting a material in the material menu. Figure B.18.
6. Specifying the disk drive for experimental data storage and retrieval, and employing the automatic save and print feature. Figure B.19.
7. Setting up the general analysis specifications for an experiment. These hold simultaneously for all probes. Figure B.20.
8. Use of the automatic repeat function for execution of successive experiments. Figure B.21.
9. Performing an experiment, where the experiment is begun at a clock setting or when the temperature of the probe stabilizes. Figure B.22.
10. Reanalyze a previous experiment or calibrate the probe from an experiment on a material of known properties. Figure B.23.
11. Manually supplying heat to the probe, initializing the Keithley, and using the function keys to store an experimental set-up. Figure B.24.

**Thermal Conductivity Measurement - Data Set Plotter.**

12. Searching through old data sets, and plotting experimental temperature rise or apparent conductivity versus natural logarithm of time for experiments and all thermal conductivity measurements for a material. Figure B.26.
-

Figure B.5

## Thermal Conductivity System Log In Procedure

**Asherworks**

The method of logging into the thermal conductivity system follows; 1) the Keithley Soft500 is loaded, and 2) the thermal conductivity system software is loaded and the Keithley Series 500 is initialized.

**1** From DOS change the default drive and directory to that containing the thermal conductivity system software.

**2** Load Keithley SOFT500 as described in the Keithley Manuals:

**3** Run the thermal conductivity system by typing in BASICA.

```
RUN "TCS\TCS <Return>
```

**4** The TCS logo should now appear on the screen. Follow the instructions on the screen prompt, which are,

```
Turn Keithley Data Acquisition and Control System On,  
Then Strike <Space Bar>
```

**NOTE,** the probes should not be connected into the Series 500 whenever the Series 500 is being turned on or off. Possible power surges from the Series 500 may damage the probes.

**5** After a brief moment the thermal conductivity system menu appears. This menu controls the two methods to transfer between all sections of the software. Use the <←, ↑, →, ↓> keys to position the cursor to the desired selection and then strike <Return>, or execute the desired transfer by typing <Alt> - <F1, F2, F3, F4, F5, F6, F7, F8, F9, or F10>. The <Alt> keys remain operational in all programs when the menu bar is operational.

Figure B.6

## Operating Procedure 1

## SERIES 500 SYSTEM CONFIGURATION - THERMAL CONDUCTIVITY APPARATUS

	Channel	Edit	Restore	Save												
<p>Install a needle probe and platinum resistance thermometer into one of the four thermal conductivity system channels.</p>																
<div style="border: 1px solid black; padding: 5px;"> <p style="text-align: center; margin: 0;"><b>Channel</b></p> <table style="width: 100%; border-collapse: collapse;"> <tr> <td style="width: 10px; text-align: right;">▶</td> <td style="width: 70%;">PROBE1,</td> <td style="width: 20%;">On</td> </tr> <tr> <td></td> <td>PROBE2,</td> <td>Off</td> </tr> <tr> <td></td> <td>PROBE3,</td> <td>Off</td> </tr> <tr> <td></td> <td>PROBE4,</td> <td>Off</td> </tr> </table> <hr style="border-top: 1px dashed black;"/> <p style="text-align: center; margin: 0;">Quick Config...</p> </div>	▶	PROBE1,	On		PROBE2,	Off		PROBE3,	Off		PROBE4,	Off	<p><b>1. Select the probe to be configured or altered:</b></p> <ol style="list-style-type: none"> <li>a. In the menu bar select "Channel".</li> <li>b. In the menu list select the probe channel . Or, select "Quick Config". The Quick Config dialog is a menu type dialog. &lt;Ins&gt; turns the channel on, and &lt;Del&gt; turns the channel off. Any function key struck directly after &lt;Ins&gt; will be saved to that particular channel. See step 5 for function key information.</li> </ol>			
▶	PROBE1,	On														
	PROBE2,	Off														
	PROBE3,	Off														
	PROBE4,	Off														
<div style="border: 1px solid black; padding: 5px;"> <p style="text-align: center; margin: 0;"><b>Edit</b></p> <p>Channel On/Off Probe Name Probe Length Probe Mount Length Probe Diameter Probe Heater Resistance Probe Heat Capacity Probe Thermal Conductivity Standard Resistance PRT Name PRT On/Off</p> </div>	<p><b>2. Edit the specifications for the channel:</b></p> <ol style="list-style-type: none"> <li>a. In the menu bar select "Edit".</li> <li>b. In the menu list select the specification to edit. A question mark is printed next to the specifications that have been altered from the original value. The channel or prt on and off states are toggled, while all other specifications require an input.</li> </ol>															
<div style="border: 1px solid black; padding: 5px;"> <p style="text-align: center; margin: 0;"><b>Restore</b></p> <p>Any or all of the altered specifications.</p> </div>	<p><b>3. Restore a specification to its original value:</b></p> <ol style="list-style-type: none"> <li>a. In the menu bar select "Restore".</li> <li>b. In the menu list select the specification to restore. Only altered items are restored. All unaltered items are grayed.</li> </ol>															
<div style="border: 1px solid black; padding: 5px;"> <p style="text-align: center; margin: 0;"><b>Save</b></p> <p>Any or all of the altered specifications.</p> </div>	<p><b>4. Save a specification as the original value:</b></p> <ol style="list-style-type: none"> <li>a. In the menu bar select "Save".</li> <li>b. In the menu list select the specification to saved. Only altered items are saved. All unaltered items are grayed. This command is ignored when the channel information to</li> </ol>															
<p>be saved has a blank probe or prt and the channel or prt, respectively , is on.</p>																
<p><b>5. All specifications for the selected channel are stored to a function key by &lt;Ctrl&gt;-&lt;F1, ..., F10&gt;. The values of a function key are recalled to any selected channel by &lt;F1, ..., F10&gt;.</b></p>																

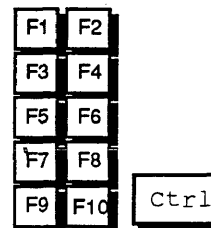


Figure B.7

## Operating Procedure 2

## TEMPERATURE RESPONSE CALIBRATION - DATA SET ACQUISITION

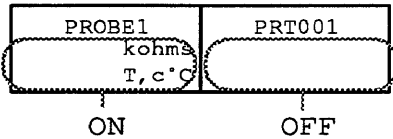
	Item	Edit	Acquisition
<p>Obtain a set of calibration points for the thermal conductivity needle probe thermistor and the platinum resistance thermometer.</p>			
<div style="border: 1px solid black; padding: 5px; margin-bottom: 5px;">Item</div> <div style="border: 1px solid black; padding: 5px; margin-bottom: 5px;">On / Off...</div> <div style="border: 1px solid black; padding: 5px;">Quick Config...</div>	<p>1. Select the probes and prt's to calibrate:</p> <ol style="list-style-type: none"> <li>a. In the menu bar select "Item".</li> <li>b. In the menu list select "On / Off".</li> <li>c. The on/off dialog is now active, and it is a menu type dialog, except that it allows for the selection of multiple items. Script appearing for the calibration display indicates that the selection is on. During any calibration process at least one probe must be selected.</li> </ol>	 <p>A probe or prt in a channel that is turned off cannot be accessed. A prt that is turned off cannot be accessed.</p>	
<div style="border: 1px solid black; padding: 5px; margin-bottom: 5px;">Edit</div> <div style="border: 1px solid black; padding: 5px;">Specifications...</div>	<p>2. Edit the steady state specifications:</p> <ol style="list-style-type: none"> <li>a. In the menu bar select "Edit".</li> <li>b. In the menu list select "Specifications".</li> <li>c. The specification dialog box is now active, and it is an edit type dialog. Input the desired check time, points per calibration, and time between points.</li> </ol>		
<div style="border: 1px solid black; padding: 5px; margin-bottom: 5px;">Acquisition</div> <div style="border: 1px solid black; padding: 5px;">           One Calibration Point            Several Calibration Points            End After Calibration Point            End Calibration         </div>	<p>3. To activate the steady state process:</p> <ol style="list-style-type: none"> <li>a. In the menu bar select "Acquisition".</li> <li>b. In the menu list select "One Calibration Point" or "Several Calibration Points".</li> </ol>		
<ol style="list-style-type: none"> <li>c. Probe resistances and prt measured temperature are determined at each steady state check. When the probe resistances are equivalent for two successive checks, it is assumed the system is at steady state. At this time the computer beeps and the actual temperature is input. To disregard the system being at steady state input a blank response.</li> <li>d. To terminate the process at any time strike &lt;Return&gt; to recall the menu list. To terminate the process immediately after the next calibration point select "End Calibration After Point", or to terminate the process immediately select "End Calibration". NOTE, the calibration process is not active while the menu list is shown.</li> </ol>			



Figure B.8  
Operating Procedure 3

**TEMPERATURE RESPONSE CALIBRATION - ANALYSIS AND PLOTTER**

Item	Analysis	Plot
<p>Determine a set of calibration coefficients and plot the calibration data set for a needle probe or a platinum resistance thermometer.</p>		
<p><b>Item</b></p> <div style="border: 1px solid black; padding: 5px;"> <p>▶ PROBE1 PROBE2 PROBE3 PROBE4</p> <hr style="border-top: 1px dashed black;"/> <p>PRT001 PRT002 PRT003 PRT004</p> </div>	<p><b>1. Select the probe or prt for the analysis or plot:</b></p> <p>a. In the menu bar select "Item".</p> <p>b. In the menu list select a probe or prt. Only a probe from a channel that is turned on or prt from from a channel and prt slot that is turned on can be selected. The current calibration coefficients are listed on the screen.</p> <p><b>2. Determine the calibration coefficients for the selected probe or prt:</b></p> <p>a. In the menu bar select "Analysis".</p> <p>b. In the menu list select "Calibration Coefficients". The calibration data sets are plotted, the calibration coefficients are calculated, and the residuals from the least squares regression are plotted. The coefficients are stored in a data file and are recalled each time the thermal conductivity system is started. A prompt will ask if the coefficients should or should not be saved.</p> <p>c. In the same menu list a subsidiary function is provided, "Order Data Sets". This structures the data in order of decreasing temperature and creates a backup file. Ordering the data enables the analysis and plotter to operate faster, but it loses the structure with which the data was obtained.</p>	
<p><b>Analysis</b></p> <div style="border: 1px solid black; padding: 5px;"> <p>Calibration Coefficients Order Data Sets</p> </div>		
<p><b>Plot</b></p> <div style="border: 1px solid black; padding: 5px;"> <p>Temperature vs Resistance Resistance vs Temperature 1/Temperature vs ln(Resistance) ln(Resistance) vs 1/Temperature Actual vs Measured Temperature</p> </div>	<p><b>3. Plot a calibration data set by:</b></p> <p>a. In the menu bar select "Plot".</p> <p>b. In the menu list select the plot. If the data for a probe is to be plotted, then one of four graph types must be selected. There is only one type of a plot for a prt.</p> <p>c. To return to the main screen strike &lt;End&gt;, and edit mode for the graph is entered by &lt;Return&gt;. Data is removed from the files thru the probe temperature versus resistance graph and the prt graph. The operation is described in the graph editor guidelines.</p>	

Figure B.9  
Operating Procedure 4

THERMAL CONDUCTIVITY MEASUREMENT - ACQUISITION AND ANALYSIS

	Channel	Edit	Execute												
<p>Selecting and setting up a probe for an experiment.</p> <div style="display: flex; justify-content: space-between;"> <div style="width: 30%; border: 1px solid black; padding: 5px;"> <p>Channel</p> <ul style="list-style-type: none"> <li>▶ PROBE1</li> <li>PROBE2</li> <li>PROBE3</li> <li>PROBE4</li> </ul> <hr style="border-top: 1px dashed black;"/> <p>Quick Config...</p> <hr style="border-top: 1px dashed black;"/> <p>Probe Set-Up...</p> <p>Show Temperature</p> </div> <div style="width: 65%;"> <ol style="list-style-type: none"> <li>1. Select the desired probe by:                             <ol style="list-style-type: none"> <li>a. In the menu bar select "Channel".</li> <li>b. In the menu list select the probe. A probe can only be selected from a channel which is turned on. To show the temperature of the selected probe select "Show Temperature" in the menu list.</li> </ol> </li> <li>2. Alter the set up of the probe by:                             <ol style="list-style-type: none"> <li>a. In the menu bar select "Channel".</li> <li>b. In the menu list select "Probe Set-Up". This activates the probe set-up dialog box, which is a full-time dialog box when the probe is assigned a material.</li> </ol> </li> </ol> <p>If the probe is not assigned a material the material menu will pop up first. The material menu can also be activated by selecting the material name in the probe set-up dialog box. The operation of the material menu is described in the next operating procedure.</p> <ol style="list-style-type: none"> <li>c. "Q" is the power per unit probe length. Its range is 0 to 99 mW/cm in steps of 0.01.</li> <li>d. "Δt" is the time step between temperature rise measurements. Its range is 0.001 to 32.767 seconds in steps of 0.001.</li> <li>e. "NΔt" is the time length of an experiment. Its range is 00:00:01 to 23:59:59.</li> <li>f. "Start" is the starting time for an experiment (only when starting an experiment from "Man"). Its range is 00:00:00 to 23:59:59.</li> <li>g. If specifying a solution "ITS" is Infinite Time Solution ("LTS" with no error analysis), "LTS" is Long Time Solution, and "STS" is Short Time Solution. The final two solutions are not an option if the probe thermal conductivity and heat capacity are not specified.</li> <li>h. Strike &lt;End&gt; to return to the main cursor, or &lt;Ctrl&gt;-&lt;End&gt; to return and save as startup. The value of "N" is calculated. If the time length is not an integer multiple of the time step, then the next highest integer is selected for "N". "N" must be greater than a hundred and less than two thousand. Otherwise, a system prompt is given and to proceed strike any key.</li> </ol> </div> </div>															
			<table style="width: 100%; border-collapse: collapse;"> <tr><td style="border-top: 1px solid black;">Q mw/cm</td><td style="border-top: 1px solid black;">10.00</td></tr> <tr><td>Δt secs</td><td>0.200</td></tr> <tr><td>NΔt</td><td>00:01:00</td></tr> <tr><td>Start</td><td>00:00:00</td></tr> <tr><td>Date</td><td></td></tr> </table>	Q mw/cm	10.00	Δt secs	0.200	NΔt	00:01:00	Start	00:00:00	Date			
Q mw/cm	10.00														
Δt secs	0.200														
NΔt	00:01:00														
Start	00:00:00														
Date															
			<table style="width: 100%; border-collapse: collapse;"> <thead> <tr><th style="border-top: 1px solid black; border-bottom: 1px solid black;">Exp</th><th style="border-top: 1px solid black; border-bottom: 1px solid black;">Min</th><th style="border-top: 1px solid black; border-bottom: 1px solid black;">Max</th></tr> </thead> <tbody> <tr><td>"N"</td><td>100</td><td>2000</td></tr> <tr><td>"Δt"</td><td>0.001</td><td>32.767</td></tr> <tr><td>"NΔt"</td><td>00:00:01</td><td>18:12:14</td></tr> </tbody> </table>	Exp	Min	Max	"N"	100	2000	"Δt"	0.001	32.767	"NΔt"	00:00:01	18:12:14
Exp	Min	Max													
"N"	100	2000													
"Δt"	0.001	32.767													
"NΔt"	00:00:01	18:12:14													

Figure B.10  
Operating Procedure 5

THERMAL CONDUCTIVITY MEASUREMENT - ACQUISITION AND ANALYSIS

■	Channel	Edit	Execute
---	---------	------	---------

Selecting a material for the selected probe and inserting, editing, or deleting a material in the material menu.

<table border="1" style="width: 100%; border-collapse: collapse;"> <tr> <td style="padding: 2px;">Edit</td> </tr> <tr> <td style="padding: 2px;">Material Menu.. Data Drive...</td> </tr> <tr> <td style="padding: 2px;">Automatic Save On Automatic Print On</td> </tr> <tr> <td style="padding: 2px;">Analysis Specs... Repeat Cycle... Maximums...</td> </tr> </table>	Edit	Material Menu.. Data Drive...	Automatic Save On Automatic Print On	Analysis Specs... Repeat Cycle... Maximums...	<ol style="list-style-type: none"> <li>1. Display the material menu :             <ol style="list-style-type: none"> <li>a. In the menu bar select "Edit".</li> <li>b. In the menu list select "Material Menu...". The material menu is pop-up dialog box of the menu type.</li> </ol> </li> <li>2. Add to or alter the material selection menu:             <ol style="list-style-type: none"> <li>a. Select a material cell. If a material is listed in the cell then that material will be edited, otherwise a new material is input to the cell.</li> </ol> </li> </ol> <p>b. Strike &lt;Ins&gt;. If adding a material respond to the system prompt to insert a new material and then input a four character code. The code must be four alphanumeric characters in length, and all experiments are saved to disk according to this code. Duplicate 4 character codes are permitted. Up to 24 materials can be added to the menu, all all names must follow IBM's conventions for filenames. For a new material and when altering a material respond to the system prompts for the material name,description, and next file number.</p> <p>NEXT FILE NUMBER: All experiments are referred to by the four character code plus the next file number. All new materials are assigned the next file number of "001". Each experiment increments this number by "001" until "999". When this number is lowered old experiments remain on disk and are written over as the number increases.</p> <ol style="list-style-type: none"> <li>3. Delete a material from the material menu:             <ol style="list-style-type: none"> <li>a. Select a material cell. If a material is listed in the cell, then that material will be deleted.</li> <li>b. Strike &lt;Del&gt;. Respond to the prompt on whether or not to delete the material.</li> </ol> </li> <li>4. Terminate the material menu and select a material.             <ol style="list-style-type: none"> <li>a. To assign the selected material to the current probe strike &lt;Return&gt;.</li> <li>b. To not change the selected material for the current probe strike &lt;End&gt;.</li> <li>c. To reset the master material menu strike &lt;Ctrl&gt;-&lt;End&gt;.</li> </ol> </li> </ol>
Edit					
Material Menu.. Data Drive...					
Automatic Save On Automatic Print On					
Analysis Specs... Repeat Cycle... Maximums...					

Example Material - Solid or Liquid, EXAM001
EXAM

Figure B.19

## Operating Procedure 11

## THERMAL CONDUCTIVITY MEASUREMENT - ACQUISITION AND ANALYSIS


Channel	Edit	Execute
<p>Specifying the disk drive for experimental data storage and retrieval, and employing the automatic save and print feature.</p> <div style="display: flex; justify-content: space-between; align-items: flex-start;"> <div style="width: 30%; border: 1px solid black; padding: 5px;"> <p><b>Edit</b></p> <hr/> <p>Material Menu.. Data Drive...</p> <hr/> <p>Automatic Save On Automatic Print On</p> <hr/> <p>Analysis Specs... Repeat Cycle... Maximums...</p> </div> <div style="width: 65%;"> <ol style="list-style-type: none"> <li>1. Assign the disk drive for the experiments by:               <ol style="list-style-type: none"> <li>a. In the menu bar select "Edit".</li> <li>b. In the menu list select "Data Drive".</li> <li>c. Respond to the system prompt for the disk drive. The software will accept drives A thru D as inputs. A blank drive value is used for the default drive. The software does not check if the specified drive is the default drive or not. The disk specification is only for the experimental data generated by thermal conductivity experiments. If using floppy disk drives there is minimal room on the thermal conductivity system disk for data storage.</li> </ol> </li>   <li>2. Automatically save an experiment after analysis by:               <ol style="list-style-type: none"> <li>a. In the menu bar select "Edit".</li> <li>b. In the menu list select "Automatic Save On". When the disk icon is shown in the lower right portion of the screen the automatic save is on. If the save feature is on then this menu list option becomes "Automatic Save Off".</li> </ol> </li>   <li>3. Automatically print an experiment after analysis by:               <ol style="list-style-type: none"> <li>a. In the menu bar select "Edit".</li> <li>b. In the menu list select "Automatic Print On". When the paper icon is shown in the lower right portion of the screen the automatic print is on. If the print feature is on then this menu list option becomes "Automatic Print Off".</li> </ol> </li>   <li>4. Edit the maximum temperature rise and thermal conductivity for an experiment:               <ol style="list-style-type: none"> <li>a. In the menu bar select "Edit".</li> <li>b. In the menu list select "Maximums...". The maximums pop-up dialog box is now active. This is an edit type dialog box. If the temperature in an experiment becomes greater than the maximum temperature the experiment is terminated. If the thermal conductivity determined during data analysis is less than zero or greater than the maximum then the data analysis is terminated.</li> </ol> </li> </ol> </div> </div> <div style="width: 30%; text-align: center; margin-top: 20px;">  </div>		

Figure B.12  
Operating Procedure 7

THERMAL CONDUCTIVITY MEASUREMENT - ACQUISITION AND ANALYSIS

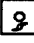
	Channel	Edit	Execute							
<p>Setting up the general analysis specifications for an experiment. These hold simultaneously for all probes.</p> <div style="border: 1px solid black; padding: 5px; width: fit-content;"> <p>Edit  </p> <table border="1" style="width: 100%; border-collapse: collapse;"> <tr> <td style="padding: 2px;">Material Menu..</td> </tr> <tr> <td style="padding: 2px;">Data Drive...</td> </tr> <tr> <td style="padding: 2px;">Automatic Save On</td> </tr> <tr> <td style="padding: 2px;">Automatic Print On</td> </tr> <tr> <td style="padding: 2px;">Analysis Specs...</td> </tr> <tr> <td style="padding: 2px;">Repeat Cycle...</td> </tr> <tr> <td style="padding: 2px;">Maximums...</td> </tr> </table> </div> <div style="margin-left: 20px;"> <p>1. Activate the analysis specifications dialog box by:</p> <ol style="list-style-type: none"> <li>a. In the menu bar select "Edit".</li> <li>b. In the menu list select "Analysis Specs...". The analysis specs is a full-time dialog box of the edit type.</li> </ol> </div>				Material Menu..	Data Drive...	Automatic Save On	Automatic Print On	Analysis Specs...	Repeat Cycle...	Maximums...
Material Menu..										
Data Drive...										
Automatic Save On										
Automatic Print On										
Analysis Specs...										
Repeat Cycle...										
Maximums...										
<p>2. Edit the analysis specifications by:</p> <ol style="list-style-type: none"> <li>a. To control the multiple experiment number.           <ol style="list-style-type: none"> <li>i. Select "<math>\Sigma</math>" and then input the number of multiple experiments desired.</li> <li>ii. During a multiple experiment run the information is stored after each experiment. To access this old data move the cursor one position to the right and strike &lt;Return&gt;. A miniture disk icon appears and the number of previous experiments is retrieved.</li> </ol> <p>NOTE: There is no checking to assure that a restarted multiple experiment is executed under the same experimental conditions.</p> </li> <li>b. Select "<math>\Delta</math>" to edit the number of point estimates for the apparent thermal conductivity.</li> <li>c. Select "<math>\Delta</math>" to edit the fractional length of the total experiment time for each apparent thermal conductivity estimate.</li> <li>d. Select one of the "<u>    </u>." locations. The first parameter controls the fractional location for the beginning of the data analysis, and the second controls the end location.</li> </ol> <div style="float: right; text-align: center; margin-top: 20px;"> <p><math>\Sigma</math></p> <p></p> <p><math>\Delta</math></p> <p><u>    </u></p> <p><u>    </u></p> </div>										
<p>3. Terminate the analysis specifications dialog box by &lt;End&gt;.</p>										

Figure B.13  
Operating Procedure 8


THERMAL CONDUCTIVITY MEASUREMENT - ACQUISITION AND ANALYSIS

n	Channel	Edit	Execute
---	---------	------	---------

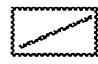

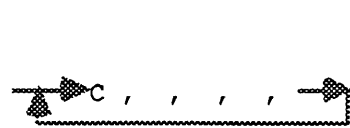
Using the automatic repeat function for execution of successive experiments.

**Edit**

Material Menu..
Data Drive...
Automatic Save On
Automatic Print On
Analysis Specs...
Repeat Cycle...
Maximums...

1. Activate the repeat dialog box by:
  - a. In the menu bar select "Edit".
  - b. In the menu list select "Repeat Cycle...". The repeat cycle is a full-time dialog box of the edit type.
2. Set up the repeat cycle by:
  - a. Select "". If the repeat icon is shown the repeat cycle is on.
  - b. Select "0, L". Input the number of experiments, L is from 1 to 99, for the repeat cycle.

During the acquisition modes the current repeat number replaces the "0".

- c. Select "". Input the viewing time after an acquisition and analysis. In this time the settings for the save and print option can be overridden. After the time expires the automatic save and print options are executed as per their settings.
- d. Select "". Input the delay time from one start time to the next. It is overridden if enough time is not given for an experiment to finish. This parameter is only used when starting an acquisition by the clocks.
- e. Alter sequence for the experiments by:
  - i. Select "" to activate the sequence cursor. Move the cursor by <←,→>.
  - ii. Strike <C>, <F1, ..., F10>, or <Space Bar> for the current screen values, for the parameters of a function key, or to clear a value, respectively. The repeat cycle iterates from the first value until a blank space or the end of the list.

NOTE: Only the parameters "Q", "Δt", and "NΔt" for the selected probe and the "Analysis Specs..." parameters are recalled by a function key. After recalling a function key the current screen values are those of the function key. Details on setting up a function key are given in a later operating procedure.

- iii. End this cursor by <End>.



0, L





Figure B.14

## Operating Procedure 9

THERMAL CONDUCTIVITY MEASUREMENT - ACQUISITION AND ANALYSIS

	Channel	Edit	Execute				
<p>Performing an experiment, where the experiment is begun at a clock setting or when the temperature of the probe stabilizes.</p>							
<table border="1" style="width: 100%; border-collapse: collapse;"> <thead> <tr style="background-color: black; color: white;"> <th style="width: 100%;">Execute</th> </tr> </thead> <tbody> <tr> <td style="padding: 5px;">           Acquisition: by Clock...            Acquisition: by Temperature...         </td> </tr> <tr> <td style="border-top: 1px dashed black; padding: 5px;">           Analysis...            Optimize...         </td> </tr> <tr> <td style="border-top: 1px dashed black; padding: 5px;">           Manual Q...            Initialize Keithley...         </td> </tr> </tbody> </table>	Execute	Acquisition: by Clock... Acquisition: by Temperature...	Analysis... Optimize...	Manual Q... Initialize Keithley...	<ol style="list-style-type: none"> <li>1. Execute an experiment by:             <ol style="list-style-type: none"> <li>a. In the menu bar select "Execute".</li> <li>b. In the menu list select "Acquisition: by Clock..." to start an experiment from a clock setting or "Acquisition: by Temperature..." to start an experiment by the temperature stabilization of the probe.</li> </ol> </li> </ol>		
Execute							
Acquisition: by Clock... Acquisition: by Temperature...							
Analysis... Optimize...							
Manual Q... Initialize Keithley...							
<ol style="list-style-type: none"> <li>2. The acquisition and analysis process then proceeds as follows:             <ol style="list-style-type: none"> <li>a. In the clock mode the experiment is immediately set up, while in the temperature mode the experiment is set up immediately before experimentation. Strike no keys to allow the mode to initiate itself. In the clock mode the system waits for the "Start" time, and in the temperature mode the system waits for stabilization of the probe thermistor temperature. Strike &lt;Return&gt; to initiate the mode and &lt;End&gt; to return control to the main cursor.</li> <li>b. During the spare time, which is a function of the time step, several functions are performed by the system; a) the converted data is plotted, b) checks if the temperature rise is less than the maximum allowable (3 Kelvin), if true the experiment continues, and c) check if &lt;End&gt; was struck anywhere in the acquisition and conversion process, if true a system prompt is given for the disposition of the experiment. &lt;Ctrl&gt;-&lt;A&gt; terminates the acquisition and &lt;Ctrl&gt;-&lt;C&gt; terminates the acquisition and conversion.</li> <li>c. In the first step of the analysis process the optimum solution region is located using the "ITS" solution. During analysis the data segment being analyzed is graphically and numerically shown. Then if requested the "LTS" or "STS" solution is performed. If errors occur during analysis the analysis terminated. The analysis is also terminated by &lt;End&gt;.</li> <li>d. After the analysis concludes a system prompt is given for the disposition of the experiment. The choices are &lt;1&gt; save and print, &lt;1&gt; save, &lt;2&gt; print, &lt;3&gt; no save or print, and &lt;Return&gt; edit mode (more on this in a later procedure).</li> </ol> </li> </ol>							

Figure B.15  
Operating Procedure 10

**THERMAL CONDUCTIVITY MEASUREMENT - ACQUISITION AND ANALYSIS**

	Channel	Edit	Execute
<p>Reanalyze a previous experiment or calibrate the probe from an experiment on a material of known properties.</p> <p><b>Execute</b>  </p> <div style="border: 1px solid black; padding: 5px; margin: 5px 0;"> <p>Acquisition: by Clock...</p> <p>Acquisition: by Temperature...</p> <hr style="border-top: 1px dashed black;"/> <p>Analysis...</p> <p>Optimize...</p> <hr style="border-top: 1px dashed black;"/> <p>Manual Q...</p> <p>Initialize Keithley...</p> </div>	<ol style="list-style-type: none"> <li>1. Reanalyze an experiment by:               <ol style="list-style-type: none"> <li>a. In the menu bar select "Execute".</li> <li>b. In the menu list select "Analysis...". This activates the file menu, which is a pop-up dialog box of the menu type. Files 1 to 4 are for the last experiment for a probe channel. Files 5 to 8 are the user assigned files. File 9 is the last accessed file. File 0 is to specify a file. Strike &lt;Ins&gt; to insert a new file and strike &lt;Del&gt; to delete the file at a file selection</li> </ol> </li> <li>2. Select from a possible solution by:               <ol style="list-style-type: none"> <li>a. Strike "ILS &lt;1&gt;, LTS &lt;2&gt;, STS &lt;3&gt;, or Last &lt;L&gt;". A data set is completely reanalyzed only if the selection is different than the previous analysis, otherwise the solution editor is activated.</li> <li>b. After a complete solution the system prompts for the experimental disposition, or return to the editor by &lt;Return&gt;. Saving or discarding refers only to changes from data reanalysis.</li> </ol> </li> <li>3. Utilize the solution editor by:               <ol style="list-style-type: none"> <li>a. The solution editor is of the graph editor type. Position the vertical edit bar to the range of data that is to be reanalyzed. The horizontal edit bar indicates a conductivity at a specified position.</li> <li>b. Strike &lt;Return&gt; to reanalyze the selected data.</li> <li>c. To edit the basis for the experiment strike &lt;E&gt;. A pop-up dialog box of the menu type appears. The possible selections are:                   <ol style="list-style-type: none"> <li>i. Select the type of solution. This is done through a pop-up dialog box of the menu type. ITS, LTS, and STS are as defined previously. PRB stands for the probe calibration solution, and it requires the sample conductivity and heat capacity.</li> <li>ii. Edit the probe properties. This is done through a pop-up dialog box of the edit type. The properties that are edited are those as specified in the in the configuration procedure.</li> <li>iii. Specify the sample properties for the probe calibration solution. This is done through a pop-up dialog box of the edit type.</li> <li>iv. Edit the material descriptions for the file only.</li> </ol> </li> <li>d. End the solution editing session by &lt;End&gt;, and respond to the prompts as to the disposition of the changes.</li> </ol> </li> </ol>		



Figure B.16

## Operating Procedure 11

## THERMAL CONDUCTIVITY MEASUREMENT - ACQUISITION AND ANALYSIS

	Channel	Edit	Execute											
<p>Manually supplying heat to the probe, initializing the Keithley, and using the function keys to store an experimental set-up.</p>														
<table border="1" style="width: 100%; border-collapse: collapse;"> <thead> <tr> <th style="text-align: left; padding: 2px;">Execute</th> </tr> </thead> <tbody> <tr> <td style="padding: 2px;">Acquisition: by Clock...</td> </tr> <tr> <td style="padding: 2px;">Acquisition: by Temperature...</td> </tr> <tr> <td style="border-top: 1px dashed black; padding: 2px;">Analysis...</td> </tr> <tr> <td style="padding: 2px;">Optimize...</td> </tr> <tr> <td style="border-top: 1px dashed black; padding: 2px;">Manual Q...</td> </tr> <tr> <td style="padding: 2px;">Initialize Keithley...</td> </tr> </tbody> </table>	Execute	Acquisition: by Clock...	Acquisition: by Temperature...	Analysis...	Optimize...	Manual Q...	Initialize Keithley...	<p>1. Manually supply heat to the probe by:</p> <ol style="list-style-type: none"> <li>a. In the menu bar select "Execute" .</li> <li>b. In the menu list select "Manual Q..." . This activates the manual Q dialog, which is a pop-up dialog box. This feature is useful in melting a formed solid away from the probe, but not melting all of the formed solid.</li> <li>c. Strike &lt;Return&gt; to show or hide the probe temperature. Strike &lt;Space Bar&gt; to turn the power to the probe on or off. The amount of power supplied to the probe can be edited.</li> </ol> <p>2. Initialize the Keithley Series 500 by:</p> <ol style="list-style-type: none"> <li>a. In the menu bar select "Execute" .</li> <li>b. In the menu list select "Initialize Keithley..." . This zeros all power to the probe thermistor and heater channels, which is the same function as when the thermal conductivity system software is first loaded. This is useful in case the Keithley is turned off while the thermal conductivity system is active.</li> </ol> <p>3. Experimental set-ups are saved and recalled by the function keys.</p> <p>One possibility is to save the set-up just to the point of beginning experimentation. For this feature to function the menu bar must have program control. The procedure to save and recall a set-up follows:</p> <ol style="list-style-type: none"> <li>a. To save an experimental set up strike &lt;Ctrl&gt; - &lt;F1, F2, F3, F4, F5, F6, F7, F8, F9, F10&gt;. The experimental set up will be saved to the function key until overrode by another save. Note, the characteristics of each probe channel are saved whether the probe channel is on or off</li> <li>b. To retrieve an experimental set up strike &lt;F1, F2, F3, F4, F5, F6, F7, F8, F9, F10&gt;. The experimental set up last saved to the function key is retrieved. The current on/off status of the probe channels are valid. Note, the current experimental set up is deleted and cannot be retrieved.</li> </ol>						
Execute														
Acquisition: by Clock...														
Acquisition: by Temperature...														
Analysis...														
Optimize...														
Manual Q...														
Initialize Keithley...														
	<table border="1" style="display: inline-table; border-collapse: collapse;"> <tbody> <tr><td style="padding: 2px;">F1</td><td style="padding: 2px;">F2</td></tr> <tr><td style="padding: 2px;">F3</td><td style="padding: 2px;">F4</td></tr> <tr><td style="padding: 2px;">F5</td><td style="padding: 2px;">F6</td></tr> <tr><td style="padding: 2px;">F7</td><td style="padding: 2px;">F8</td></tr> <tr><td style="padding: 2px;">F9</td><td style="padding: 2px;">F10</td></tr> </tbody> </table> <table border="1" style="display: inline-table; border-collapse: collapse; margin-left: 20px;"> <tbody> <tr><td style="padding: 2px;">Ctrl</td></tr> </tbody> </table>			F1	F2	F3	F4	F5	F6	F7	F8	F9	F10	Ctrl
F1	F2													
F3	F4													
F5	F6													
F7	F8													
F9	F10													
Ctrl														

Figure B.17

Operating Procedure 12

THERMAL CONDUCTIVITY MEASUREMENT - FILE SEARCH AND PLOTTER

☐	Item ←	Item →	Edit	Search	Plot
---	--------	--------	------	--------	------

Searching through old data sets, and plotting experimental temperature rise or apparent conductivity versus natural logarithm of time for experiments and all thermal conductivity measurements for a material.

**Search** |

Specifications...
List...
Edit Specifications...

1. Edit the specifications to search by:
  - a. In the menu bar select "Search".
  - b. In the menu bar select "Edit Specifications". This activates the specification dialog box. It is a full-time dialog box of the edit type.
  - c. Select a specification and edit the range to search. "→" indicates that the specification will be searched, and toggles between on by <Ins> and off by <Del>. If the material is selected, then use the material menu to alter the selection.
2. Search according to the specifications by:
  - a. In the menu bar select "Search".
  - b. In the menu bar select "Specifications..". This activates the search specification dialog box. It is a pop-up dialog box of the menu type. After a few moments the search is completed.
  - c. Move the cursor to view the files. Save the selected file as "Item←" file by <Return>, or cancel the selection by <End>.

**Item←** |

▶ EXAM001
EXAM002
EXAM003
EXAM004
NUL
NUL
NUL
NUL
File Menu...

3. Select the file to plot by:
  - a. In the menu bar select "Item←" or "Item→".
  - b. In the menu list select the desired file or select "File Menu..." to specify a file. To plot two files on the same graph select a file for both items.
4. Plot the data by:
  - a. In the menu bar select "Plot".
  - b. In the menu list select the desired type of plot. After a few moments the plot appears.
  - c. Edit mode, except for 2 file plots, is entered by <Return>, and control returns to the file search and plot program by <End>. Data removed only from the material graph.

**Plot** |

Temperature Rise, Apparent Conductivity for an Experiment, and Conductivities for a Material.
---

---

## B.2 PROGRAM CODE

---

The program code and variable and data file documentation is available through the Colorado School of Mines, Chemical Engineering Department, E. Dendy Sloan. The general flow of all programs is:

